NLRC3: a NEW PLAYER at the CROSSROADS of INFLAMMASOME REGULATION, CELL PROLIFERATION and IMMUNE TOLERANCE

by

Elif EREN

M.Sc., Paris VI Pierre-Marie Curie University, 2008

B.Sc., Paris V René Descartes University, 2006

Submitted to the Institute for Graduate Studies in
Science and Engineering in partial fulfillment of
the requirement for the degree of
Doctor of Philosophy

Graduate Program in Molecular Biology and Genetics

Boğaziçi University

2015

ACKNOWLEDGEMENTS

First of all, I would like to thank my thesis director Prof. Nesrin Özören for giving me the freedom to ask new questions, design experiments and for her guidance and support. I would like also to thank past and present members of AKIL for being such great friends and colleagues.

The second part of this thesis was performed at Massachusetts Institute of Technology (Boston, MA, USA). I would like to thank Assistant Prof. Ömer Yılmaz (M.D., PhD) for his critical review and all Yılmaz laboratory members, with special thanks to Naniye Malli (PhD) for showing me organoid cultures and Tuomas Tammela (PhD) from Jacks Laboratory (MIT) for providing me U6-sgRNA-EFS-turboRFP plasmid. I would also like to acknowledge TUBITAK 2214A for supporting my six months at MIT.

I would also like to thank my thesis evaluation committee members Assoc. Prof. Devrim Gözüaçık and Prof. Esra Battaloğlu, who have been in my jury since the beginning of my PhD. Thank you for following my work every six months and for guiding me during this long journey. I would also like to acknowledge Assoc. Prof. Ayça Sayı and Assoc. Prof. Arzu Çelik for evaluating the final version of my thesis.

I also thank Stefan Kostler (PhD) for taking confocal images, Genreg laboratory for providing pLenti-CMV-Blast vector and Retina laboratory for sharing their immunostaining protocols.

Finally, I am very thankful to my friends from the department who were always with me and made my life much easier.

ABSTRACT

NLRC3: a NEW PLAYER at the CROSSROADS of INFLAMMASOME REGULATION, CELL PROLIFERATION and IMMUNE TOLERANCE

NLR family proteins are cytoplasmic receptors responsible for the regulation of inflammation. Whereas some NLRs such as Cryopyrin form protein complexes recognizing pathogens and activating inflammation called the inflammasome; the function of other NLRs is still to be characterized. NLRC3, one of the less studied members of this family, was found to be a negative regulator of T-cell activation, NFκB pathway and STING-dependent cytokine secretion. In this thesis, we investigate the role of NLRC3 in the regulation of the Cryopyrin inflammasome, in cell proliferation and its possible involvement in immune tolerance mechanisms.

By overexpression and knock-down analyses, we identified whether NLRC3 inhibits Cryopyrin-induced IL-1β cleavage and secretion in response to different stimuli. We determined that NLRC3 exerts its suppressive effect downstream of Cryopyrin by interacting with diffused ASC protein and pro-Caspase-1 via their respective CARD domains and thus may disrupt complex assembly.

Secondly, potential regulation of stem cell proliferation by NLRC3 was clarified. Nlrc3 was gradually silenced in more proliferative Apc and Apc Kras organoids. Nlrc3 KO primary tissues were generated using CRISPR/Cas9 techniques and organoid formation capacity of Nlrc3 KO, KD and overexpressing cells were measured. Suppression of Nlrc3 expression increased cell proliferation and organoid formation whereas the opposite phenotype was observed in NLRC3 overexpressing cells. We showed that Nlrc3 KO increases the expression of stem cell (Lgr5) and cell cycle (CyclinD1) markers.

Finally, we showed that NLRC3 could be involved in immune tolerance mechanisms since it is expressed in cell lines and tissues from these sites. Furthermore, NLRC3 localized in the nucleus, suggesting that it could act as a transcription factor.

ÖZET

NLRC3: ENFLAMAZOM DENETİMİ, HÜCRE ÇOĞALMASI ve İMMÜN AYRICALIK YOLAKLARININ KESİŞİMİNDEKİ YENİ ÜYE

NLR protein ailesi ödemi (enflamasyonu) denetleyen sitoplazmik almaçlardır. Cryopyrin gibi bazı NLR'ların enflamazom adı verilen kompleksler oluşturduğu ve patojeni tanıyıp enflamasyonu tetiklerken; aileyi oluşturan diğer NLR'ların görevi tam olarak bilinmemektedir. Bu az araştırılmış üyelerden biri olan NLRC3'ün, T hücresi aktivasyonunu baskıladığı, NFκB yolağını susturduğu ve STING'e bağlı sitokin salınımını olumsuz etkilediği belirlenmiştir. Bu tez kapsamında, NLRC3'ün Cryopyrin enflamazomunun düzenlenmesi, hücre çoğalması ve immün tolerans mekanizmalarındaki olası görevi araştırılmaktadır.

Hücrelerde aşırı anlatımını sağlayarak veya shRNA ile susturarak, NLRC3'ün, Cryopyrin enflamazomuna bağlı IL-1β kesilim ve salımınını olumsuz etkilediği bulunmuştur. NLRC3'ün, yolakta Cryopyrin'in altında yer alan ASC ve pro-Caspase-1 proteinleri ile CARD bölgeleri sayesinde etkileştiği ve kompleks oluşumunu engellediği görülmüştür.

Tezin ikinci bölümünde ise, NLRC3'ün kök hücre çoğalmasına etkisi araştırılmıştır. Nlrc3 seviyelerinin, tümöre daha yatkın olduğu bilinen Apc ve Apc Kras hücrelerinde azaldığı tespit edilmiştir. CRISPR/Cas9 tekniğini kullanarak Nlrc3 KO birincil dokular üretilmiş ve Nlrc3 KO, KD ve Nlrc3 aşırı anlatımı olan hücrelerin organoid oluşturma kapasitesi ölçülmüştür. Nlrc3'ün susturulması hücre çoğalmasını ve organoid oluşumunu arttırırken, Nlrc3'ü aşırı anlatan hücrelerde aksi fenotip gözlenmiştir. Nlrc3 susturulduğunda kök hücre (Lgr5) ve hücre çoğalması (CyclinD1) belirteçlerinin daha yüksek olduğu gösterilmiştir.

Son olarak, Nlrc3'ün immün ayrıcalık dokularında ve hücre hatlarında anlatımının olduğu ve hücrelerin çekirdeğinde yer aldığı için bu dokularda transkripsiyon faktörü olabileceği öne sürülmüştür.

TABLE OF CONTENTS

LIST OF FIGURES

LIST OF TABLES

LIST OF SYMBOLS

a.u.	Arbritrary Unit
bp	Base Pairs
g	Gravity
gr	Gram
kb	Kilobase
kDa	Kilodalton
L	Liter
M	Molar
mA	Milliamper
mg	Milligram
mM	Millimolar
min	Minute
ng	Nanogram
rpm	Revolutions Per Minute
sec	Second
V	Volt
°C	Centigrade Degree
α	Alpha
β	Beta
γ	Gamma
µg	Microgram
µl	Microliter
ϰ	Kappa

LIST OF ACRONYMS/ABBREVIATIONS

AIM2	Absent in Melanoma 2
AP-1	Activator Protein-1
APC	Adenomatous Polyposis Coli
APS	Ammonium Persulfate
ASC	Apoptosis-Associated Speck-Like Protein Containing a CARD
ATP	Adenosine Triphosphate
BCA	Bicinchoninic Acid
BSA	Bovine Serum Albumin
BRCC3	BRCA1-BRCA2-Containing Complex
CARD	Caspase Activation and Recruitment Domains
Caspase	Cysteine-Dependent Aspartate-Directed Proteases
Cas9	CRISPR Associated Protein 9
CD	Cluster of Differentiation
CIITA	Class II, Major Histocompatibility Complex, Transactivator
CMV	Cytomegalovirus
CpG	C-Phosphate-G
CRISPR	Clustered Regularly-Interspaced Short Palindromic Repeats
cDNA	Complementary DNA
DAMP	Danger-Associated Molecular Pattern
DAPI	4',6-Diamidino-2-Phenylindole
DSS	Dextran Sulfate Sodium
DMEM	Dulbecco's Modified Eagle Medium

DMSO	Dimethyl Sulfoxide
DNA	Deoxyribonucleic Acid
EDTA	Ethylenediaminetetraacetic Acid
EFS	Embryonal Fyn-Associated Substrate
ELISA	Enzyme-Linked Immunosorbent Assay
ERK1/2	Extracellular Signal-Regulated Protein Kinases 1 and 2
FBS	Fetal Bovine Serum
GFP	Green Fluorescent Protein
HBS	Hepes Buffered Saline
HLA	Human Leukocyte Antigen
IgG	Immunoglobulin G
IKK	IκB Kinase
IκB	Inhibitor of Kappa B
IRES	Internal Ribosome Entry Site
IRF-3	Interferon Regulatory Factor 3
IL-1β	Interleukin 1β
IFNβ	Interferon Beta
IP	Immunoprecipitation
IPAF	Ice Protease-Activating Factor
IRAK	Interleukin-1 Receptor-Associated Kinase 1
KO	Knock-Out
KD	Knock-Down
LPS	Lipopolysaccharide
LRR	Leucine Rich Repeat
LGR5	Leucine-Rich Repeat-Containing G-Protein Coupled Receptor 5

LB	Luria Broth
MHC	Major Histocompatibility Complex
MDP	Muramyl Dipeptide
MSU	Monosodium Urate
MOI	Multiplicity of Infection
MyD88	Myeloid Differentiation Primary Response Gene 88
NBD	Nucleotide Binding Domain
NEAA	Non-Essential Amino Acid
NLR	NOD-Like Receptor
NLS	Nuclear Localization Signal
NFκB	Nuclear Factor Kappa-Light-Chain-Enhancer of Activated B Cells
NLS	Nuclear Localization Signal
NOD2	Nucleotide-Binding Oligomerization Domain Containing 2
NP-40	Nonidet P-40
OD	Optical Density
PAMP	Pathogen-Associated Molecular Pattern
PBS	Phosphate-Buffered Saline
PCR	Polymerase Chain Reaction
PI3K	Phosphoinositide 3-kinase
PFA	Paraformaldehyde
PMA	Phorbol Myristate Acetate
PNK	Polynucleotide Kinase
PRR	Pattern Recognition Receptors
PVDF	Polyvinylidene difluoride
P_2RX_7	Purinergic Receptor P2X

ROS	Reactive Oxygen Species
shRNA	Small Hairpin
sgRNA	Single Strand Guide RNA
STING	Stimulator of interferon genes
TAK1	Transforming Growth Factor Beta-Activated Kinase 1
TBST	Tris-Buffered Saline and Tween 20
TBK1	TANK-binding kinase 1
TEMED	Tetramethylethylenediamine
TRAF6	TNF Receptor-Associated Factor 6
tRFP	Turbo Red Fluorescent Protein
TRIF	TIR-Domain-Containing Adapter-Inducing Interferon-β
TNFα	Tumor Necrosis Factor Alpha
TLR	Toll Like Receptor
TBST	Tris-Buffered Saline and Tween 20
TCA	Trichloroacetic Acid
WCL	Whole Cell Lysate
WT	Wild-type

1. INTRODUCTION

1.1. Inflammation and TLR/NLR Proteins

The immune system is divided into two branches that cooperate to maintain tissue homeostasis: the innate immune system is mainly mediated by cellular receptors and cytokines, and the adaptive immune system that is acquired and involves the action of specialized cells able to keep a memory of the stimulants. In this thesis, the main focus will be on the innate immune system.

Organisms are protected from external pathogens by physical (skin, hair, membranes) and chemical barriers (tears, mucus, acidic pH) but in case of infiltration, they have developed systems to recognize and get rid of pathogens to which they are continually exposed in their environment. This system uses receptor molecules located in the plasma membrane or the membranes of the endosomal system (TLRs, toll-like receptors) or in the cytoplasm (NLRs, nucleotide-binding domain leucine-rich repeats) (Franchi *et al*., 2008 and Schroder *et al*., 2010). Recognition of pathogen-associated molecular patterns (PAMPs) and endogenous signals that induce cell damage (danger-associated molecular pattern, DAMPs) by these pattern recognition receptors (PRRs) present on macrophages, dendritic cells and mast cells, activates signaling pathways modulating immune responses (Martinon *et al*., 2007 and Franchi *et al*., 2008).

1.1.1. TLRs and NFκB Pathway

Among the pattern recognition receptors, TLRs are the most conserved and most studied receptors up to now. TLRs were first characterized in humans on the plasma membrane as inducers of NFκB pathway-dependent cytokine expression (Medzhitov *et al*., 1997*)*. Up to 11 TLRs were identified in mammals and each one recognizes different PAMPs. For instance, TLR3 is activated by double stranded RNA, whereas TLR4 senses LPS; TLR7 and TLR8 recognize imidazoquinolines and TLR9 is specific to CpG DNA (Takeda *et al*., 2005).

Upon stimulation, TLR receptors signal through their intracellular TIR domains, which are structurally similar to the IL-1β receptor (TIR for Toll/IL-1). MyD88 or TRIF adaptor proteins are recruited to the TIR domain (Takeda *et al*., 2004). While the MyD88-dependent pathway activates the NFκB pathway, the TRIF-dependent signaling leads to IRF-3 activation (Takeda *et al*., 2005). At the basal stage, the transcription activator heterodimer p50/p65 is maintained in the cytoplasm by the inhibitor IκB. Stimulation of TLRs induces a cascade of activation of some kinases including IRAK1, TRAF6, TAK1 and IκK. Active IκK phosphorylates IκB that in turn gets poly-ubiquitinated and is degraded by the proteasome. Therefore, the inhibition on p50/p65 is taken off and p50/p65 translocates to the nucleus, binds to NFκB sites on the DNA and induces the expression of target genes (Figure 1.1).

Activation of NFκB and/or IRF-3 pathways by different components listed above results in initiation of the immune responses through the induction of cytokines and chemokines' expression at the transcriptional level.

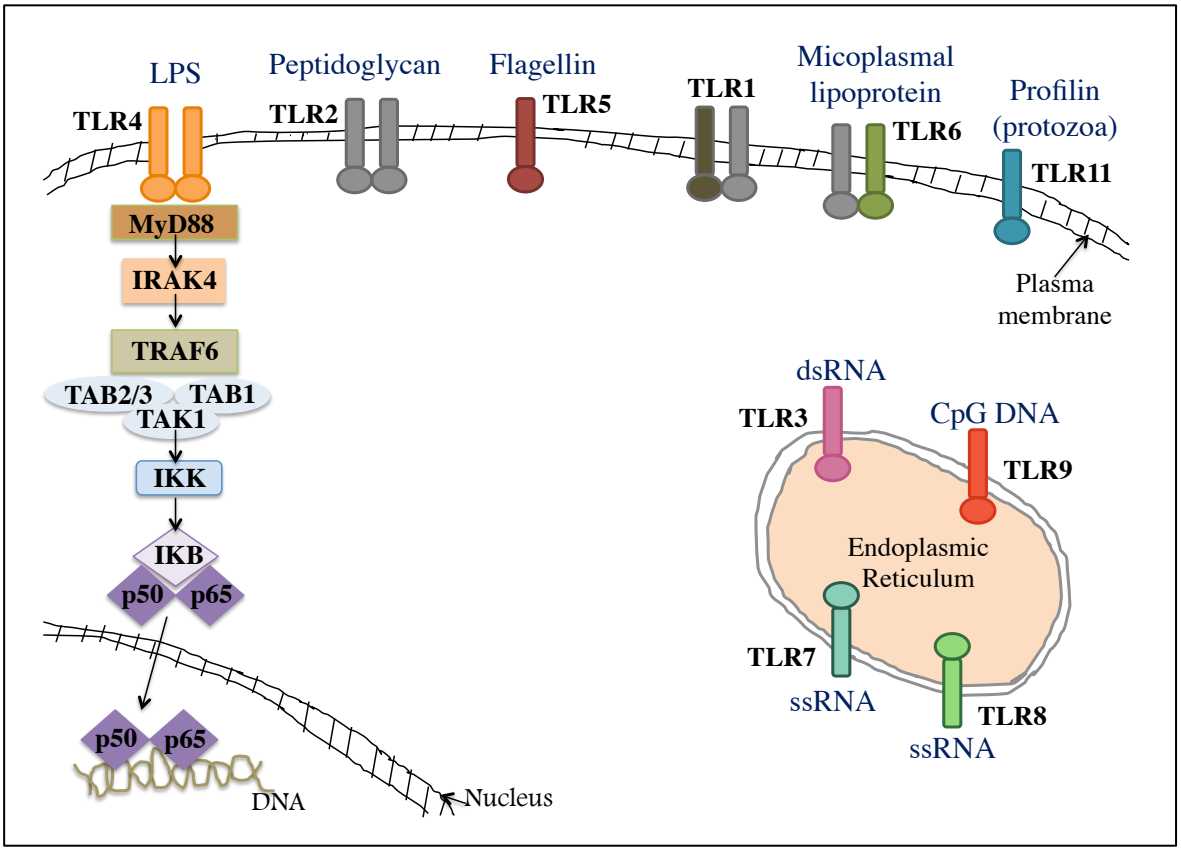

Figure 1.1. TLR receptors and NFκB pathway. Adapted from Kaufmann *et al*., 2007.

1.1.2. NLRs and Inflammasomes

In most of the cases, TLR stimulation is essential for inducing cytokine/chemokine expression but needs the cooperative effects of NLRs to fully activate the immune system. NLRs are cytoplasmic proteins that recognize cytoplasmic PAMPs and activate immunity. Up to now, 23 NLRs were described in humans. NLRs contain a regulatory NACHT domain and LRR (Leucine Rich Repeats) domain (only NLRP10 does not have a LRR domain), which senses pathogen. These 23 NLRs were classified into four subgroups depending on their functional domains (Figure 1.2): NLRA (NLR containing an activator domain), NLRB (NLR containing a BIR domain), NLRC (NLR containing a CARD domain) and NLRP (NLR containing a pyrin domain) (Shaw *et al*., 2008).

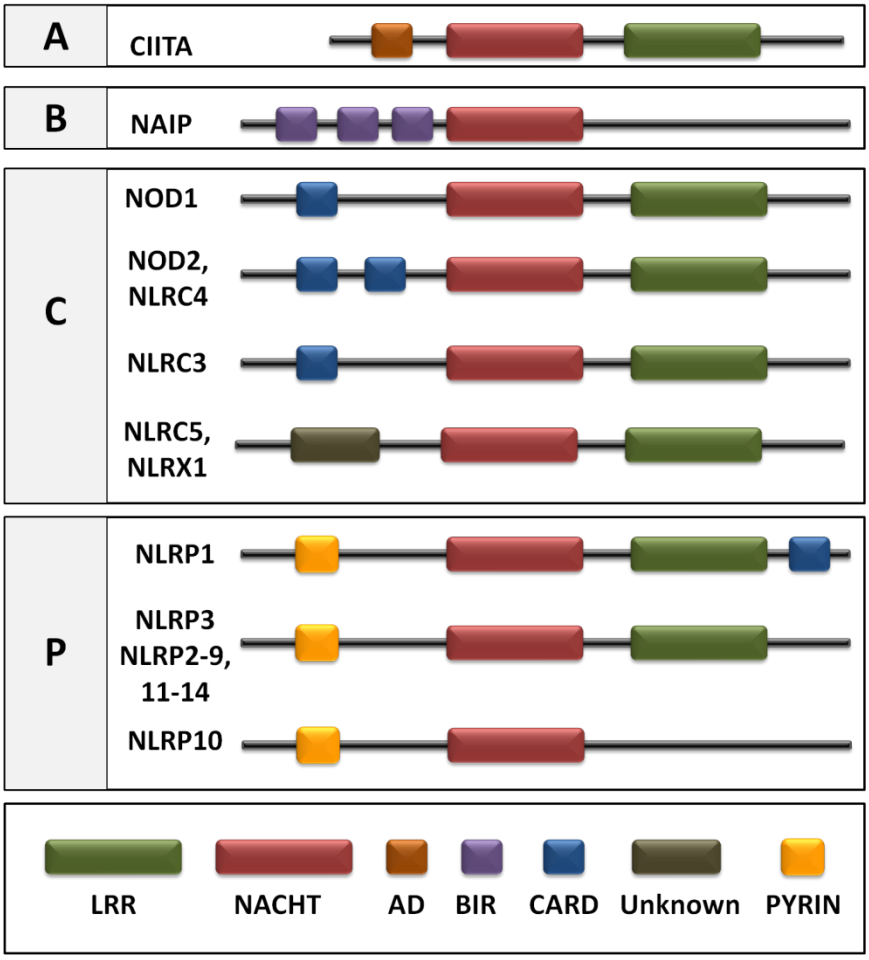

Figure 1.2. Classification of NLR proteins. Different NLR proteins are schematically represented. Each domain of NLR proteins is represented with a different color.

NLR proteins can be either pro-inflammatory or anti-inflammatory proteins. Some pro-inflammatory NLRs assemble into protein complexes called "inflammasome". Inflammasomes induce the maturation and secretion of IL-1β, which binds to its receptor located on neighboring cells and stimulates the secretion of other pro-inflammatory cytokines, chemokines as well as its own secretion. These secreted molecules attract other innate immune cells to the infection site to fight pathogens. This process is called "inflammation" and is characterized by swelling, redness, heat and pain caused by vasodilatation of vessels and leukocyte infiltration (Murphey *et al*., 2008).

To date, four different inflammasomes have been characterized, namely the NALP1, NLRC4 (IPAF), AIM2 and Cryopyrin (NLRP3) inflammasomes (Schroder *et al*., 2010).

Most attention has been attributed to the Cryopyrin inflammasome due to its wide range of activator molecules and its involvement in the physiopathology of several auto-inflammatory diseases.

All inflammasomes have in common the target pro-inflammatory cytokine IL-1β, the effector Caspase-1 and the adaptor ASC protein. They only differ by their receptor proteins that sense ligands (Figure 1.3).

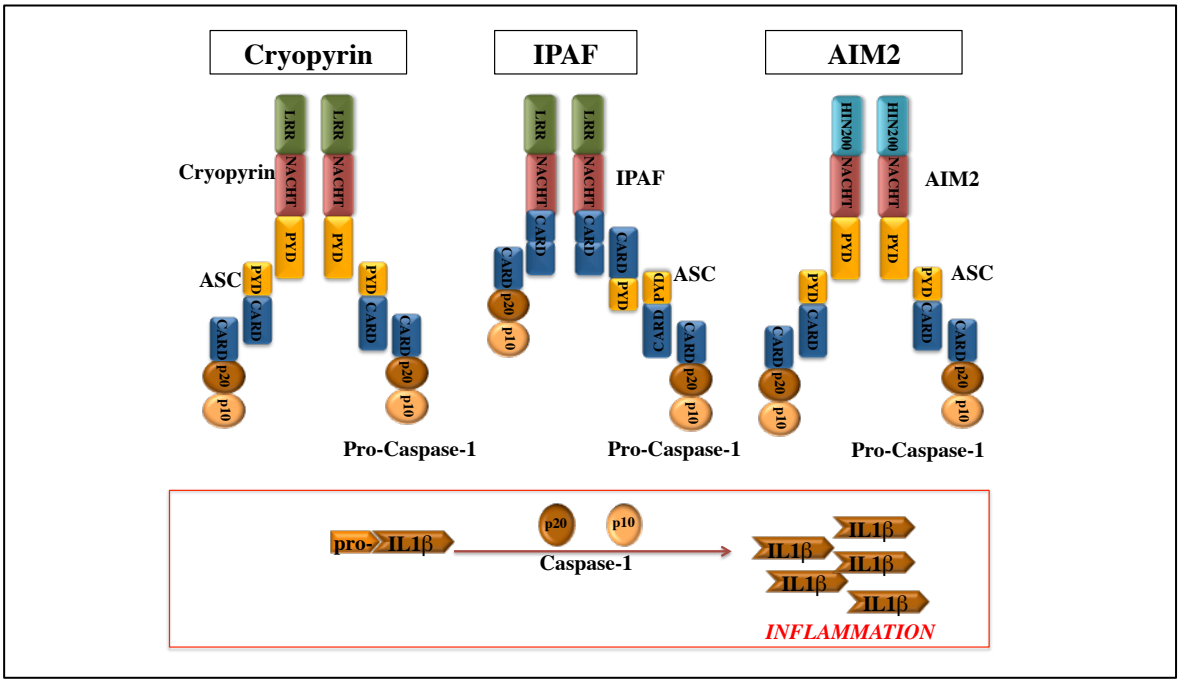

Figure 1.3. Inflammasomes. Schematical representation of three different inflammasomes and their components.

1.1.2.1. Cryopyrin Inflammasome as an Example of Pro-Inflammatory NLR. Three proteins form the Cryopyrin inflammasome: Cryopyrin itself, the adaptor protein ASC and the immature cysteine-aspartic protease pro-Caspase-1. Upon its activation, by mechanisms that are still unknown, Cryopyrin binds to ASC and induces pro-Caspase-1 cleavage into its active form Caspase-1. Active Caspase-1 is then able to induce pro-IL-1β by proteolytic digestion into IL-1β. Mature IL-1β is secreted from cells and initiates inflammation (Mariathasan *et al*., 2007).

Many types of molecules have been shown to activate the Cryopyrin inflammasome: living bacteria (*Staphylococcus aureus, Listeria monocytogenes*; Mariathasan *et al*., 2006), purified bacterial components (LPS, MDP; Martinon *et al*., 2004 and Özören *et al*., 2006), small synthetic RNAs (R837; Kanneganti *et al*., 2006) and crystals (MSU; Martinon *et al*., 2006). All of these molecules have been found to induce pro-Caspase-1 cleavage and IL-1β secretion in a Cryopyrin and ASC-dependent manner. Moreover, the Cryopyrin inflammasome has been shown to be important in linking innate immunity to the adaptive immune system (Eisenbarth *et al*., 2009 and Chen *et al*., 2011).

To avoid accidental induction of inflammation, Cryopyrin inflammasome activation is tightly regulated in cells. Two signals are necessary to activate the Cryopyrin inflammasome. First of all, Cryopyrin and ASC protein levels are maintained at a basal level in the resting cell and are then upregulated by NFκB pathway activation: this is the "priming" step (Bauernfeind *et al*., 2009). A second signal is required for the "activation" step. Despite the knowledge of multitude of the molecules inducing inflammasome formation, the molecular mechanism of its activation by these molecules is still poorly understood.

Three signals have been described to induce Cryopyrin activation: potassium efflux, reactive oxygen species (ROS) generation and lysosomal damage (Yu *et al*., 2008; Jin *et al*., 2010 and Bauernfeind *et al*., 2011). ATP or Nigericin treatment of macrophages induces decrease in intracellular potassium (K+) levels (Perregaux *et al*., 1994) and this K+ efflux is necessary for inflammasome activation (Bauernfeind *et al*., 2011).

On the other hand, stimulation of P_2RX_7 receptors by ATP also showed to increase intracellular reactive oxygen species (ROS) production and ROS generation was correlating with inflammasome activation (Cruz *et al*., 2007). Moreover, Caspase-1 cleavage in response to ROS production was PI3K and ERK1/2 activation-dependent (Martinon *et al*., 2010).

The third mechanism proposed to activate the Cryopyrin inflammasome is the lysosomal rupture. Crystals (MSU or silica) are taken into the cells by phagocytosis and phagosomes containing crystals fuse with late lysosomes to form phagolysosomes. Due to

the highly acidic environment of lysosomes, crystals release ammonium and increase cellular osmolarity. Lysosomes take up water, swell and are destabilized. Then leakage occurs and the lysosomal content is released into the cytoplasm (Hornung *et al*., 2008). The inflammasome complex has been shown to be activated as a result of these events.

These three mechanisms are not independent but can cooperate with each other to activate the Cryopyrin inflammasome. Still, the molecular signals that lead to Cryopyrin activation through these mechanisms have to be elucidated.

1.1.2.2. Auto-Inflammatory Diseases and Cryopyrin Inhibition. Familial cold auto-inflammatory syndrome, Muckle-Wells syndrome and neonatal-onset multi-system inflammatory disease are auto-inflammatory diseases characterized by increased IL-1β secretion. Mutations in the *Cryopyrin* gene have been identified in patients affected by these diseases (Dode *et al*., 2002; Aganna *et al*., 2002; Verma *et al*., 2008 and Yu *et al*., 2011) and functional studies showed that *Cryopyrin* mutations are constitutively activating the inflammasome complex even in the absence of any stimulation (Dowds *et al*., 2004). Similarly, in our recently published paper we showed that two novel *Cryopyrin* mutations (V200M and T195M) are linked to Behçet's Syndrome (Yüksel *et al*., 2014). Thus, Cryopyrin inflammasome inactivation is also an important process to avoid aberrant secretion of IL-1β and auto-inflammatory symptom manifestation.

Until recently, the main focus was on the Cryopyrin inflammasome activation and recent studies started to identify how the Cryopyrin inflammasome can be inactivated. Autophagy has been implicated in destruction of the activated Cryopyrin inflammasome (Shi *et al*., 2012). Stimulation of Cryopyrin inflammasome activity resulted in autophagy activation and inflammasome components co-localized with autophagosomes.

Another recent publication proposed that de-ubiquitination of the Cryopyrin protein on K63 and K48 by BRCC3 protein activates the inflammasome. G5 selectively inhibited Cryopyrin inflammasome by preventing its de-ubiquitination by BRCC3 (Py *et al*., 2013).

1.1.3. A New Player within the NLR family: NLRC3

Besides the pro-inflammatory NLR proteins described in the previous sections, a few NLRs such as NLRC5 and NLRX1 were found to inhibit the NFκB pathway (respectively Cui *et al*., 2010 and Xia *et al*., 2011). Upon stimulation, NLRX1 dissociates from TRAF6 and binds to IKK and the association of NLRX1 with IKK inhibits the NFκB pathway (Allen *et al*., 2011). NLRC5 and NLRX1 proteins are members of the NLR proteins containing an N-terminal CARD or CARD-like domain. NLRC3 is also in this group and its function is still uncharacterized.

NLRC3 (CATERPILLER 16.2) was first described as a NLR protein family member negatively regulating T-cell activation (Conti *et al*., 2005). The human *NLRC3* gene is located on chromosome 16p13.3 and is formed by 20 exons (NCBI NC_000016.9; ENSEMBL; Conti *et al*., 2005). The NLRC3 protein (NP_849172.2) contains a nucleotide binding domain (NBD) encoded by a large exon, 16 leucine-rich-repeats (LRR) encoded by 14 exons (Conti *et al*., 2005) and a CARD domain encoded by the first 60 amino-acids located in N-terminal part. The *NLRC3* gene gives rise to 4 protein coding, 5 processed and 1 polymorphic pseudogene transcripts (ENSEMBL).

NLRC3 was shown to be expressed in T-cell lines such as Jurkat and Raji by real-time PCR and in bone marrow, thymus, lymph nodes, B-cells, $CD4^+$ T-cells and $CD8^+$ T-cells mostly using human and mouse micro-array analyses (Conti *et al*., 2005). NLRC3 subcellular localization in HeLa cells was shown to be cytoplasmic (Conti *et al*., 2005).

Interestingly, activation of primary T-cells by anti-CD3 antibody or PMA and Ionomycin treatments resulted in decrease in NLRC3 mRNA levels whereas IL-2 and its receptor IL-2R expressions, which are markers of T-cell activation, were upregulated (Conti *et al*., 2005).

Luciferase reporter gene assays showed that overexpression of NLRC3 in combination with PMA or TNF treatment decreases NFκB, AP-1 pathways in HEK293T and Jurkat cells (Conti *et al*., 2005). Furthermore, IκB degradation (hallmark of NFκB activation) was delayed in NLRC3 overexpressing cells. Moreover, overexpression of

NLRC3 in activated Jurkat cells led to downregulation of IL-2 and CD25 mRNA levels (Conti *et al*., 2005) suggesting that NLRC3 has a negative effect on T-cell activation.

Four years after this first publication, the NLRC3 homolog in catfish was identified. cNLRC3 was expressed in kidney, intestine, spleen, T-cells, B-cells and macrophages. Bacterial infection of cNLRC3 expressing cells did not change cNLRC3 levels suggesting that cNLRC3 did not have a pro-inflammatory role after bacterial stimulation (Sha *et al*., 2009).

Based on these findings, we started to study NLRC3's functions in our laboratory in 2009. NLRC3 was cloned into different mammalian expression vectors and the inhibitory effect of NLRC3 on the NFκB pathway was shown by luciferase assays (Gültekin, 2011). NLRC3 also co-localized with ASC and Caspase-1 in cells overexpressing transiently these proteins.

Over the years, NLRC3 KO mice were generated and the inhibition of NFκB pathway by NLRC3 was confirmed by other groups (Schneider *et al*., 2012). NLRC3 was shown to target TRAF6 protein necessary to activate IKK to proteosomal degradation. Thus, IKK could not phosphorylate IκB and IκB was stabilized and retained p50/p65 in the cytoplasm.

In another study, a Nlrc3-like protein was found to be mutated in microglial cell-deficient zebrafish. Nlrc3-like protein has 25% identity with the human NLRC3. Macrophages from these mutants secreted more pro-inflammatory cytokines (IL-1β, TNFα, IL-8 and IL-12α) and the overall number of macrophages was decreased. Macrophages and dendritic cells aberrantly migrated into the brain in Nlrc3-like mutants; mimicking inflammatory conditions. The observed phenotype was rescued by injection of WT Nlrc3-like protein. Indeed, Nlrc3-like protein has been shown to interact with ASC adaptor protein via its Pyrin domain. Overall, Nlrc3-like protein was found to be an inhibitor of inflammation in the zebrafish brain (Shiau *et al*., 2013).

One year later, the anti-inflammatory role of NLRC3 was shown in mouse and human cells. NLRC3 inhibited STING dependent IFNβ, TNFα and IL-6 secretions in

response to cytoplasmic DNA stimulation. NLRC3 altered STING and TBK1 interaction by directly binding to TBK1 and STING. NLRC3 KO mice responded more efficiently to HSV-1 virus infection since IFNβ levels were higher in the sera of these mice compared to WT NLRC3 expressing mice (Zhang *et al*., 2014). Finally, expression analysis of NLRC3 mRNA revealed that NLRC3 is down-regulated in patients with colorectal cancer (Liu *et al*., 2015).

Taken all the published data together, NLRC3 appears to act as a negative regulator of both the NFκB pathway and inflammation. However, its role on Cryopyrin inflammasome formation and on its activity is not known yet.

1.2. NLRs and Cancer

1.2.1. Inflammation and Colorectal Cancer

Chronic inflammation is generally associated with increased tumorigenesis. For instance, infection of the stomach by *Helicobacter pylori* can cause gastric cancers (Polk *et al*., 2010). Similarly, inflammatory bowel diseases such as Crohn's Disease can lead to colorectal cancer (Gillen *et al*., 1994).

Inflammatory diseases of the intestine are modeled in the mouse by inducing colitis with dextran sulfate sodium (DSS) treatment (Yan *et al*., 2009). Acute DSS-induced colitis is characterized by weight loss, colon shortening and degeneration of the epithelial structure. Pathogenesis of DSS-induced colitis is characterized by increased pro-inflammatory cytokines such as IL-1β and IL-6. Caspase-1 was shown to be an essential player in the induction of colitis since DSS-treated Caspase-1 KO mice did not develop severe colitis (Siegmund *et al*., 2001). Furthermore, KO of Cryopyrin and ASC also had a protective role against DSS-induced colitis (Bauer *et al*., 2010). Thus, DSS-induced acute colitis was shown to be specifically mediated by the Cryopyrin inflammasome. On the

other hand, the induction of chronic inflammation in the intestine by combined AOM and DSS treatments can cause ulcerative colitis and evolve into colorectal cancer.

Besides Cryopyrin, other NLRs were shown to also have a protective effect on inflammation-induced tumorigenesis in the intestine. Knocking-out NLRP12 (Zaki *et al.,* 2011) or NLRP6 (Chen G. *et al.,* 2011) or NOD1 (Chen *et al*., 2008) led to more tumor formation in the colon in response to chronic inflammation. On the other hand, mutations of the NOD2 protein caused susceptibility to inflammation-induced cancer (Roberts *et al*., 2006).

Similarly, AIM2 protein expression was shown to protect against colorectal cancer (Man *et al*., 2015). AIM2 KO mice developed more inflammation-induced cancer compared to AIM2 expressing WT mice. Moreover, expression of AIM2 inhibited the organoid formation in the intestine (Man *et al*., 2015).

Recently, analysis of the microarray database of patients with colorectal cancer showed that anti-inflammatory NLRs such as NLRC3 and NLRX1 were down-regulated in human patients with colorectal cancer compared to healthy counterparts (Liu *et al*., 2015). However, the effect of NLRC3 on cell proliferation is still not known.

1.2.2. Structure of the Intestine and Wnt Pathway Implicated in Cancer

The intestine is a good model for stem cell and cancer studies. It is one of the most regenerative tissues of the body. The intestines contain stem cells that express the *Lgr5* gene at the bottom of their crypts and differentiate to give rise to Lysozyme^{+} Paneth cells and other cells necessary for functioning such as enterocytes, Goblet cells and enteroendocrine cells (Figure 1.4).

Stem cells, Paneth cells and transit amplifying cells can be isolated by using the Lgr5-EGFP-IRES-Cre^{ERT2} knock-in mouse model (Barker *et al*., 2007). In this model, EGFP is expressed under the control of Lgr5 promoter specific to stem cells. So, stem cells

have high GFP expression (GFP^{high}) and lose this GFP expression gradually when they divide and form transit amplifying cells (GFP^{low}). Olfm4 expression can also be used for stem cell identification. Paneth cells that are supportive immune cells of the intestine can be isolated by anti-c-kit antibody staining (Sato *et al*., 2011). The Paneth cells express high levels of Lysozyme necessary for defense against pathogens (Sato *et al*., 2011). Moreover, Paneth cells were shown to express high levels of NOD2 protein which is a cytoplasmic receptor that senses bacterial components. NOD2 mutations are associated with Crohn's diseases (Ogura *et al*., 2003).

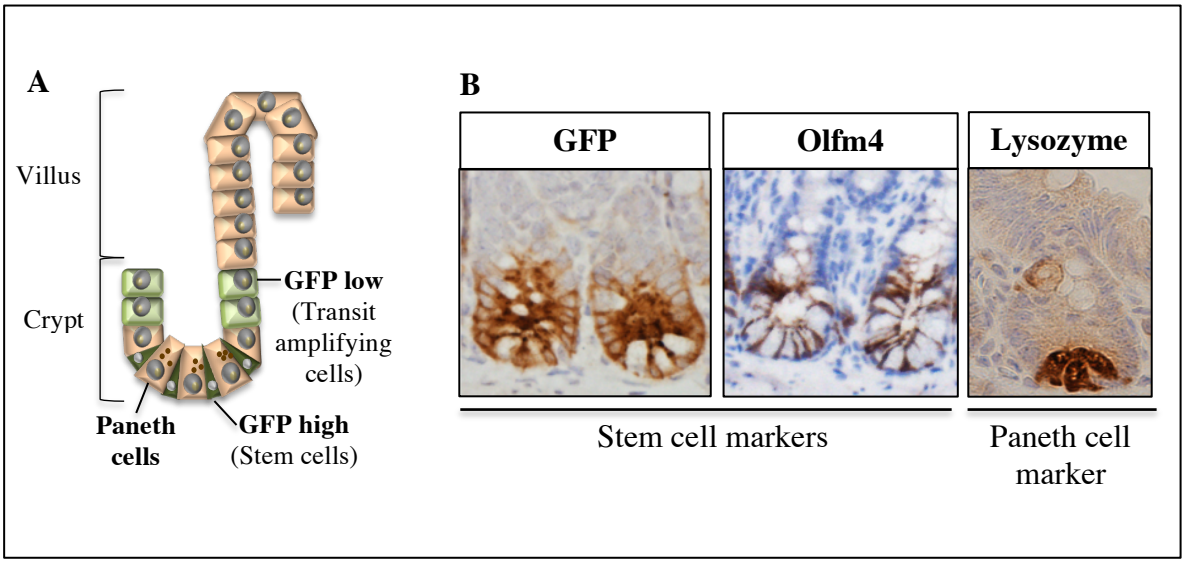

Figure 1.4. Structure of the intestine. (A) Representative cartoon of the intestinal crypt structure and the localization of stem cells and Paneth cells in Lgr5-EGFP knock-in mouse model. (B) Result of the immunohistochemistry staining of the stem cells and Paneth cells with specific markers.

It has been found that *in vitro* culture of isolated $Lgr5^{+}$ stem cells or intestinal crypts form mini-gut structures in three dimensions (Sato *et al*., 2009). These structures also called "organoids", reflect the capacity of the intestinal cells to proliferate and are a measurement of stemness (Sato and Clevers, 2013).

Colorectal cancers are associated with APC mutations (Gregorieff *et al*., 2005). APC is implicated in the regulation of the Wnt signaling pathway that is important for stem cell properties. In non-stimulated cells, APC binds to β-Catenin and other adaptors and induces

the degradation of β-Catenin. Upon stimulation of the Frizzled receptor, Axin2 is recruited to the receptor and dissociates the inhibitory complex formed by APC. Then, β-Catenin is released and can translocate to the nucleus to activate the expression of Wnt target genes (Clevers *et al*., 2006).

The accumulation of mutations aggravates the cancer phenotype. In general, initial mutations occur in the *APC* gene that leads to the rise of dysplastic crypts. Kras and p53 mutations can be acquired and give rise to carcinoma (Fearon *et al*., 1990).

Lineage tracing analysis demonstrated that $Lgr5^+$ stem cells that acquire deleterious mutations proliferate and give rise to adenocarcinoma (Schepers *et al*., 2012). These cells were named "cancer stem cells".

1.3. Immune Tolerance

1.3.1. Adaptive Immunity and T-Cell Development

Our body is protected from external attacks by anatomical and physiological barriers such as skin, mucous, tears, cilia and others. If a pathogen succeeds entering into our tissues despite these protections, then innate immune cells residing in our tissues get involved as described previously. Monocytes, macrophages and dendritic cells recognize pathogens and with the help of TLR and NLRs and inflammation are activated in order to recruit more immune cells to the site of infection (Murphy *et al*., 2007).

Dendritic cells and macrophages are also known as antigen presenting cells and as their name indicates, they circulate from the infection sites to central or peripheral immune sites to present antigens to T-cells and B-cells. $CD8^+$ T-cells recognize self-antigens

presented by MHC class I molecules whereas $CD4^+$ T-cells interact with MHC class II molecules presenting foreign antigens (Murphy *et al*., 2007).

During T-cell development, cells are clonally selected according to their affinity to self-antigen. The first selection called central selection occurs in the thymus. First of all, cells that interact very weakly with self-antigens or are not interacting at all are eliminated by apoptosis (phenomenon called death by neglect). Secondly, strong recognition of self-antigen leads also to elimination of T-cells (negative selection), thus preventing auto-immunity or are committed to form regulatory T-cell linage. Only cells that interact weakly with self-antigens are selected positively and can pursue their maturation in the periphery where selection is also occurring (Hogquist *el al*., 2005; Vallejo *et al*., 2004; Starr *et al*., 2003). As a result, adaptive immune system can differentiate between self and non-self and develop an immune reaction to eliminate non-self.

1.3.2. Immune Tolerance and Its Potential Mechanisms

However, non-self is not always harmful to organisms. For instance, in the case of pregnancy, the mother is carrying another organism expressing its mother's, its father's and its own antigens. To survive and reproduce, our immune system was educated to "tolerate" some non-self antigens. Medawar introduced for the first time the notion of acquired immune tolerance and obtained the Nobel Prize in 1960 for his works. Medawar co-worker Billigham showed that some parts of our body are immune privileged: the immune system access to these sites is either restricted or if it has access, the inflammatory response is dampened. The brain, eye, testis, pregnant uterus, and placenta have been defined as immune-privileged sites (Billigham *et al*., 1964).

Several physiological and molecular models have been proposed to be underlying immune tolerance. First of all, immunological ignorance was proposed to be the mechanism. The presence of anatomical barriers (between the mother and the fetus, the blood-brain barrier or blood-eye barrier) was thought to prevent host immune cells to pass into the organ and induce our immune response. However, it is now well known that many exchanges take place between the fetus and mother such as nutrients, gas, growth factors

and cells. Fetal DNA in the blood of the mother has been characterized 20 years after birth proving that exchanges in both directions occur (Bianchi *et al*., 2012).

Secondly, some antigens have been shown to be down-regulated in immune-privileged sites. For instance, fetal antigens have been found to be reduced in the placental part that is in contact with maternal cells. Trophoblastic cells do not express MHC class Ia molecules HLA-A and HLA-B. They only express MHC class Ia molecule HLA-C and MHC class Ib molecules HLA-E, HLA-F and HLA-G at low expression levels (Redman *et al*., 1984).

The third mechanism involved in immune tolerance is the modulation of the host's immune system. Especially T-cell populations have been shown to be markedly altered during pregnancy. $CD4^+$ and $CD8^+$ T-cell levels were found to be decreased (Carter *et al*., 1983; Tallon *et al*., 1984; Watanabe *et al*., 1997*)* suggesting an important role of T-cells during pregnancy. $CD4^+$ $CD25^+$ T-reg cells were enriched in peripheral blood, lymph nodes and spleen of the mother starting from early phases of pregnancy (Koch *et al*., 2007; Saito *et al*., 2007). A subset of these regulatory T-cells accumulated in the placenta (Saito *et al*., 2007). There is growing evidence of the critical role of different subtypes of T-cells in mediation of immune tolerance during pregnancy. However, the exact mechanism is still unknown.

The last mechanism important in immune tolerance was proposed to be site-specific immune suppression. Different types of molecules such as complement proteins, amino-acids, and hormones have been reported to have a site-specific inhibitory effect (Schjenken *et al*., 2012).

All these models are still under investigation and it is clear that maternal immune tolerance implies coordinated action of many players. Characterization of immune tolerance mechanisms will solve a fundamental immunological phenomenon and will be important to find out treatments to prevent spontaneous abortions and to increase the rate of organ transplantation acceptance.

1.3.4. NLR Proteins in Immune Tolerance Sites

One of the important immune privileged site is the pregnant uterus. Hydatidiform mole is characterized by the growth of the trophoblast which does not contain any embryo. This miscarriage results from the fertilization of an oocyte without any nucleus. NLRP7 mutations have been associated with hydatidiform moles (Murdoch *et al*., 2006). Similarly, some NLRP2 polymorphisms are associated with recurrent miscarriages (Huang *et al*., 2013). These findings point out the importance of NLR protein in pregnancy. However, the exact functions of these proteins and the mechanisms by which they induce miscarriage are not known.

1.3.5. Regulation of HLA Molecules' Expression by NLR Proteins

CIITA was the first NLR family member identified to regulate MHC molecules' expression. CIITA was identified as a transcriptional co-activator that binds to DNA and activates the expression of MHC class II molecules HLA-DR, HLA-DP and HLA-DQ as well as HLA-DM, HLA-DO and invariant chain in different cell types (Steimle *et al*., 1994).

On the opposite, the other family member NLRC5 was shown to specifically regulate MHC class I molecules' expression (Meissner *et al*., 2010). NLRC5 induced HLA-A, HLA-B, HLA-C, HLA-E, HLA-F, HLA-G and β_2M molecules expression in response to interferon stimulation (Meissner *et al*., 2010). NLRC5 translocated to the nucleus, bound to the promoter of MHC class I molecules and activated their expression (Meissner *et al*., 2012).

Besides their role in the modulation of the innate immune response through the regulation of inflammation, NLR family members also control the expression of MHC molecules that play an important role in the adaptive immune system.

2. PURPOSE

The first and primary aim of this PhD thesis is to elucidate the role of NLRC3 protein in the regulation of the Cryopyrin inflammasome. Toward this end, NLRC3's exogenous and endogenous effects on Cryopyrin-induced inflammation will be investigated. Endogenous interaction of NLRC3 with Cryopyrin inflammasome components will be determined and domains responsible for this interaction will be characterized. Furthermore, a correlation between NLRC3's *in vivo* expression and Cryopyrin-induced inflammation will be established. Since NLRC3 has been shown to be an inhibitor of the NFκB pathway and based on its domains' structure, we hypothesize that NLRC3 may inhibit Cryopyrin inflammasome activation.

Secondly, NLRC3's effect on stemness and cell proliferation will be determined. Nlrc3 KO primary tissues will be generated with CRISPR and proliferation of these cells will be measured. Since inflammasome forming proteins were shown to have a role in tumor formation, we hypothesized that NLRC3 may also have an effect on cell proliferation and/or stemness.

Finally, NLRC3's implication in immune tolerance mechanisms as an immune suppressor protein will be investigated. Expression of NRLC3 in different cell lines and tissues from immune tolerant sites will be determined. Potential regulation of MHC class molecules by NLRC3 will be tested. NLRC3 may induce tolerance by producing an anti-inflammatory environment through the inhibition of Cryopyrin inflammasome or by down-regulating MHC molecules expression.

3. MATERIALS

3.1. Cell Lines

Table 3.1. Cell lines used in this study.

Name of cell lines	Catalog number	Main source	Provider
HEK293FT	R700-07	Invitrogen, USA	Kind gift of Prof. Maria Soengas, Spanish National Cancer Research Center, Spain
THP-1	ATCC TIB-202	ATCC, USA	Kind gift of Prof. Ahmet Gül, Istanbul University, Turkey
HEK293FT-ASC-EGFP	-	From HEK293FT cells	Generated at AKIL laboratory
THP-1-ASC-EGFP	-	From THP-1 cells	Generated at AKIL laboratory
Swan 71	Generated by Prof. Gil G. Mor	ATCC, USA	Kind gift of Prof. Gil G. Mor, Yale University, USA
HEC-1-A	ATCC HTB-112 (Lot 58087755)	ATCC, USA	ATCC, USA
HEC-1-B	ATCC HTB-113 (Lot 3903111)	ATCC, USA	ATCC, USA
JAR	ATCC HTB-144 (Lot 5006454)	ATCC, USA	ATCC, USA
Tera-2	ATCC HTB-106 (Lot 4018167)	ATCC, USA	ATCC, USA

3.2. Chemicals, Plastic and Glassware

Chemicals used in this study were purchased from Sigma (USA) or Merck (Germany).

Plastics were from TPP (Switzerland) or Axygen (USA).

3.3. Buffers and Solutions

3.3.1. Cell Culture

Media used in cell culture (DMEM, RPMI 1640, McCoy's 5A, DEM/F12, FBS, Penicillin/Sterptomycin, NEAA, L-Glutamine, HEPES and DMSO) were from Gibco, Invitrogen, USA.

Table 3.2. Cell culture solutions used in this study.

10X PBS	1,37 M NaCl 27 mM KCl 81 mM Na_2HPO_4 15 mM KH_2PO_4 pH7,2-7,4
2X HBS	2,5 ml Hepes 0,73 g NaCl 0,01g Na_2HPO_4 for 50 ml, pH7
2M $CaCl_2$	11,098 g in 50 ml ddH2O
Freezing Medium	10% DMSO 90% FBS
0,05% Trypsin	0,53 mM EDTA 0,5 g/L Trypsin 8 g/L NaCl 0,4 g/L KCl 0,06 g/L KH_2PO4 1 g/L D-Glucose 0,048 g/L Na_2HPO4 0,35 g/L $NaHCO_3$, pH 7,5-8

3.3.2. PCR

Reagents used for PCR (Taq buffer, MgCl2, dNTP, Q5 Buffer, Q5 polymerase) were from Fermentas, Canada.

3.3.3. Agarose Gel Electrophoresis

Table 3.3. Solutions used in agarose gel eletrophoresis.

10X TAE	48,4 g Tris Base/L 11,4 ml Acetic acid/L 3,7 g EDTA/L
1% Agarose Gel	1 g Agar in 100 ml 1X TAE Buffer
Ethidium Bromide	Merck, Germany
Gene Ruler Mix	Fermentas, Canada
6X Loading Dye	Fermentas, Canada

3.3.4. Bacterial Growth and Transformation

Table 3.4. Solutions for bacterial growth and transformation.

LB Medium	Sigma, Germany
LB-Agar	Sigma, Germany
Ampicillin (100 mg/ml)	Applichem, Germany
Kanamycin (50 mg/ml)	Applichem, Germany

3.3.5. Western Blotting

Table 3.5. Solutions used in Western blotting.

NP-40 Lysis Buffer	150 mM NaCl 1% or 0,2% NP-40 50 mM Tris, pH8
25X Complete EDTA	1 tablet into 2 ml lysis buffer
30:0,8 Acrylamide: Bisacrylamide	30 g Acrylamide 0.8 g Bisacrylamide in 100 mL water
4% Stacking gel	66 ml 30:0,8 Acrylamide:bisacrylamide 126 ml 0,5 M Tris-HCl pH6,8 5 ml 10% SDS in 500 ml water
15% Resolving Gel	500 ml 30:0.8 Acrylamide: Bisacrylamide 10 ml 10% SDS 200 ml 1,875M Tris pH8.8 in 1L

Table 3.5. Solutions used in Western blotting (cont).

10% APS	Applichem, Germany
TEMED	Sigma, Germany
Running Buffer	0,9 g Tris-Base 4,32 g Glycin 0,1% SDS qsp 3 L water
10X Wet Transfer Buffer	144 g Glycin/L 30 g Tris Base/L
10X TBS	1,5 M NaCl 0,5 M Tris pH7,5
TBST	0,15 M NaCl 0,05 M Tris 0,001% Tween-20 pH7,5
10% w/v BSA	Bovine serum albumin fraction V (Roche, Germany) in TBST
Sodium azide	Roche, Germany
Protein Ladder	Fermentas, Canada
Substrate Reagent Pack	Roche, Germany
Sensitive Substrate	Roche, Germany
PVDF 0,45 µ	Roche, Germany
PVDF 0,2 µ	Roche, Germany
Nitrocellulose 0,2 µ	Roche, Germany
Methanol	Merck, USA
Stripping Buffer	62,5 mM TrisHCl pH6,8 2% SDS 0,7% beta-mercaptoethanol
5X Laemnli Buffer	1,5 M Tris-HCl, pH 6,8 10 ml Glycerol 5 ml beta-mercaptoethanol 2 g SDS 1 ml 1% bromophenol blue in 20 ml ddH_2O
80% TCA	Merck, USA

3.3.6. Immunoprecipitation

Table 3.6. Solutions and reagents used in immunoprecipitation.

Protein A/G Beads	Pierce, USA
0.2% NP-40 Buffer	150 mM NaCl 0.2% NP-40 50 mM Tris pH 8

3.3.7. Immunohistochemistry and immunocytochemistry

Table 3.7. Solutions used in immunohistochemistry and immunocytochemistry.

10% PFA	40 g PFA in 1L PBS warmed at 60°C, pH adjusted with 1M NaOH and 0,45µm filter sterilized
20% Sucrose	20 g Sucrose (Sigma, Germany) in 1X PBS
Permeabilization Buffer	0,1% Triton in PBS
Blocking Buffer	1% Glycin 0,1%BSA 0,1% Tween20 5% Donkey Serum
Wash Buffer	0,01% Tween20 in PBS
DAPI	0,02 µg/ml

3.3.8. Subcellular Fractionation

Table 3.8. Solutions used in subcellular fractionation.

Hypotonic Buffer	20 mM Tris-HCl pH7,4 10 mM NaCl 3 mM $MgCl_2$
Cell fractionation buffer	20 mM Tris-HCl pH7,4 10 mM NaCl 1% Triton X-100 1 mM EDTA 10% Glycerol 0,1% SDS

3.4. Kits

Table 3.9. Kits used in this study.

Human IL-1beta/IL-1F2	R&D Systems
High Pure PCR Product Purification	Roche, Germany
RNA isolation kit	Roche, Germany
RT-PCR kit	Promega, ImProm-II™ Reverse Transcription System
High Pure Plasmid Isolation	Roche, Germany
Genopure Plasmid Midi Kit	Roche, Germany
Genopure Plasmid Maxi Kit	Roche, Germany

3.5. Equipment

Table 3.10. Equipment used in this study.

Autoclaves	MAC 601, Eyala, Japan ASB260T, Astell, UK
Centrifuges	Allegra X22-R, Beckman, USA Himac CT4200C, Hitachi Koki, Japan J2-MC Centrifuge, Beckman, USA J2-21 Centrifuge, Beckman, USA
Freezers	2021D, Arçelik, Turkey 4250T, Arçelik, Turkey
Incubator	Hepa ClassII Forma Series, Thermo, USA
Heat Block	VWR, USA
Laminar Flow	Class II A, Tezsan, Turkey Class II B, Tezsan, Turkey
Magnetic Stirrer	Yellowline MSH Basics, USA
Microscopes	Zeiss, Axio Observer, Germany ZI Inverted Mic., Germany Leica, TCSSP5II, Germany Nikon, Eclipse TS100, Japan
Microwaves	Arçelik, Turkey
pH Meter	H221, Hanna Instruments, USA

Table 3.10. Equipment used in this study (cont).

Pipettes	Gilson, USA
Plate Reader	VersaMax, Molecular Devices, USA
Pipettors	Greiner Bio One, UK
Power Supplies	Power Pac Universal, BIO-RAD, USA
Shakers	Polymax 1040, USA Polymax 1010, USA Heildophl, Germany
Spectrophotometer	Nanodrop ND-100 Thermo, USA
Water Bath	GFL, Germany Memmert, Germany
Water Filter	UTES, Turkey
Western Blot Visualization	Stella Raytest, Germany
Western Blotting Electrophoresis System	MiniPROTEAN 4Cell, BIO-RAD, USA
Western Blotting Transfer System	BIO-RAD, USA

3.6. Fine Chemicals

3.6.1. Antibodies

All antibodies were prepared in 1% BSA at 1:1000 concentration for primary antibodies and 1:2000 for secondary antibodies for Western blot analysis. Concentrations are indicated in the text for immunoprecipitation and immunohistochemistry.

Table 3.11. List of antibodies used in this study.

	Type	**Company**	**Catalog number**	**Clonality**	**Species**
NLRC3	Primary	Abcam, UK	ab77817	Polyclonal	Rabbit
ASC	Primary	Kindly provided by Prof. Masumoto, Japan	-	Monoclonal	Mouse
ASC	Primary	Novus	NBP1-02966	Polyclonal	Mouse
Caspase-1 p10	Primary	Santa Cruz Biotechnology, USA	sc-515	Polyclonal	Rabbit

Table 3.11. List of antibodies used in this study (cont).

IL-1β	Primary	Cell Signaling, USA	12242	Monoclonal	Mouse
IL-1β	Primary	Cell Signaling, USA	12703	Monoclonal	Rabbit
Cryopyrin	Primary	Abcam, UK	17267	Monoclonal	Mouse
DYDDDK Tag	Primary	Cell Signaling, USA	2368	Polyclonal	Rabbit
Myc	Primary	Cell Signaling, USA	2272	Polyclonal	Rabbit
Ha	Primary	Cell Signaling, USA	3768	Monoclonal	Rabbit
β−Actin	Primary	Cell Signaling, USA	4967	Polyclonal	Rabbit
Lamina B	Primary	Santa Crutz	Sc6216	Polyclonal	Goat
RhoDGI alpha	Primary	Santa Crutz	Sc-360	Polyclonal	Rabbit
Mouse	Secondary	Cell Signaling, USA	7076	-	Horse
Rabbit	Secondary	Cell Signaling, USA	7074	-	Goat
Goat	Secondary	Santa Crutz	Sc-2020	-	Donkey
Alexa-Fluor 555	Secondary	Life Technologies	A-31572	-	Donkey
Alexa-Fluor 488	Secondary	Life Technologies	A-21202	-	Donkey

3.6.2. Enzymes

All enzymes used in this study were from NEB, England.

3.6.3. Drugs

Table 3.12. Drugs used in this study.

	Company
PMA	100 μg/ml stock in DMSO
Puromycin	Sigma, 50 mg/ml in water
Blasticidin	Sigma, 10 mg/ml stock in hepes buffer

Table 3.12. Drugs used in this study (cont).

10 mM Ionomycin	1 mg in 141 ul 100% DMSO
Nigericin	Sigma 20 mM stock in ethanol
ATP	200 mM stock in water
10 mM Chloroquine	0,005 g in 10 ml ddH2O
1000X Polybreen	4 mg/ml in water
Monosulfate Urate	Sigma, USA

3.6.4. Plasmids

Table 3.13. Plasmids used in this study.

Name	Source
pcDNA3-FLAG	Nunez Lab (UMICH, USA)
pcDNA3-MYC	Nunez Lab (UMICH, USA)
pcDNA3-HA	Nunez Lab (UMICH, USA)
pcDNA3-Empty	Nunez Lab (UMICH, USA)
pcDNA3-FLAG-Caspase-1	Nunez Lab (UMICH, USA)
pcDNA3-hASC	Nunez Lab (UMICH, USA)
pcDNA3-FLAG-Cryopyrin	Nunez Lab (UMICH, USA)
IL-1β-IRES-GFP	AKIL (BU, Turkey)
pcDNA3-MYC-NLRC3	AKIL (BU, Turkey)
pcDNA3-FLAG-NLRC3	AKIL (BU, Turkey)
pcDNA3-HA-NLRC3	AKIL (BU, Turkey)
pEGFP-C3-NLRC3	AKIL (BU, Turkey)
pEGFP-C3	Retina Lab (BU, Turkey)
pLKO-shNLRC3-D5	Broad Institute, the RNAi Consortium (clone ID: TRCN0000168436, kind gift of Yılmaz Lab, USA)
pLKO-shNLRC3-D6	Broad Institute, the RNAi Consortium (clone ID: TRCN0000168401, kind gift of Yılmaz Lab, USA)
pLKO-shNLRC3-D7	Broad Institute, the RNAi Consortium (clone ID: TRCN0000168383, kind gift of Yılmaz Lab, USA)
pLKO-shNLRC3-D8	Broad Institute, the RNAi Consortium (clone ID: TRCN0000168587, kind gift of Yılmaz Lab, USA)
pLKO-shNLRC3-D9	Broad Institute, the RNAi Consortium (clone ID: TRCN0000168194, kind gift of Yılmaz Lab, USA)

Table 3.13. Plasmids used in this study.

pLKO-shNLRC3-D8	Broad Institute, the RNAi Consortium (clone ID: TRCN0000168587, kind gift of Yılmaz Lab, USA)
pLKO-shNLRC3-D9	Broad Institute, the RNAi Consortium (clone ID: TRCN0000168194, kind gift of Yılmaz Lab, USA)
pLKO-shLuciferase	Tamer Önder's Lab (Koç University, Turkey)
pLenti-CMV	Tolga Emre's Lab (Bogazici University)
pCMVdeltaR8.74	Deisseroth Lab (Stanford University, USA)
pMD2.G	Deisseroth Lab (Stanford University, USA)

Table 3.14. Plasmids generated during this study.

Name
pcDNA3-MYC- NLRC3- CARD
pcDNA3-MYC- NLRC3- NACHT
pcDNA3-MYC- NLRC3- LRR
pcDNA3-MYC- NLRC3- CARD/NACHT
pcDNA3-MYC- NLRC3- NACHT/LRR
pET30a-His-NLRC3-CARD
pET30a-His-NLRC3-LRR
pLenti-CMV-NLRC3
U6-sgmNLRC3-Guide1-EFS-tRFP
U6-sgmNLRC3-Guide2-EFS-tRFP
U6-sgtdTomato- EFS-tRFP
pLKO.1-shNLRC3-D9-PGK-tRFP
pLKO.1-shNLRC3-D7-PGK-tRFP
pSECC- sgmNLRC3-Guide2
pSECC- sgmtdTomato
pUSCC-sgmApc
pLenti-CRISPR-tRFP
pLenti-CRISPR-tRFP-sgmNLRC3-Guide2
pLenti-CRISPR-tRFP-sgmApc
pLenti-CRISPR-tRFP-sgtdTomato

3.6.5. Primers and Oligonucleotides

Primers and oligonucleotides were synthesized by Macrogen, Korea. Primers were prepared as 250 or 100 μM stock solutions.

Table 3.15. Cloning primers used in this study. (RS: Restriction Site)

	Sequence (5' to 3')	**RS**
N3CARDF	AAAAAGATCTAGGAAGCAAGAGGTG	BglII
N3CARDR	TTTTCCATGGTCAGTCATTGCTGCAG	NcoI
N3NACHTF	AAAAGAATTCACTCAAGGATACAGAGGC	BglII
N3NACHTR	TTTTAAGCTTTCAGGTGTCCAGCCT	HindIII
N3LRRF	AAAAAGATCTAACCAGTTCCAGGACC	EcoRI
N3LRRR	TTTTAAGCTTTCACATTTCAACAGTGCA	HindIII
Nlrc3-f	TAAGTCTAGAAGGAAGCAAGAGGTGCGG	XbaI
N3CSTR	TATGCGGCCGCTCAGTCATTGCTGCA	NotI
N3NF	GCGGGCTAGCTCAAGGATACAGAGG	NheI
N3NSTR	TAATGCGGCCGCTCACTGGGCACAG	NotI
N3LF	ATGGTCTAGTGAGGCCAACCTGTCC	XbaI
N3LSTR	TTGCGGCCGCTCAATCACATTTCAACAG	NotI
N3CNF	GGGGTCTAGAAGGAAGCAAGAGGTGCGG	XbaI
MCNR	TAA GCG GCC GCT CAC TGG GCA CAG G	NotI
N3NLF	CTGGGCTAGCTCAAGGATACAGAGGCA	NheI
N3NLSTR	TCGGCGGCCGCTCAATCACATTTCAAC	Not-I
turboRFP-F	AATCACCGACCTCTCTCCCCAGGGGGATC CCCATGAGCGAGCTGATCAAGGAGAACA TG	BamHI
turboRFP-R	TGTAAGTCATTGGTCTTAAAGGTACCTTA TCTGTGCCCCAGTTTGCTAGGG	KpnI

Table 3.16. qPCR Primers used in this study.

mNLRC3F	CAGATTGGTAACAAAGGAGCCA
mNLRC3R	CGTTCGGTTTATCTTCAGAGCA
hNLRC3F	GTGCCGACCGACTCATCTG
hNLRC3R	GTCCTGCACTCATCCAAGC
mActinF	GGCTGTATTCCCCTCCATCG
mActinR	CCAGTTGGTAACAATGCCATGT
hActinF	CATGTACGTTGCTATCCAGGC

Table 3.16. qPCR Primers used in this study (cont).

hActinR	CTCCTTAATGTCACGCACGAT
CyclinD1F	GCGTACCCTGACACCAATCTC
CyclinD1R	CTCCTCTTCGCACTTCTGCTC
cMycF	ATGCCCCTCAACGTGAACTTC
cMycR	CGCAACATAGGATGGAGAGCA

Table 3.17. Sequencing primers used in this study.

T7a	AATACGACTCACTATAG
CMV-F	CGCAAATGGGCGGTAGGCGTG
SV40	TATTTATGCAGAGGCCGAGG
BGH-R	TAGAAGGCACAGTCGAGG
hU6	GACTATCATATGCTTACCGT
hPGK	GTAGTGTGGGCCCTGTTCCT
KON3G1F	GTGGAGGACAGGAAGAGCTG
KON3G1R2	CACAGCTCTGCTCCAGTGAG
KON3G2F2	AGAGCCAAAGTCCAAGTCCA
KON3G2R2	TAGGCCAGGCATGTCTCTCT
M13F (-21)	TGTAAAACGACGGCCAGT

Table 3.18. Guide RNAs used in this study.

sgNLRC3 Guide 1-Sense	CACCGTGGCGTGATCAGTGTGATAA
sgNLRC3 Guide 1-Antisense	AAACTTATCACACTGATCACGCCAC
sgNLRC3 Guide 2-Sense	CACCGGAGACAACATAGGTTCCCCA
sgNLRC3 Guide 2-Antisense	AAACTGGGGAACCTATGTTGTCTCC
sgmApc Sense	CACCGTCTGCCATCCCTTCACGTT
sgmApc Antisense	AAACAACGTGAAGGGATGGCAGAC
sgtdTomato Sense	CACCGGCCACGAGTTCGAGATCGA
sgtdTomato Antisense	AAACTCGATCTCGAACTCGTGGCC

4. METHODS

4.1. Cell Culture

Hec1A and **Hec1B** (purchased from ATCC) that are cells isolated from patient with stage IA endometrium cancer were maintained respectively in McCoy's 5A Medium supplemented with 10% Fetal Bovine Serum (FBS), 1 mM Non-Essential Amino Acid (NEAA), 1 mM L-Glutamine and 1 mM Penicillin/Streptomycin and MEM alpha medium containing 10% FBS, 1 mM NEAA, 1 mM L-Glutamine and 1 mM Penicillin/Streptomycin. **Swan71** cells (kind gift from Yale University) were immortalized first trimester trophoblastic cell lines and they were cultured into DMEM:F12 media supplemented with 1 mM sodium pyruvate, 10 mM HEPES, 10% FBS, 1 mM NEAA, 1 mM L-Glutamine and 1 mM Penicillin/Streptomycin. **JAR** cell lines (purchased from ATCC) were placental choriocarcinoma cells. **Tera-2** cell lines (purchased from ATCC) are testicular seminomas maintained in McCoy's medium supplemented with 15% FBS, 1 mM NEAA, 1 mM L-Glutamine and 1 mM Penicillin/Streptomycin. **MIO-M1** cell lines (kindly provided by Prof. Dr. Kuyaş Buğra) are human Müller cells grown in DMEM supplemented with 10% FBS, 1 mM NEAA, 1 mM L-Glutamine and 1 mM Penicillin/Streptomycin. **Jurkat** cell lines (kindly provided by İzmir Yüksek Teknoloji Enstitüsü) were immortalized T-lymphocytes isolated from 14-year-old boy with T cell leukemia. **THP-1** cells which are human monocytic cell lines were kindly provided by Prof. Dr. Ahmet Gül. JAR, Jurkat and THP-1 cells were maintained in RPMI 1640 containing 10% FBS, 1 mM NEAA, 1 mM L-Glutamine, 1 mM Penicillin/Streptomycin. **HEK293FT** (kindly provided by Prof. Dr. Maria Songeas) cells are from human embryonic kidney and are cultured in DMEM supplemented with 10% FBS, 1% NEAA, 1 mM L-Glutamine and 1 mM Penicillin/Streptomycin. All cells were grown at 37°C, 5% CO_2. All FBS used in these experiments were heat-inactivated at 60°C and filtered by 0,2µ filter. Cells were frozen in FBS with 10% DMSO and stored at -80°C or -150°C for longterm storage.

4.2. Virus Production, Cell infection and Selection

For 6 well-plate transfection, 2 μg plasmid encoding the shRNA or sgRNA and 750 ng of psPax2 and 250 ng of MD2G plasmids were prepared in a total volume of 219,5 μl water. 30,5 μl of 2 M $CaCl_2$ were added dropwise to the cells and incubated 5 minutes at room temperature. Then, 250 μl of 2X HBS buffer were added dropwise, incubated 5 minutes at room temperature and the mixtures was added to the cells. Media were changed into 20% FBS containing full media 16 hours after transfection. The next day, supernatants were passed through 0,45 μm filter, aliquoted and stored at -80°C or directly used for infection after addition of 4 μg/ml polybreen.

Target cells were put into 6 well-plate the day before infection and media was changed into Optimem containing 5% FBS before adding virus. Cells were changed into regular 10% FBS containing media until the next day and selection antibiotic was added 5 days after infection.

4.3. Activation of Cryopyrin and IPAF Inflammasomes

10^6 THP-1 cells were plated in 6 well-plate in 1 ml RPMI 1640 the day before treatment. THP-1 monocytes were differentiated into macrophages by adding 0,5 μM PMA to the cells for 3 hours at 37°C, 5% CO_2 and treated cells were left overnight to let them fully differentiate. The next day, macrophages were treated with 100 ng/ml LPS (from *E. coli* 0111:B4, Alexis Biochemicals, San Diego, CA-USA) for 2 hours for MSU and 3 hours for ATP and Nigericin treatments. Then, 150 μg/ml homemade MSU crystals; 5 mM ATP or 20 μM Nigericin were added and cells and supernatants were harvested at different time points.

To activate IPAF inflammasome, THP-1 monocytes were differentiated into macrophages with 0,5 μM PMA treatment as previously described, primed with 3 hours 100 ng/ml LPS and stimulated with 75 MOI living *Pseudomonas aeroginosa*. A pre-culture of *P. aeroginosa* was prepared the day before infection and 1/10 of this O/N culture was further grown at 37°C with shaking until OD reached 0,4-0,6. Cells were counted and prepared for infection into DMEM.

4.4. Total Protein Lysate Preparation

Cells were washed twice with ice-cold PBS, trypsinized and centrifuged at 2 000 rpm for 2 minutes. Cell pellets were dissolved into 500 µl lysis buffer A (20 mM HEPES pH 7,5, 50 mM KCl, 150 mM NaCl, 1 mM EDTA, 0,5% NP-40, 1 mM DTT, 1,5 mM $MgCl_2$) per 10^6 cells. Prior to use, 1 tablet of EDTA-free protease inhibitor cocktail (Roche) was added to 50 ml lysis buffer. Cells were lysed 15 minutes at 4°C or overnight at -20°C. After lysis, centrifugation at 4°C 13 000 rpm for 30 minutes was performed and supernatant was saved at -20°C for future experiments.

4.5. Determination of Protein Concentration

Pierce Thermo Scientific BCA (bicinchoninic acid) Assay Kit was used for protein quantification. 194 µl BCA Reagent A and 4 µl BCA Reagent B are prepared for each sample. 25 µl of lysates or standard were incubated with this mixture for 30 minutes at 37°C. BSA (Bovine Serum Albumine Fraction V, Roche) standards ranging from 25 pg/ml to 2500 pg/ml were prepared into appropriate lysis buffer. Absorbance was measured at 562 nm with Versamax Plate Reader. Protein concentrations were determined by SoftMax Pro v5 software.

Thermo Scientific Pierce Coomassie Plus Protein Assay kit was also used to determine protein concentrations. 5 µl of Bovine Serum Albumin (BSA) at different concentrations and protein samples were mixed with 300 µl Coomassie Blue (Pierce, #1856210) and protein concentration was measured with VERSAmax turable microplate reader (Molecular Devices) at 595 nm.

Measurements were repeated three times for each well and the average concentration for each sample was calculated.

4.6. Subcellular Fractionation

5 x 10^6 cells were washed with ice old PBS and collected in PBS by scraping. After centrifugation at 2000 rpm 2 minutes, the pellet was dissociated in 500 µl hypothonic buffer by pipetting up and down and incubated on ice for 15 minutes. 25 µl of 10% NP-40 was added and samples were vortexed 10 seconds. Nuclear and cytoplasmic fractions were separated by centrifugation at 3000 rpm for 10 minutes at 4°C. The cytoplasmic fraction (supernatant) was transfer to a new tube. The pellet was resuspended in 50 µl complete cell extraction buffer and incubated 30 minutes on ice. The sample was centrifuged 30 minutes at 14000 g at 4°C and the supernatant that is the nuclear fraction was saved for analysis.

4.7. Immunoprecipitation

50 µl of Protein A/G mixture (Thermo Scientific, #20422) were washed three times in 500 µl cold 0,1% NP-40 lysis buffer and cell lysates were pre-cleaned to eliminate proteins that bind non-specifically protein A/G by incubating them with washed protein A/G beads for 1 hour at 4°C. Beads and cell lysate mixture was centrifuged 1 minute at 4 °C and 13000 rpm and the supernatant (cleaned cell lysate) was kept at - 20°C until usage.

For immunoprecipitation, 50 µl of cleaned protein A/G were incubated for 3-4 hours with the appropriate concentration of antibody and cell lysates overnight at 4°C with shaking. The next day, samples were centrifuged 1 minute at 13 000 rpm and supernatants were kept as remaining fractions. The pellet was washed three times and dissolved in 30 µl 5X Laemnli Buffer.

4.8. Western blotting

Protein samples were boiled at 95°C for 10 minutes in 5X Laemnli Buffer and loaded on acrylamide. The gel was run 1h at 100V in running buffer. Wet transfer was performed at 100V 1h30. For this purpose, a sandwich was made with respectively two Watman papers (QuickDraw Blotting Paper, 0,2 µm pore size, Sigma) wet in transfer buffer, the

acrylamide gel, a PVDF membrane (Immobilon Transfer Membrane 0,2 µm pore size, Millipore) activated in methanol and two others Watman papers.

After the transfer, membrane was blocked with dry-milk powder (Blocking Grade Blocker Non-Fat Dry Milk, Biorad) or BSA (Roche, #10735094001) for 1 hour and incubated in primary antibody overnight. The next day, the membrane was washed three times for 5 minutes in TBST and incubated 1 hour at room temperature with the HRP-coupled secondary antibody. Finally, the membrane was washed three times for 10 minutes in TBST and visualized with Stella Raytest machine by using enhanced chemiluminescence system (Lumi-Light Western Blotting Substrate, Roche). If necessary, membranes were stripped in stripping solution for 30 minutes at 50°C and washed two times 10 minutes in PBS at room temperature.

Western blot results were quantified with ImageJ v.1.42q software. All measurements were repeated three times.

4.9. RNA Isolation

RNA was isolated from cells using Roche High Pure RNA Isolation kit. 10^6 cells were suspended in 200 µl PBS and lysed with 400 µl Lysis/Binding Buffer. Lysates were transferred to column and centrifuged 30 seconds at 8 000 g. Samples were treated with DNase I (10 µl DNase I in 90 µl DNase Incubation Buffer per sample) for 15 minutes at room temperature. Lysates were washed with 500 µl Wash Buffer I and 500 µl Wash Buffer II respectively with 30s centrifugation at 8 000 g between each wash. A final wash was done with 200 µl Wash Buffer II and centrifugation at 13 000 g for 2 minutes. Total RNAs were eluted with 50 µl Elution Buffer and centrifugation at 8 000 g for 2 minutes. Concentration and purity of RNAs were measured with Nanodrop.

4.10. RT-PCR

cDNA was synthesized from total RNA by using Promega ImProm-IITM Reverse Transcription System. 1 μg total RNA were incubated with OligodT primers 5 minutes at 72°C and then on ice for 5 minutes. Reaction mix containing 6,25 mM $MgCl_2$, 1X ImProm-II reaction buffer, 0,5 mM PCR nucleotide mix, rRNasin Ribonuclease inhibitor and ImPro-II reverse transcriptase was prepared and incubated at 42°C for 1 hour and reverse transcriptase was inactivated at 70°C during 15 minutes.

4.11. Primer Design and Cloning

Primer 3 software and NCBI Primer-Blast were used to design primers. Oligo-calc online tool was used to check self-complementary and hairpin formation. For qPCR, primers were chosen from the primers of MGH primer bank encompassing intron/exon junctions and blasted against the target genome. For plasmid cloning Vector NTI or Snapgene were used.

4.12. pLKO.1-tRFP Plasmid Generation

pLKO.1-shD7 and pLKO.1-shD9 were kindly provided by the Broad Institute, USA. Turbo RFP was amplified from pTRIPZ-tRFP by using turboRFP-F and turboRFP-R primers (see meaterials). Puromycin selection cassette of the original pLKO.1 vector was replaced by tRFP by Gibson cloning. Briefly, KpnI and BamHI-HF digested pLKO.1-shD7 and pLKO.1-shD9 were purified from gel and ligated with pure tRFP PCR product for 30 minutes at 50°C. 4 μl of the ligation reaction was transformed and cloning was verified by sequencing. Functionality of tRFP was determined by transfection of the plasmid to HEK293FS cells.

4.13. pLenti-CMV-NLRC3 Cloning

Full length NLRC3 was cloned into Addgene pLenti-CMV vector (kindly provided by Assoc. Prof. Tolga Emre) and newly obtained vector was named pLenti-CMV-NLRC3. Full length NLRC3 was extracted from pET30a-NLRC3 vector by BglII and XhoI digestion and was ligated 1 hour at 22°C (Fermentas T4 Ligase) in a 3:1 insert/vector molar ratio into pLenti-CMV vector digested with BamHI and XhoI enzymes. Bacteria were transformed with ligation mixture and plasmids were isolated from single colonies. Analytic digestion was performed with XbaI enzyme and positive colonies were sent to Macrogen for sequencing with universal CMV-F and SV40-F sequencing primers. The generated plasmid was named pLenti-CMV-NLRC3.

4.14. U6-sgRNA Plasmid Cloning

U6-filler-EFS-tRFP vector (kindly provided by Jacks lab) was digested with BsmBI at 55°C for 30 minutes and gel purified. sgRNA directed against mouse Nlrc3 were designed by using Benchling online software. sgNlrc3-Guide1 and sgNlrc3-Guide2 sense and antisense oligonucleotides were annealed by mixing 1 µl of each sense and antisense 100 µM stocks of the oligonucleotides with 1 µl of 10X T4 DNA ligase buffer, 0,5 µl of T4 PNK enzyme and water up to 10 µl. The reaction was first incubated at 37°C for 30 minutes, then at 95°C for 5 minutes and the temperature was ramped down to 25°C at 5°C /min. 1 µl of phospho-annealed oligonucleotides and 50 ng of BsmBI digested pure U6-tRFP fragment were ligated into T4 ligation buffer in a final volume of 20 µl for 2 hours at room temperature and transformed to bacteria.

4.15. Immunohistochemistry

Mouse brain was dissected and incubated 4 hours in 4% PFA pH 7,4 at 4°C for fixation. Then the tissue was washed three times for 10 minutes with PBS and incubated in 20% sucrose for cryopreservation until the tissue shrinks. Samples were embedded into OCT and incubated 5 minutes at -146°C. 10 µm sections of the brain were taken with cryostat onto positively charged slides. Slides were permeabilized for 5 minutes and

blocked for 1 hour at room temperature. Slides were then incubated with the primary antibody O/N at 4°C (1:100 anti-NLRC3 antibody or blocking buffer for the negative control). The next day, samples were washed three times for 10 minutes and incubated with the secondary antibody for an hour at room temperature (1:1000 anti-rabbit Alexa-Fluor antibody for NLRC3). DAPI staining was performed for 5 minutes with 0,02 μg/ml DAPI and washed three times for 10 minutes. Finally, stained sections were visualized under fluorescent microscope.

4. 16. Cellular staining

A sterile coverslip was placed into wells of 6 well-plates and the cells were seeded on top of these coverslips. Treatments were performed as usual and cells were washed with ice-cold PBS, fixed in PFA for 10 minutes and stained as described previously.

4.17. Speck Isolation

HEK293FT cells were transfected with 4 μg mCherry-ASC plasmid in 10 cm plate. Cells from four 10 cm plates were scraped in PBS 24 hours after transfection, sonicated 3 times 5 seconds 50% power and spined down at 2400 g for 5 minutes. Then samples were vortexed until filaments were formed and seen by eye. Tubes were left 5 minutes at room temperature and supernatant was transferred to a new tube, spined down at 200 g 1 hour. The pellet was dissolved in 30 ml PBS, passed through 5 μm filter, spined down at 2400 g 1 hour. The final pellet containing ASC specks was dissociated in 500 μl PBS. Purity of ASC specks was verified under microscope.

4.18. Competent Bacteria Preparation

Overnight culture of competent bacteria was grown 1:100 in LB until the OD_{600} reaches 0,4-0,6. Then bacterial culture was centrifuged at 3000 rpm at 4°C for 10 minutes and the pellet was re-suspended in 50 mM ice-cold $CaCl_2$ and aliquots were stored at -80°C.

4.19. Bacterial Transformation

For re-transformation, 10 ng of plasmid were incubated 5 minutes on ice with competent *E. coli* TOP10 bacteria or Stable3 if it is a lentiviral plasmid. Heat shock was performed by incubating samples at 42°C for 40 seconds and then on ice for 5 minutes. Resulting transformed bacteria were grown in 400 µl LB for 1 hour at 37°C (30°C for lentiviral plasmids) with shaking and spread on appropriate antibiotic containing LB plates.

4.20. Plasmid Amplification

Mini-, midi- and maxipreparations were performed by using Roche kits as indicated by the manufacturer. Bacterial cultures were grown into 10 ml LB for mini, 200 ml LB for midi and 1L of LB for maxipreparations.

4.21. ELISA

R&D DuoSet ELISA Development kit was used. 4 µg/ml mouse anti-human IL-1β capture antibody was coated on 96 well-plate overnight at room temperature. The next day, coated wells were washed three times with 400 µl Wash Solution (0,05% Tween 20 in PBS, pH7,2) and the liquid was removed completely after the last wash. Then, blocking was performed with 300 µl Reagent Diluent (1% BSA in PBS pH 7,2-7,4) 1 hour at room temperature. After washing three times with 400 µl Wash Solution as described previously, wells were completely dried and 100 µl of IL-1β standards in Reagent Diluent or 100 µl of samples were added to the each well and incubated 2 hours at room temperature. The wells were washed to remove the excess of protein and were incubated with 100 µl of Streptavidin-HRP at room temperature for 20 minutes. A last wash was performed and 100 µl of Substrate Solution (1:1 Color Reagent A (H_2O_2): Color Reagent B (Tetramethylbenzidine)) was added to the wells and was incubated 20 minutes at room temperature on dark. Finally, 50 µl of Stop Solution (2M H_2SO_4) was used to stop the reaction and optical density is measured at 450 and 570 nm with Versamax machine.

4.22. IL-1β Precipitation and Endogenous IL-1β Western Blotting

Proteins in the serum-free cell-free supernatant were precipitated by addition of 1% TCA and incubation 30 minutes on ice. After 10 minutes centrifugation at 15 000 g 10 minutes, equal volume of 80% acetone was added to the pellet and dissolved by vortexing. The sample was spined down at 15 000 g for 10 minutes and the pellet was dried for 30 minutes at room temperature and resuspended in 5X Laemnli buffer.

4.23. ASC Speck Assay

HEK293FT-ASC-EGFP cells were grown in 6 well-plate and transfected with different amounts of Cryopyrin, NLRC3, NLRC3's domain or empty vector. Each condition was transfected in two different wells. The next day, ASC specks were counted under fluorescent microscope in eight different fields that were randomly chosen for each well.

4.24. Crypt Isolation and Culture

C57BL6, C57BL6-Villin-Cre^{ERT2};Lox-STOP-Lox-Cas9-EGFP mice were used. C57BL6- Villin-Cre^{ERT2}-Cas9-EGFP mice were injected with 2 doses of tamoxifen prior to isolation. Mice were sacrificed by cervical dislocation and small intestine and colon were isolated, flushed with ice-cold PBS, linearized and incubated into PBS-EDTA for 30 minutes at room temperature. Colon crypts were scraped whereas crypts from the small intestine were isolated by shaking. Crypt cultures were set into 100 µl matrigel in 24 well-plate and crypts were grown at 37°C and 5% CO_2 into homemade WRN media plus Y-factor (1:1000) to obtain cystic organoids. Tamoxifen (5 nM) was added to the culture of crypts from Villin-CreERT2-Cas9-EGFP mice.

4.25. Organoid Infection

Organoids in 24 well-plate were broken down by pipetting and spined down at 300 g 5 minutes to discard the matrigel. Organoids were trypsinized with TriplE express 5 minutes at 32°C to get single cells. Trypsin was stopped by S-MEM. Single cells were mixed with virus and spinoculated 1 hour at 750 g 32°C in a 24 well-plate. After spinoculation, the plate was incubated 6 hours in the incubator and cells were collected, spined down to discard the virus and plated with matrigel.

4.26. Surveyor Assay

Thermo Fischer Scientific TOPO TA-Cloning kit was used. Region encompassing guides were amplified by PCR, purified from gel and overhang 3'-A were added by incubation of the PCR product with Taq polymerase, dATP for 15 minutes at 72°C. 4 µl of PCR product was ligated into 1 µl pCR2.1 TOPO vector (10 ng) in presence of 1 µl salt (1,2M NaCl and 0.06M $MgCl_2$) into a final volume of 6 µl at room temperature for 15 minutes. 40 µl of competent DH5a bacteria were transformed with 2 µl TOPO reaction. Plasmids were isolated from resulting colonies and sent to sequencing with the sequencing primer M13F (-21).

5. RESULTS

5.1. NLRC3's Role in Cryopyrin Inflammasome Regulation

5.1.1. NLRC3 Protein is Expressed in Human Cell Lines

Experiments published so far were based on mRNA levels of NLRC3 or detection of tagged NLRC3 proteins. To visualize endogenous expression of NLRC3 and work in a more physiological setting, we optimized Western blotting for the commercially available NLRC3 antibody (Abcam ab77817, polyclonal anti-rabbit antibody, see procedures part for details). THP-1 human monocytic cell lines and HEK293FT human embryonic kidney cells were tested for NLRC3 expression (Figure 5.1). Because NLRC3 was shown to be expressed in T-cells, Jurkat human T-cell lines were used as positive control of NLRC3 expression.

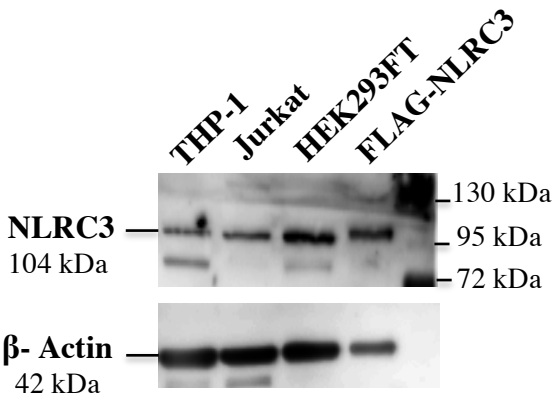

Figure 5.1. NLRC3 protein is expressed in human cell lines. 60 μg protein were loaded on a 10% gel and transferred to 0.45 μm PVDF membrane. NLRC3 antibody was used overnight at 1:1000 concentration in 5% BSA.

Depending on the batch of antibody used and the cell lysate tested, NLRC3 antibody detected several bands. To determine the band corresponding to NLRC3 protein, Myc-, Flag- or Ha- tagged NLRC3 proteins expressed in HEK293FT cells were used as control (Figure 5.1). NLRC3 protein was localized just above the 100 kDa band of the protein ladder as suggested by the predicted 104 kDa weight by the antibody producer. Myc-,

Flag- and HA- tags that are about 1 kDa more than NLRC3 were slightly higher as expected.

The specificity of the NLRC3 band was further confirmed in knock-down cells where this band disappeared or had a lower intensity in KD lines compared to the control (Figure 5.4b). In summary, NLRC3 protein was shown to be expressed in human HEK293FT, THP-1 and Jurkat cells.

5.1.2. NLRC3 Inhibits Cryopyrin Inflammasome in Overexpression System

In our recently published paper, we showed that when overexpressed together with Cryopyrin, NLRC3 decreases IL-1β cleavage in HEK293FT (Gültekin *et al*., 2014). As a result of the maturation by cleavage, IL-1β gets secreted from the cell and can be detected in the supernatant by ELISA. In order to confirm this previous Western blotting result, we transfected HEK293FT cells with Cryopyrin, NLRC3 or Cryopyrin and NLRC3 together with other Cryopyrin inflammasome components: ASC, Caspase-1 and IL-1β and measured the amount of secreted IL-1β by ELISA (Figure 5.2).

As expected, Cryopyrin transfection induced IL-1β secretion in cell-free supernatants in a dose-dependent manner (496,3 ± 42,7 pg/ml IL-1β for 250 ng Cryopyrin vs 2903,7 ± 229,8 pg/ml IL-1β for 1000 ng Cryopyrin, $p=10^{-5}$) compared to ASC, Caspase-1 and IL-1β transfected sample (10 ± pg/ml IL-1β).

Absence of IL-1β secretion in cells only transfected with ASC, Caspase-1 and IL-1β showed us that the endogenous Cryopyrin level in HEK293FT cells is not enough to induce inflammasome formation and that the IL-1β release observed in our experimental setting is Cryopyrin-dependent. Moreover, the priming step required for inflammasome activation was by-passed by overexpression of the components. Transfection of Cryopyrin assembled ASC and Caspase-1 proteins, induced IL-1β cleavage and its release from the cell. Thus, this system is suitable for testing of Cryopyrin inflammasome activation.

In order to determine NLRC3's impact on Cryopyrin-induced inflammasome activation, NLRC3 was co-transfected with Cryopyrin, ASC, Caspase-1 and IL-1β. Interestingly, when co-transfected with NLRC3, Cryopyrin-induced IL-1β secretion was significantly reduced and this decrease was depending on NLRC3 concentration (Figure 5.2b, 2903,7 ± 229,8 pg/ml IL-1β for 1000 ng NLRC3 compared to 1949,328 ± 171,998 pg/ml IL-1β for 500 ng NLRC3, p=0,0018 and 1403,537 ± 48,14 pg/ml for 1000 ng NLRC3, $p=10^{-5}$).

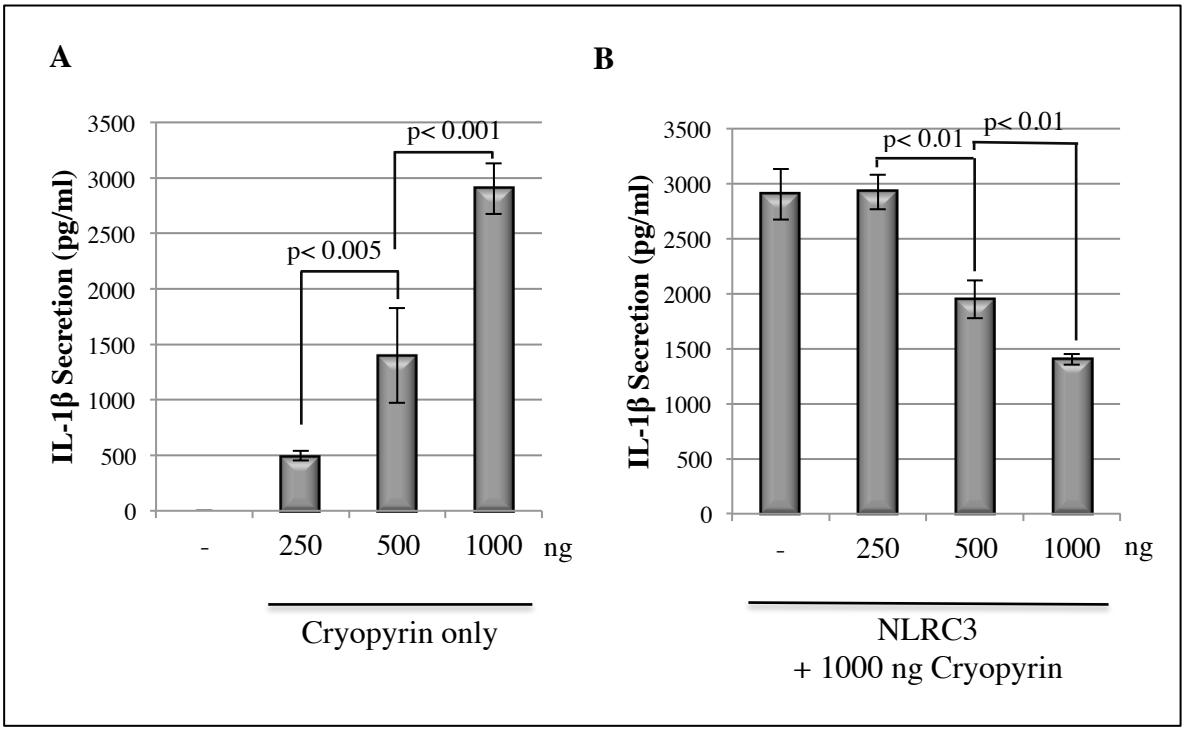

Figure 5.2. NLRC3 inhibits Cryopyrin-induced IL-1β secretion. In all conditions, 500 ng pro-IL-1β, 250 ng ASC and 250 ng pro-Caspase-1 plasmids were transfected. IL-1β was quantified 24h after transfection in cell supernatants by ELISA. (A) Cryopyrin transfection. (B) Co-transfection of 1000 ng Cryopyrin and indicated amount of NLRC3. The amount of transfected plasmid is shown in ng/ml. Equal amount of DNA was transfected for each condition by using empty vector. Each condition was duplicated.

Taken together, these data suggest that NLRC3 has an inhibitory effect on Cryopyrin inflammasome activation. Because all the components are overexpressed, this inhibition is not exerted at the transcriptional level through NFκB inhibition as previously described

(Conti *et al*., 2005) or other uncharacterized transcriptional mechanisms. NLRC3 may modulate Cryopyrin inflammasome at the post-translational level by triggering protein degradation (as shown for TRAF6, Schneider *et al*., 2012) or by interfering with the assembly of the complex.

5.1.3. Establishment of Cryopyrin Inflammasome Activation Protocol

Overexpression based studies showed an inhibitory effect of NLRC3 on the Cryopyrin inflammasome and that this inhibition is post-transcriptional. In order to confirm the endogenous effect of NLRC3 on the Cryopyrin inflammasome, inflammasome activation protocol was established in WT THP-1 cells (Figure 5.3). THP-1 human monocytic cell lines were differentiated into macrophages by using PMA, primed with LPS and treated with different known Cryopyrin inflammasome activators. IL-1β concentrations were measured in the cell supernatants as a read-out of Cryopyrin inflammasome activation.

Treatment of WT THP-1 cells with 5 mM ATP increased IL-1β secretion significantly in a time dependent manner (Figure 5.3a). Whereas 1 hour ATP treatment did not change IL-1β secretion (100,78 ± 22,2 pg/ml for 1 hour compared to 157,96 ± 61,03 pg/ml for the control sample harvested 4 hours after the treatment), IL-1β secretion started to increase significantly 2 hours after ATP stimulation and reached a maximum at 4 hours (1468,22 ± 48,22 pg/ml for 2 hours vs 2489,72 ± 78,86 pg/ml for 4 hours, p=0,004). Thus, the cells were primed with 100 ng/ml LPS for 4 hours and treated with 5 mM ATP for 4 hours to activate the Cryopyrin inflammasome in the upcoming experiments.

Similarly, Nigericin treatment of THP-1 cells increased IL-1β secretion in a time dependent way (Figure 5.3b). IL-1β secretion started to increase significantly 15 minutes after stimulation (Control: 455,07± 16,74 pg/ml, 15': 724,43 ± 67,89 pg/ml, p=0,03) and the highest secretion was observed 1 hour after stimulation (30': 6472,07 ± 224,76 pg/ml vs 1h: 9361,355 ± 76,01 pg/ml, p=0,003). Thus, cells were primed with 100 ng/ml LPS for 4 hours and treated with 20 μM Nigericin for 1 hour to activate the Cryopyrin inflammasome for upcoming experiments.

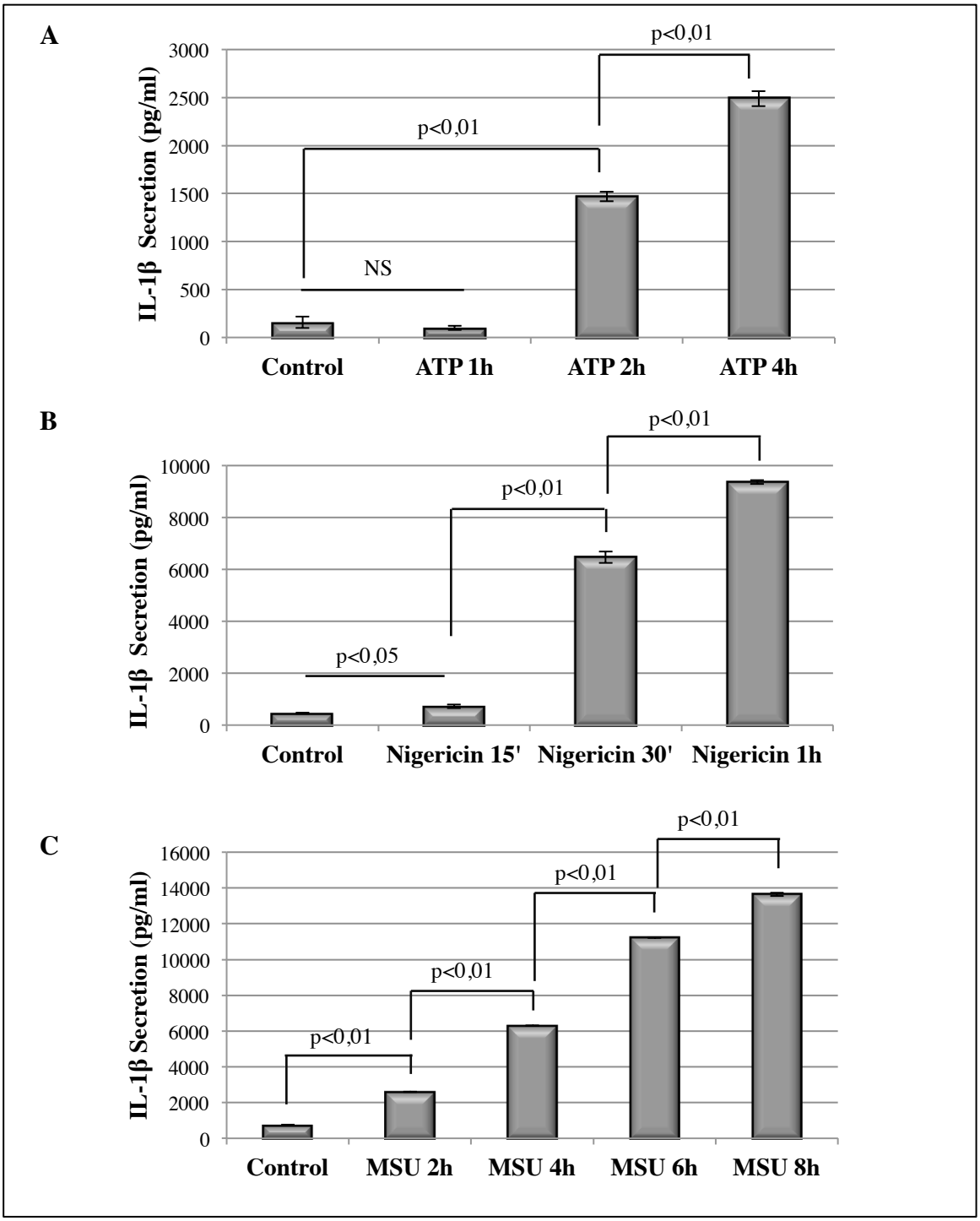

Figure 5.3. Cryopyrin inflammasome activation in WT THP-1 cells. IL-1β secretion was measured in cell supernatants by ELISA in cells (A) primed with 100 ng/ml LPS for 4 hours and treated with 5 mM ATP, (B) primed with 100 ng/ml LPS for 4 hours and treated with 20 μM Nigericin and (C) primed with 100 ng/ml LPS for 2 hours and treated with 150 μg/ml MSU. Cell supernatants were harvested at the indicated time points.

Finally, the Cryopyrin inflammasome activation in response to MSU treatment was optimized (Figure 5.3c). IL-1β secretion significantly increased until 8 hours in response to MSU stimulation (Control: 732,147 ± 224,76 pg/ml, 2h: 2600,539 ± 9,25 pg/ml, 4h: 6302,398 ± 1,13 pg/ml, 6h: 11214,348 ± 1,27 pg/ml and 8h: 13640,726 ± 96,2 pg/ml, $p<0,001$). Thus, cells were primed with 100 ng/ml LPS for 2 hours and treated with 150 μg/ml MSU for 8 hours to activate the Cryopyrin inflammasome.

5.1.4. NLRC3 Is Stably Knocked-Down in HEK293FT and THP-1 Cells

To test the endogenous effect of NLRC3 on the Cryopyrin inflammasome, four available shRNAs against human NLRC3, namely shD6, shD7, shD8 and shD9, were obtained from the Broad Institute (MIT, USA). Whereas shD6 targets exon 5 encoding for the central NACHT domain, shD7, shD8 and shD9 target exons coding for the C-terminal LRR domain (Figure 5.4a). Blast of shRNA's target sequences to the whole human genome and transcripts or to the sequences of other NLR proteins did not give any significant match suggesting that these RNAs specifically recognize NLRC3 mRNA.

First of all, efficacy of these shRNAs was tested in HEK293FT cells. These cells were transduced with viruses containing shRNA directed to luciferase (shLuc) as control or shRNAs directed against NLRC3 and NLRC3 protein expression was verified by Western blotting 1 week after transduction (Figure 5.4b). NLRC3 protein was absent in all transduced HEK293FT cells compared to the shLuc transduced cells (Figure 5.4b). Once we determined that shRNAs against NLRC3 are effective, stable NLRC3 KD THP-1 cells were generated. NLRC3 expression was verified in puromycin selected stable THP-1 cells by Western blotting (Figure 5.4c). NLRC3 protein levels were reduced by 34% for shD6 and 74% for shD9 THP-1 cells compared to the NLRC3 level in control THP-1 shLuc cell lines (Figure 5.4d). Thus, stable THP-1 shD9 cells were chosen for further analysis and will be referred as shNLRC3 in the following sections.

On the other hand, these shRNAs proved that the 100 kDa band predicted to be NLRC3 was indeed NLRC3 since shRNAs did not affect levels of non-specific higher molecular weight bands but decreased significantly only the 100 kDa bands (Figure 5.4b).

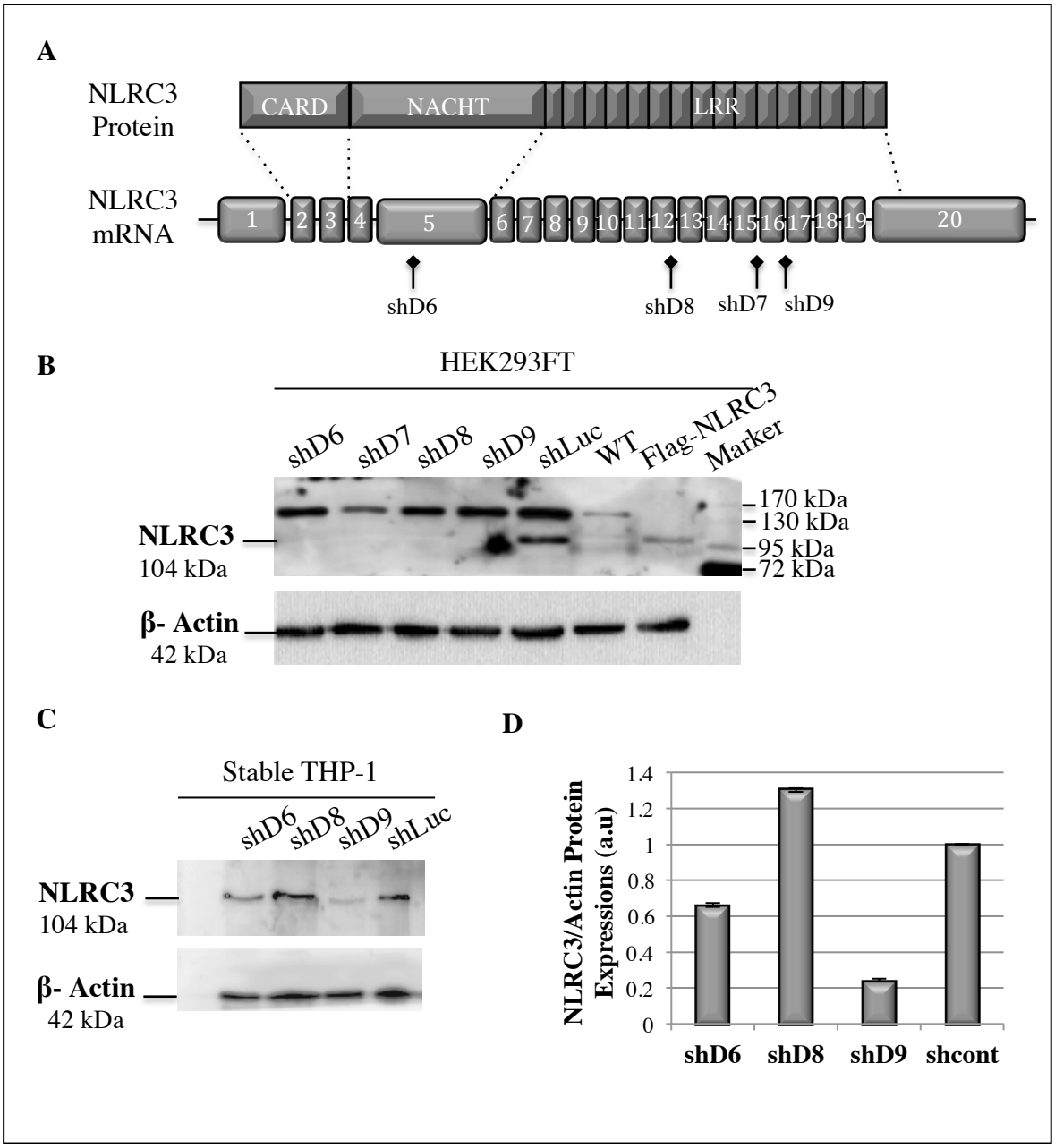

Figure 5.4. NLRC3 is stably knocked-down in HEK293FT and THP-1 cells. (A) Schematic representation of target sites of different shRNAs against NLRC3. Exons are shown as gray boxes. (B) NLRC3 expression in HEK293FT cells 1 week after transduction with indicated shRNA containing viruses. (C) NLRC3 protein levels in stable THP-1 NLRC3 KD cell lines. (D) NLRC3 and Actin ratios were calculated from Western bands with Image J and the ration for shLuc was assigned as 1 arbitrary unit and the other ratios were normalized to shLuc.

5.1.5. NLRC3 KD Results in Higher Levels of IL-1β Secretion

In order to confirm the results obtained using the overexpression systems, the effect of endogenous NLRC3 protein on Cryopyrin inflammasome regulation was investigated in THP-1 stable lines knocked down for NLRC3 (Figure 5.5). Towards this end, shNLRC3 and shLuc stable THP-1 cells were differentiated into macrophages and stimulated by Nigericin, ATP or MSU that are known activators of Cryopyrin inflammasome.

Cryopyrin inflammasome activation by MSU treatment resulted in significantly higher IL-1β secretion in shNLRC3 cells compared to the control. IL-1β levels in the supernatants negatively correlated with NLRC3 expression: it was higher in shD9, shD6 compared to shD8 that was similar to the control (not shown). Selected shD9 THP-1 stable lines were tested with other Cryopyrin stimulants. Cells were not single cloned and were used as a mixed population of different colonies because we did not want to select by chance a clone that has a random insertion of shRNAs into a functional part of the genome that could affect Cryopyrin activity and give us false negative or positive results.

In all the treatments tested, NLRC3 KD resulted in higher IL-1β secretion, thus, higher Cryopyrin inflammasome activation (Figure 5.5). Whereas the concentration of IL-1β in the supernatant of Nigericin treated shLuc cells was 3760,13 ± 182,39 pg/ml, shNLRC3 cells released 14253,37 ± 2239,9 pg/ml IL-1β in response to the same treatment (Figure 5.5A**,** $p<0,05$). Similarly, shNLRC3 cell lines secreted significantly higher IL-1β compared to control shLuc cells in response to ATP (Figure 5.5b, 1746 ± 71 pg/ml for shLuc vs 6376 ± 1473 pg/ml for shNLRC3, $p<0,001$) and MSU stimulations (Figure 5.5c, 7312,36 ± 230,1 pg/ml for shLuc vs 24971,5 ± 1801,37 pg/ml for shNLRC3, $p<0,001$).

In conclusion, endogenous NLRC3 downregulation results correlated with overexpression data: NLRC3 inhibited IL-1β secretion induced by Cryopyrin inflammasome activation in response to Nigericin, ATP and MSU treatments in THP-1 cells. Thus, NLRC3 is a novel inhibitor of the Cryopyrin inflammasome under endogenous expression conditions.

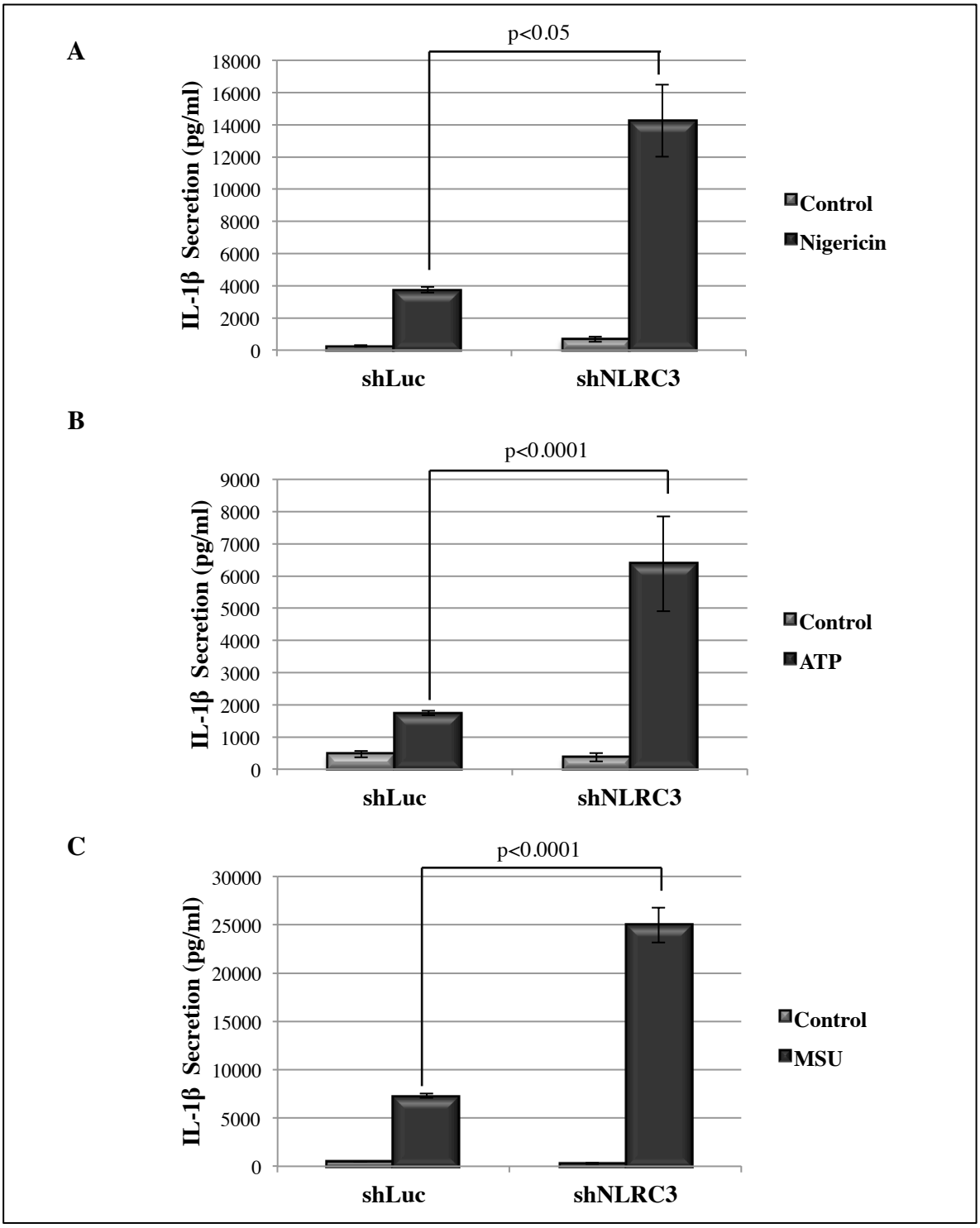

Figure 5.5. Endogenous NLRC3 inhibits the Cryopyrin inflammasome. IL-1β secretion in response to: (A) Nigericin stimulation. Representative result of three independent sets of experiments. (B) ATP stimulation. Combined results of two independent sets of experiments. (C) MSU stimulation. Representative result of four independent sets of experiments.

5.1.6. NLRC3 Inhibits pro-IL-1β Maturation

Since Cryopyrin inflammasome activation results in pro-IL1β cleavage in the cell and secretion of the cleaved IL1β, mature IL-1β levels were measured in the cell and the supernatant of shLuc and shNLRC3 cells stimulated by Nigericin (Figure 5.6).

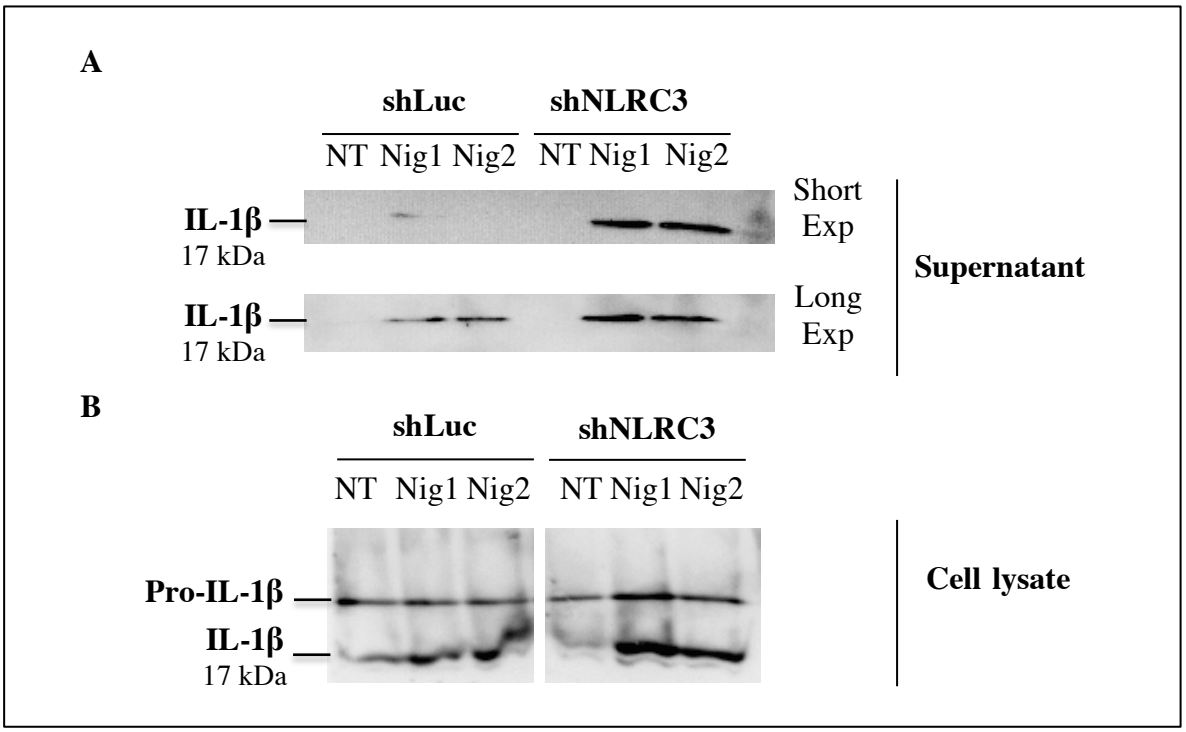

Figure 5.6. NLRC3 inhibits IL-1β maturation. IL-1β maturation in response to Nigericin treatment in shLuc and shNLRC3 THP-1 cells was assessed by Western blotting. (A) Cleaved IL-1β in the cell-free supernatant precipitated by TCA. (B) Cleaved IL-1β and pro-IL-1β in cell lysates. NT: control cells non-treated by Nigericin. Two independent samples were treated by Nigericin (Nig1 and Nig2).

Whereas pro-IL-1β levels were more or less similar in the cell lysates (Figure 5.6b), pro-IL-1β got processed more in shNLRC3 cells compared to control shLuc cells in response to Nigericin stimulation both in the cell lysate (Figure 5.6a) and in the supernatant (Figure 5.6a). In correlation with the previous ELISA results showing IL-1β secretion (Figure 5.6), NLRC3 inhibited pro-IL-1β cleavage and reduced mature IL-1β levels in the cell and the supernatant.

5.1.7. NLRC3 Is Also an Inhibitor of the IPAF Inflammasome

Different types of inflammasomes have been described so far. While they differ from each other in their receptor protein, the downstream effectors ASC, Caspase-1 and IL-1β are common. Since NLRC3 has an inhibitory role on the Cryopyrin inflammasome, we wanted to determine whether this effect is specific to Cryopyrin or whether NLRC3 can also modulate other inflammasomes.

Pseudomonas aeroginosa is a Gram-negative bacterium, which has been previously shown to activate specifically the IPAF inflammasome in Bone Marrow Derived Macrophages (BMDM) through the type III secretion system (Sutterwala *et al*., 2007). *P. aeroginosa* induction of IL-1β secretion was independent of Cryopyrin as Cryopyrin KO cells still secreted IL-1β upon *P. aeroginosa* stimulation (Sutterwala *et al*., 2007).

First of all, the IPAF inflammasome activation protocol was established in PMA-differentiated and LPS-primed THP-1 cells by stimulation with live *Pseudomonas aeroginosa* bacteria (Figure 5.7a). 75 MOI was enough to significantly activate IL-1β secretion (Control: 460,155 ± 20,58 pg/ml compared to 4084,63 ± 282,27 pg/ml for 75 MOI and 4492,28 ± 95,06 pg/ml for 100 MOI, $p<0,001$).

Then, shLuc and shNLRC3 stable lines were stimulated with 75 MOI live *P. aeroginosa* in order to activate the IPAF inflammasome. Similarly, *P. aeroginosa* induced higher IL-1β secretion in shNLRC3 cells compared to the control cell lines (Figure 5.7b, 9493,92 ± 1256,744 pg/ml for shNLRC3 compared to 3099,963 ± 1392,53 pg/ml for shLuc, $p<0,05$).

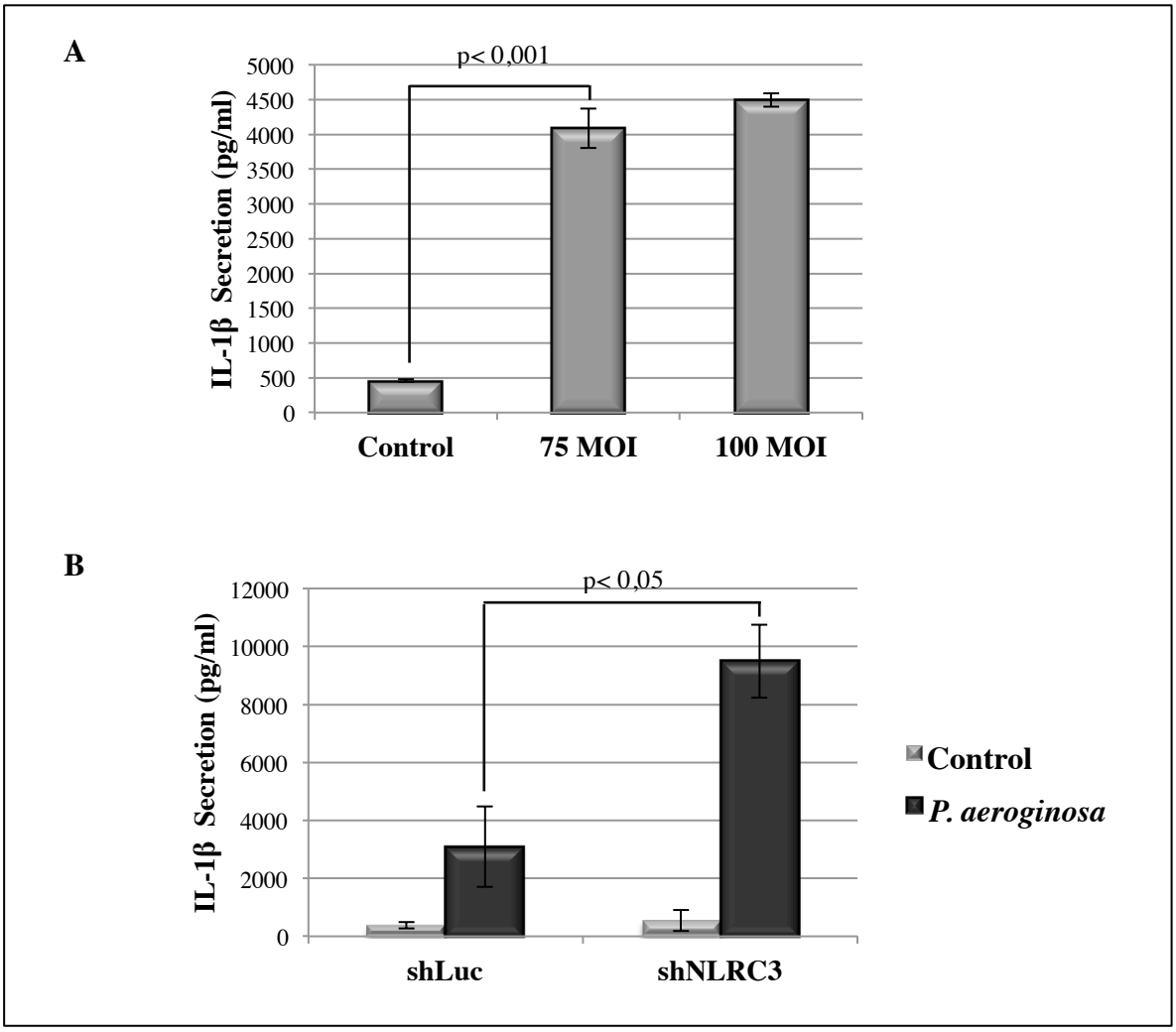

Figure 5.7. NLRC3 is also an inhibitor of the IPAF Inflammasome. (A) IL-1β secretion in WT THP-1 cells in response to *Pseudomonas aeroginosa* infection. MOI: multiplicity of infection (number of bacteria/cell). (B) IL-1β secretion in shLuc and shNLRC3 cell lines in response to 4 hours 75 MOI *P. aeroginosa* stimulation. Combined result of two independent sets of experiments.

Thus, NLRC3 inhibits both Cryopyrin and IPAF inflammasomes. Because the only difference between these two inflammasomes is their receptor proteins, we hypothesize that NLRC3 may act downstream of the receptor proteins.

5.1.8. Post-Translational Regulation of Cryopyrin, ASC and IL-1β by NLRC3

NLRC3 was shown to induce TRAF6 protein degradation by targeting it to the proteasome (Schneider *et al*., 2012). To test whether NLRC3 has such an effect on Cryopyrin inflammasome components, Cryopyrin, ASC and IL-1β were overexpressed in HEK293FT cells with increasing concentrations of NLRC3. Protein levels were assessed by Western blotting.

Overexpression of ASC, Cryopyrin or pro-IL-1β with increasing concentrations of NLRC3 did not affect Cryopyrin (Figure 5.8a), ASC (Figure 5.8b) and pro-IL-1β (Figure 5.8c) protein levels. If NLRC3 were inducing degradation of proteins, one would expect to observe a decrease in protein levels with higher NLRC3 protein levels. Western blotting results did not show such a change in protein levels. Thus, NLRC3 does not modulate the inflammasome by decreasing protein levels.

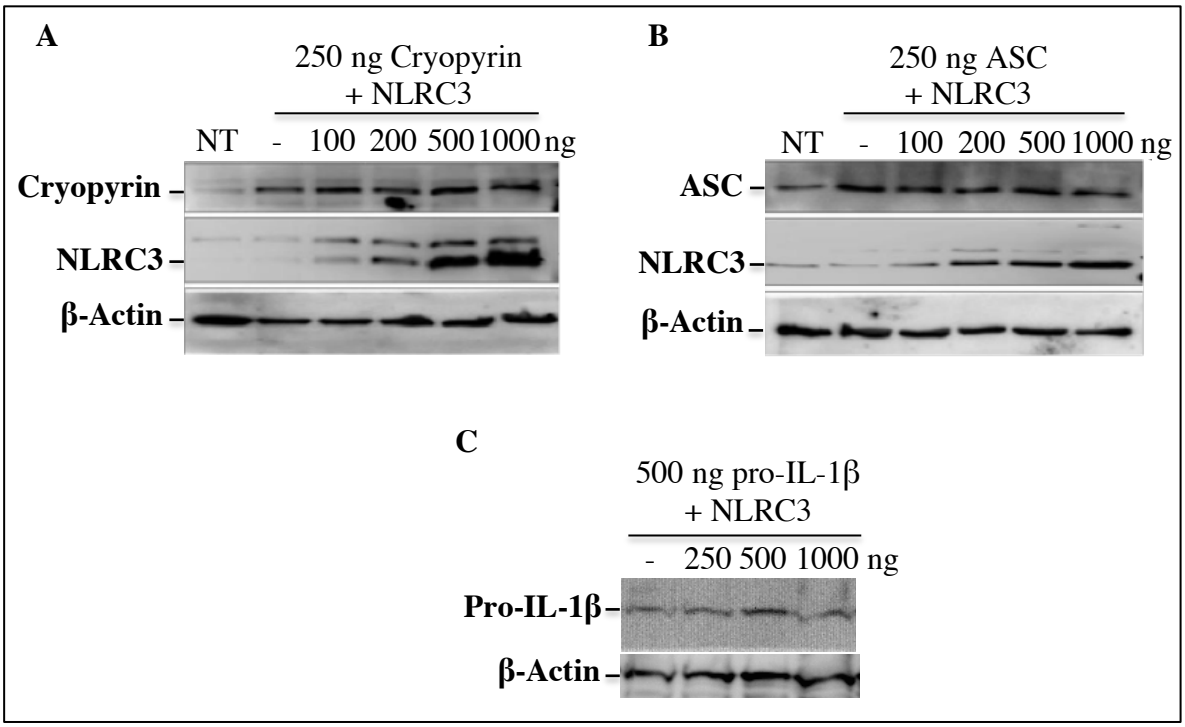

Figure 5.8. Regulation of protein levels by NLRC3. HEK293FT cells were transfected with 250 ng Cryopyrin (A) or 250 ng ASC (B) or 500 ng pro-IL-1β (C) and increasing concentrations of NLRC3. Cells were harvested 48 hours after transfection and protein levels were determined by Western blotting. Cryopyrin:107 kDa, Flag-NLRC3: 105 kDa, ASC: 24 kDa, pro-IL-1β:, B-Actin: 42 kDa.

Because proteins were overexpressed, any potential transcriptional regulation was excluded. Nonetheless, proteins may require some post-translational modifications such as ubiquitination or phosphorylation in order to be degraded directly by or through NLRC3. Because we used a human cell line and human protein encoding plasmids and the amount of overexpressed plasmid is close to the physiological level (250 ng), we expect these modifications to happen in our setting.

Regulation of protein levels by NLRC3 could not be investigated endogenously in THP-1 cells where Cryopyrin inflammasome was activated because NLRC3 is known to modulate the NFκB pathway and NFκB in turn regulates transcription of Cryopyrin inflammasome proteins. Thus, distinction between transcriptional and post-translational regulation would not be possible. Furthermore, pro-Caspase-1 and pro-IL-1β are cleaved upon Cryopyrin inflammasome activation and are secreted from the cells. Similarly, ASC protein forms a multi-protein complex (see next section) and is secreted from the cells. Thus, distinction between protein degradation induced by NLRC3 and protein secretion or transcriptional regulation would not be possible. It may require additional interventions such as inhibition of the transcription or blockage of the secretion and that would not be representative of the physiological mechanisms.

Overall, these data suggest that NLRC3 does not regulate Cryopyrin, ASC and pro-IL-1β protein levels. Inhibition of the Cryopyrin inflammasome by NLRC3 could be through disruption of the assembly of the inflammasome complex.

5.1.9. NLRC3 Disrupts ASC Speck Formation

Another outcome of Cryopyrin inflammasome activation is the formation of aggregates containing ASC proteins called “specks” (Fernandes-Alnemri *et al*., 2007). Upon Cryopyrin induction, ASC adaptor protein binds to Cryopyrin and recruits pro-Caspase-1. ASC proteins together with many pro-Caspase-1 molecules form huge ASC speck complexes, interestingly only one per cell.

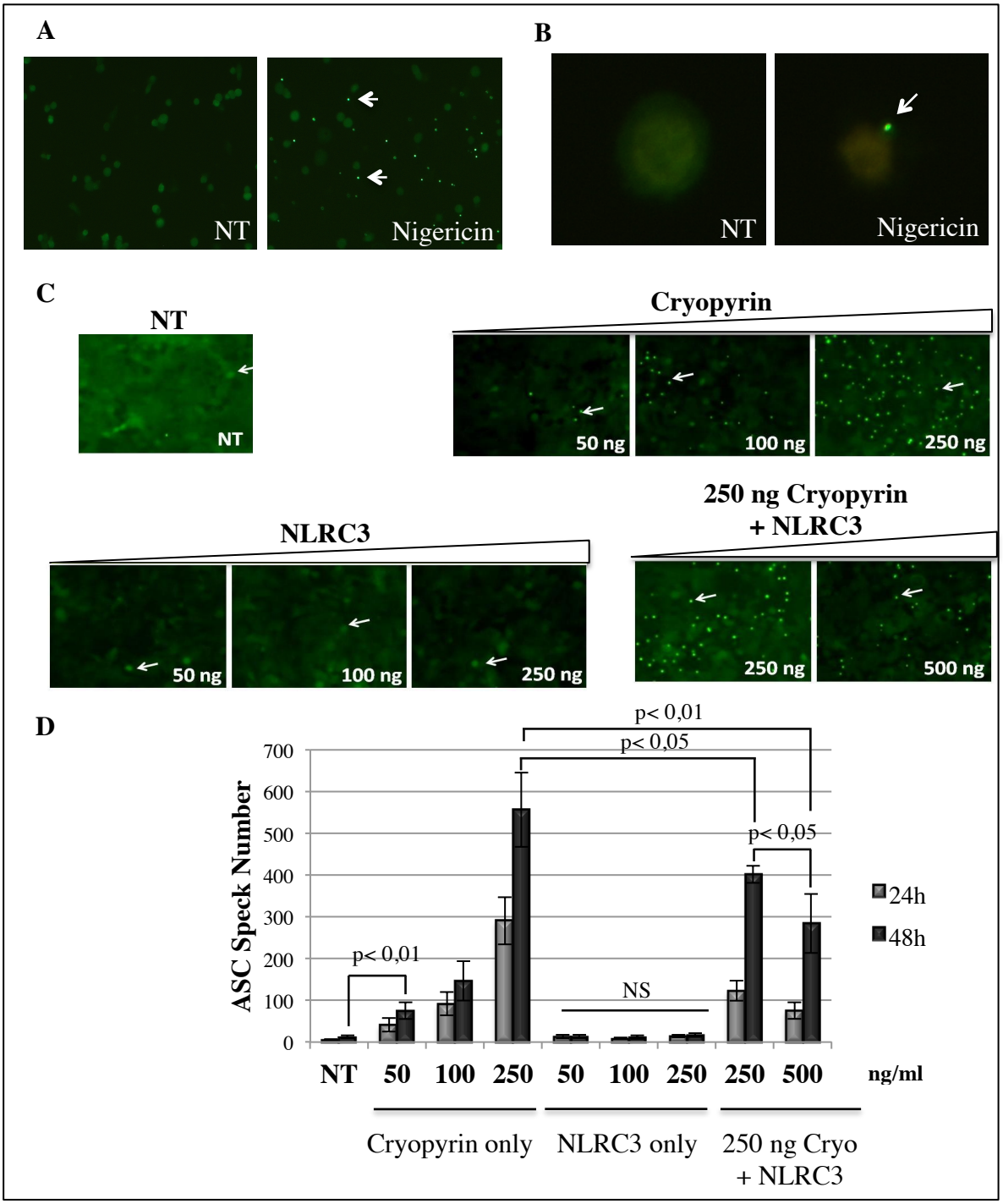

Figure 5.9. NLRC3 disrupts ASC speck formation. (A) ASC specks in THP-1-ASC-EGFP treated with 20 μM Nigericin for 4 hours (10X) and (B) THP-1 stained with anti-ASC antibody (20X). (C) Representative images of transfected HEK293FT-ASC-EGFP. (D) Speck numbers counted in 8 randomly chosen fields. Each condition was repeated twice and the experiment was performed three times. Total amount of DNA was equalized with empty pcDNA3 plasmid for each condition. Arrows show ASC specks.

To confirm the physiological relevance of ASC specks and prove that they are specifically formed in response to inflammasome activation, THP-1 cells stably expressing ASC-EGFP fusion protein were differentiated into macrophages and stimulated with Nigericin. Whereas under normal conditions ASC-EFGP protein appeared diffuse in the cytoplasm, activation of Cryopyrin inflammasome by Nigericin assembled ASC-EGFP proteins that appeared as bright green dots under the microscope (Figure 5.9a). To confirm that complexes that are seen are not an artifact of overexpression of ASC-EGFP protein but are really ASC protein complexes, WT THP-1 cells were stimulated with Nigericin and endogenous ASC was stained with anti-ASC-specific antibody (Figure 5.9b). Similar to ASC-EGFP expressing cells, endogenous ASC specks formed and appeared as complexes smaller in size. ASC specks were found one per cell in the cytoplasm or secreted from the cells.

Besides activation with known ligands, overexpression of Cryopyrin in HEK293FT-ASC-EGFP cells also induced ASC speck formation in a dose- and time-dependent manner (Figure 5.9c, upper left panel). Whereas 26 ± 4,9 specks were counted for the control transfected with empty vector, transfection of 50 ng of Cryopyrin induced the formation of 76,8 ± 15,7 specks and 529 ± 81 specks for 250 ng Cryopyrin 48 hours after transfection.

Next, the effect of NLRC3 alone on ASC speck formation was investigated (Figure 5.9c, lower left panel). NLRC3 had no significant effect on speck formation on its own (26 ± 4,9 specks for empty vector vs 15,8 ± 3,3 specks for 50 ng NLRC3 and 21,3 ± 1,7 specks for 250 ng NLRC3, 48 hours after transfection).

To elucidate whether NLRC3 has an effect on Cryopyrin-induced ASC speck formation, Cryopyrin and NLRC3 plasmids were co-transfected. Interestingly, NLRC3 reduced the number of specks triggered by Cryopyrin (529 ± 81 specks for 250 ng Cryopyrin alone and 413 ± 31,3 specks for 250 ng Cryopyrin + 250 ng NLRC3 vs 270 ± 92,7 specks for Cryopyrin + 500 ng NLRC3, $p<0,05$, 48 hours after transfection; Figure 5.9d, right panel).

These results indicate that the inhibitory effect of NLRC3 exerted on the Cryopyrin inflammasome is not at the transcriptional level and that NLRC3 prevents complex assembly. Experiments conducted so far showed that NLRC3 inhibits the formation of the Cryopyrin inflammasome. The next step will be to find out the molecular mechanism of this inhibition.

5.1.10. Interaction of NLRC3 with Inflammasome Components

Since NLRC3 inhibited complex assembly, we decided to test whether it can interact with different Cryopyrin inflammasome components. In a previous work done in our laboratory, we showed that NLRC3 interacts with Caspase-1 and ASC by co-immunoprecipitation in overexpression systems (Gültekin *et al*., 2014). To determine whether NLRC3 interacts with Cryopyrin, HEK293FT cells were transfected with Flag-Cryopyrin and Myc-NLRC3 or Flag-Cryopyrin, Myc-NLRC3 and ASC (Figure 5.10a).

Immunoprecipitation of Cryopyrin with anti-Flag antibody and blotting with anti-Myc-tag antibody (Figure 5.10a left panel) or immunoprecipitation of NLRC3 with anti-Myc antibody and blotting with anti-Flag antibody (Figure 5.10a right panel) did not reveal any bands suggesting that Cryopyrin and NLRC3 are not interacting with each other. Because interactions are known to be homotypic, we investigated whether NLRC3 and Cryopyrin interaction could be through the adaptor protein ASC, which contains both a Pyrin domain that binds to Cryopyrin and a CARD domain that binds NLRC3. The presence of ASC did not lead to NLRC3 and Cryopyrin binding either (Figure 5.10a, second lanes). Thus, NLRC3 and Cryopyrin did not interact with each other even in the presence of the adaptor protein ASC in overexpression systems.

NLRC3 and Cryopyrin interaction was further investigated endogenously (Figure 5.10b). Immunoprecipitation of endogenous NLRC3 in THP-1 cells differentiated into macrophages and treated or not treated with Cryopyrin ligands did not pull down endogenous Cryopyrin. We conclude that NLRC3 and Cryopyrin do not interact endogenously.

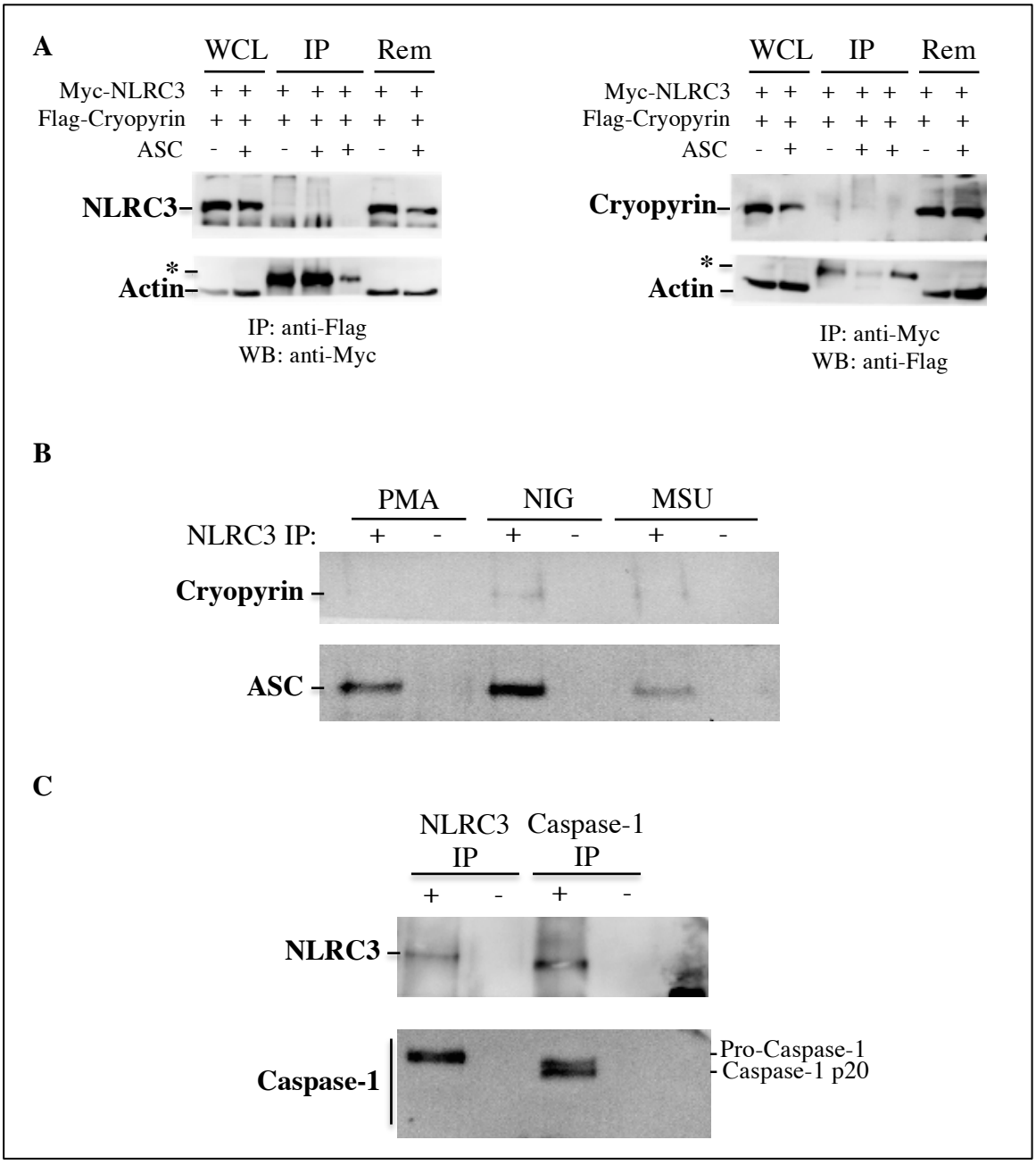

Figure 5.10. NLRC3 interaction with inflammasome components. (A) HEK293FT transfected with 6 μg plasmids. Irrelevant anti-HA antibody was used as negative control. WCL: whole cell lysates, Rem: remaining fraction after IP, * IgG heavy chains (55 kDa). (B) Interaction of endogenous NLRC3 with endogenous Cryopyrin and ASC. IP was with anti-NLRC3 antibody in PMA-differentiated THP-1 cells and Nigericin and MSU treated THP-1 cells. (C) Interaction with endogenous Caspase-1. +: IP with anti-NLRC3 or anti-Caspase-1 antibody. -: IP with anti-rabbit IgG antibody.

To validate our previous overexpression data, we tested NLRC3 interaction with ASC and Caspase-1 endogenously. NLRC3 interacted with ASC both in resting macrophages and those with active Cryopyrin complex (Figure 5.10b).

On the other hand, immunoprecipitation of NLRC3 revealed a pro-Caspase-1 band and similarly, a NLRC3 band was detected when cell lysates were immunoprecipitated with anti-Caspase-1 antibody (Figure 5.10c). Commercially available anti-Caspase-1 antibody was generated against the p10 subunit of Caspase-1 and recognized pro-Caspase-1, active p20 Caspase-1 and active p10 subunits. Visualization of only the pro-Caspase-1 on the gel after anti-NLRC3 immunoprecipitation suggests that NLRC3 interacts with immature Caspase-1 and not active Caspase-1 proteins. Thus, NLRC3 and pro-Caspase-1 interact through their CARD domain and dissociate after pro-Caspase-1 cleavage into their mature form.

In summary, NLRC3 interacts with ASC and Caspase-1 but not Cryopyrin endogenously, which explains its ability to inhibit both Cryopyrin and IPAF inflammasomes, since ASC and Caspase-1 are downstream effectors common to these two pathways.

5.1.11. Co-Localization of NLRC3 with ASC

Immunocytochemistry was performed in order to see if ASC and NLRC3 proteins co-localize endogenously (Figure 5.11a, right panel, orange color). In inactive inflammasome containing cells, diffused ASC and NLRC3 co-localized as suggested by our immunoprecipitation results. However, NLRC3 was not present in ASC specks in MSU stimulated cells (Figure 5.11a, right panel arrow). Moreover, NLRC3 was also absent in ASC specks isolated from treated cells (Figure 5.11b).

Thus, NLRC3 interacts and co-localizes with cytoplasmic and diffuse ASC protein in absence of stimulation, but once the Cryopyrin inflammasome is activated and ASC protein forms specks, NLRC3 is excluded from the specks.

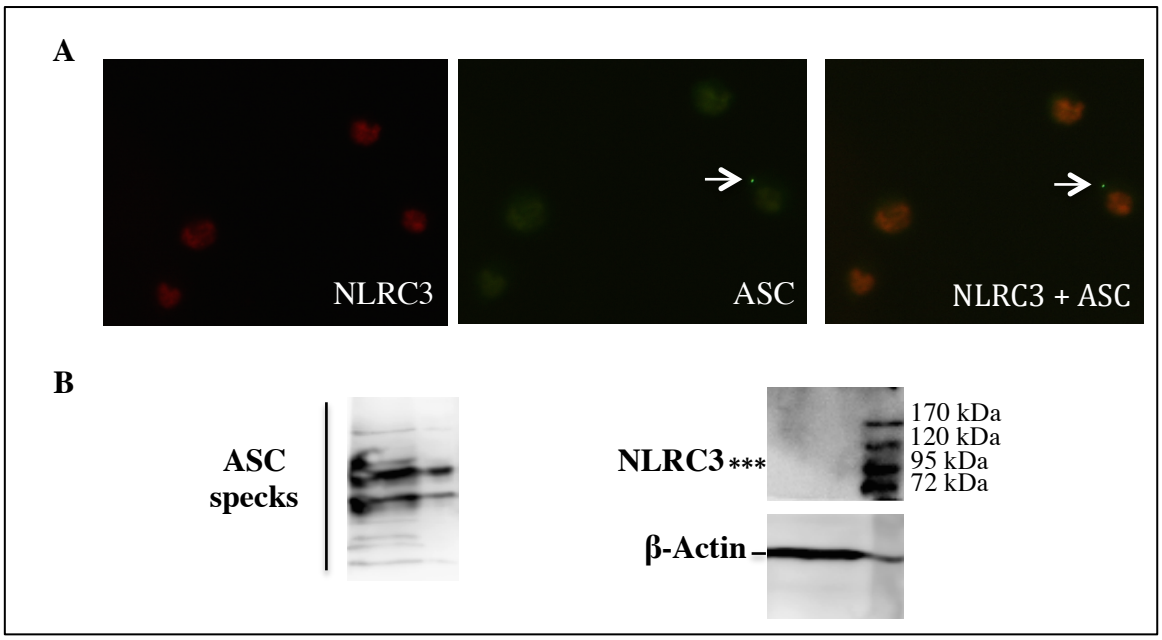

Figure 5.11. Co-localization of NLRC3 with ASC and its expression in ASC specks. (A) Endogenous ASC (green) and NLRC3 (red) co-localization in MSU treated THP-1 cells. Arrow shows ASC speck. (B) NLRC3 expression in ASC specks isolated from mCherry-ASC transfected HEK293FT. 12 µl of pure ASC specks were loaded on gel. Left panel: ASC mono- and oligomers. Right panel: NLRC3 and Actin blot. ***: position where NLRC3 band is expected to be (104 kDa).

5.1.12. Cloning and Expression of NLRC3 Domains

CARD, NACHT, LRR, CARD/NACHT and NACHT/LRR domains were cloned into N-terminal Myc-tag containing plasmid (Figure 5.12a and methods section) and were transfected to HEK293FT cells to control their expression by Western blotting with anti-Myc-tag antibody (Figure 5.12b).

The molecular weight of each domain was calculated by an online tool. All cloned domains were expressed and appeared at expected molecular weights on the membrane. Only the CARD domain that was predicted to be 7 kDa could not be detected with the transfer conditions we used in this experiment.

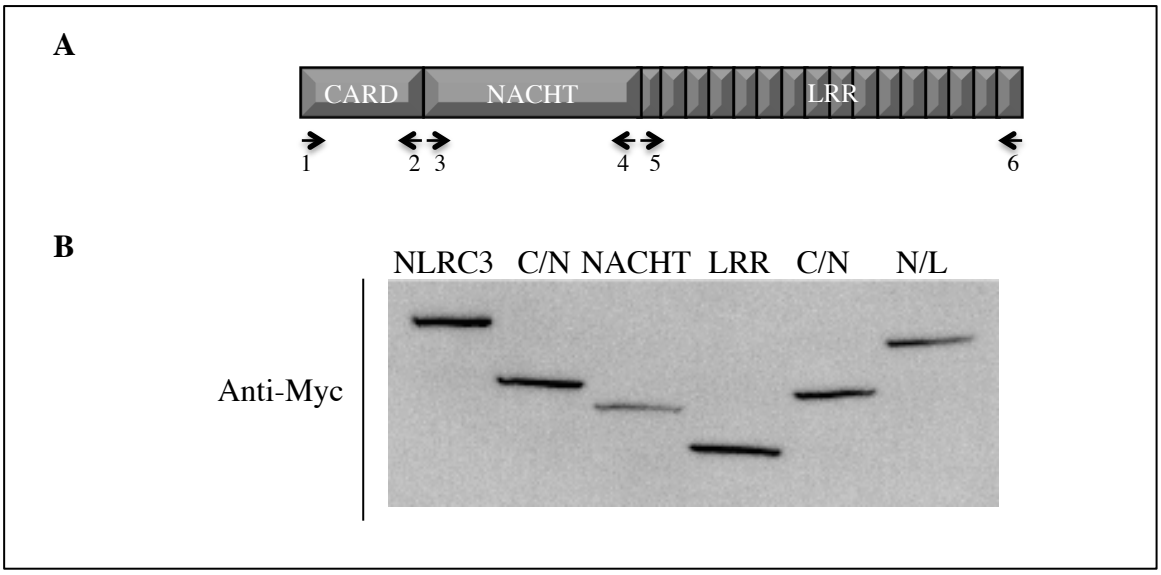

Figure 5.12. Cloning and expression of NLRC3 domains. (A) Schematic representation of cloning strategy. Primer 1: Nlrc3-F with XbaI site, 2: N3CSTR: STOP codon and NotI site, 3: N3NF with NheI site, 4: N3NSTR with Stop codon and NotI site, 5: N3LF with XbaI site, 6: N3LSTR with STOP codon and NotI site. (B) Western blot result showing expression of Myc-tagged full length NLRC3 and separate domains. Anti-Myc antibody was used. C/N: CARD/NACHT; N/L: NACHT/LRR.

5.1.13. Effect of Domains on ASC Speck Formation

We have previously shown that full length NLRC3 inhibits ASC speck formation (Figure 5.9). To identify the domain responsible for this disruption, NLRC3's domains were transfected to HEK293FT-ASC-EGFP cells and the number of ASC specks was counted (Figure 5.13).

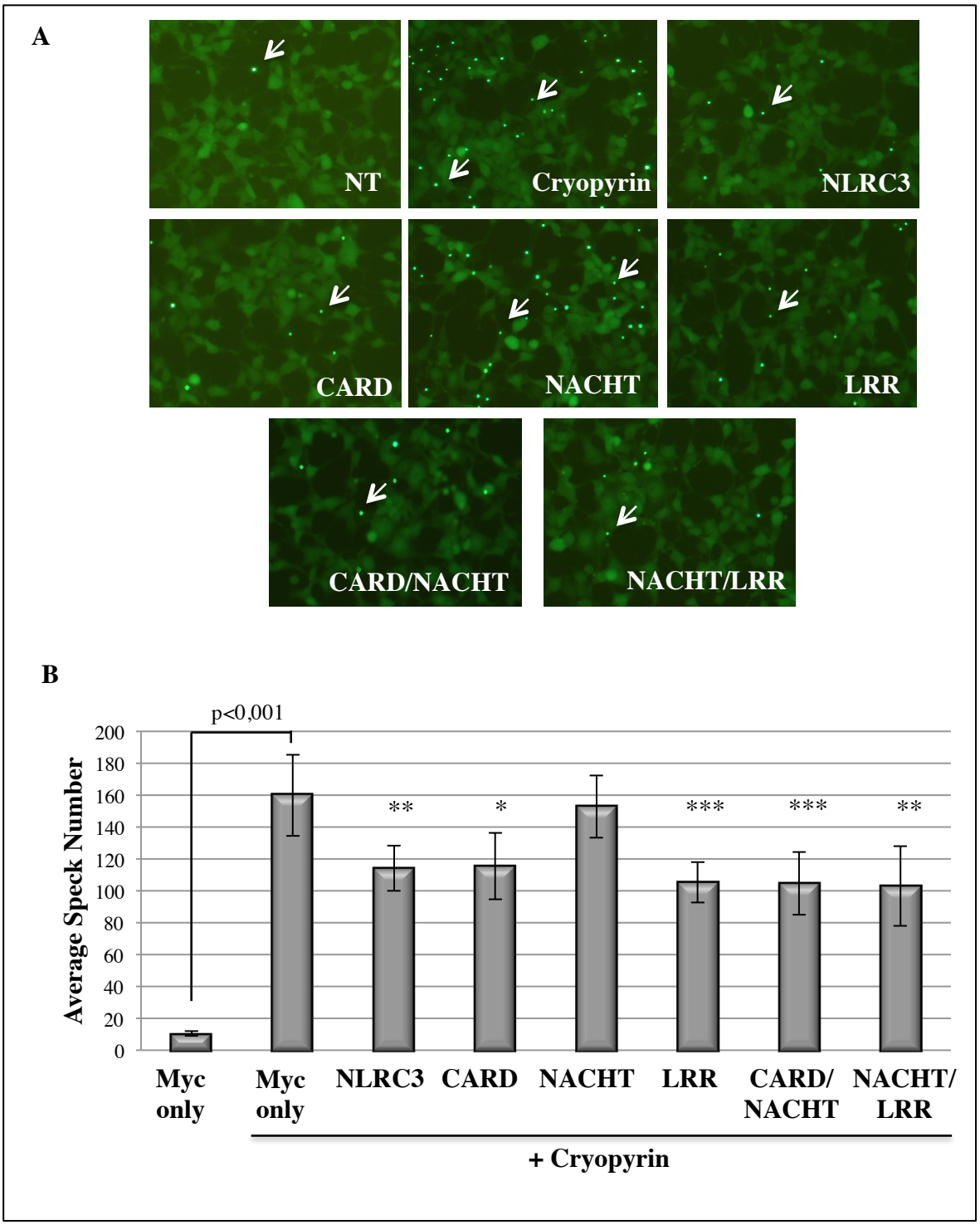

Figure 5.13. The CARD and LRR domains affect ASC speck formation. (A) Representative pictures of the effect of NLRC3 domains on ASC speck formation induced by Cryopyrin. (B) Quantification of ASC specks formed in presence of NLRC3 domains. *p<0,05, **p=0,001, ***p<0,001 (Cryopyrin only compared to the indicated condition).

Similar to the full-length protein, NLRC3 domains transfected separately had no effect on ASC speck formation (not shown). Whereas Cryopyrin transfected cells induced ASC speck assembly strongly (160 ± 25,5 compared to 10,6 ± 1,5, p<0,0001), full-length NLRC3 (114,1 ± 14,2, p=0,001), CARD (115,5 ± 20,8, p=0,003), LRR (105,4 ± 12,8, p=0,0002), CARD/NACHT (104,8 ± 19,7, p=0,0006) and NACHT/LRR (103 ± 24,9, p=0,001) domains significantly reduced ASC speck number (Figure 5.13). Only the NACHT domain had no effect on Cryopyrin-induced speck formation (152,9 ± 19,6, p=0,56). According to these results, both CARD and LRR domains affect ASC speck formation.

5.1.14. Regulation of Nlrc3 Expression During *in vivo* Inflammation- DSS-Induced Colitis Model

To investigate the effect of NLRC3 on *in vivo* inflammation, acute colitis was induced in C56BL6 mice by treatment with 3% DSS for 7 days.

As expected, DSS treated mice lost weight compared to controls (Figure 5.14a), underwent colon shortening (Figure 5.14b and c) and presented all clinical signs of colitis such as bloody intestinal content and diarrhea. Intestinal crypts were isolated from the colon of control and DSS-treated mice and qPCR was performed. Nlrc3 mRNA levels were reduced nearly by half in DSS-treated mice compared to control counterparts (Figure 5.14d).

Since our previous findings suggest that Nlrc3 is an anti-inflammatory protein that regulates the Cryopyrin inflammasome, down-regulation of its level during an inflammatory disease involving the activation of the Cryopyrin inflammasome strengthened our hypothesis.

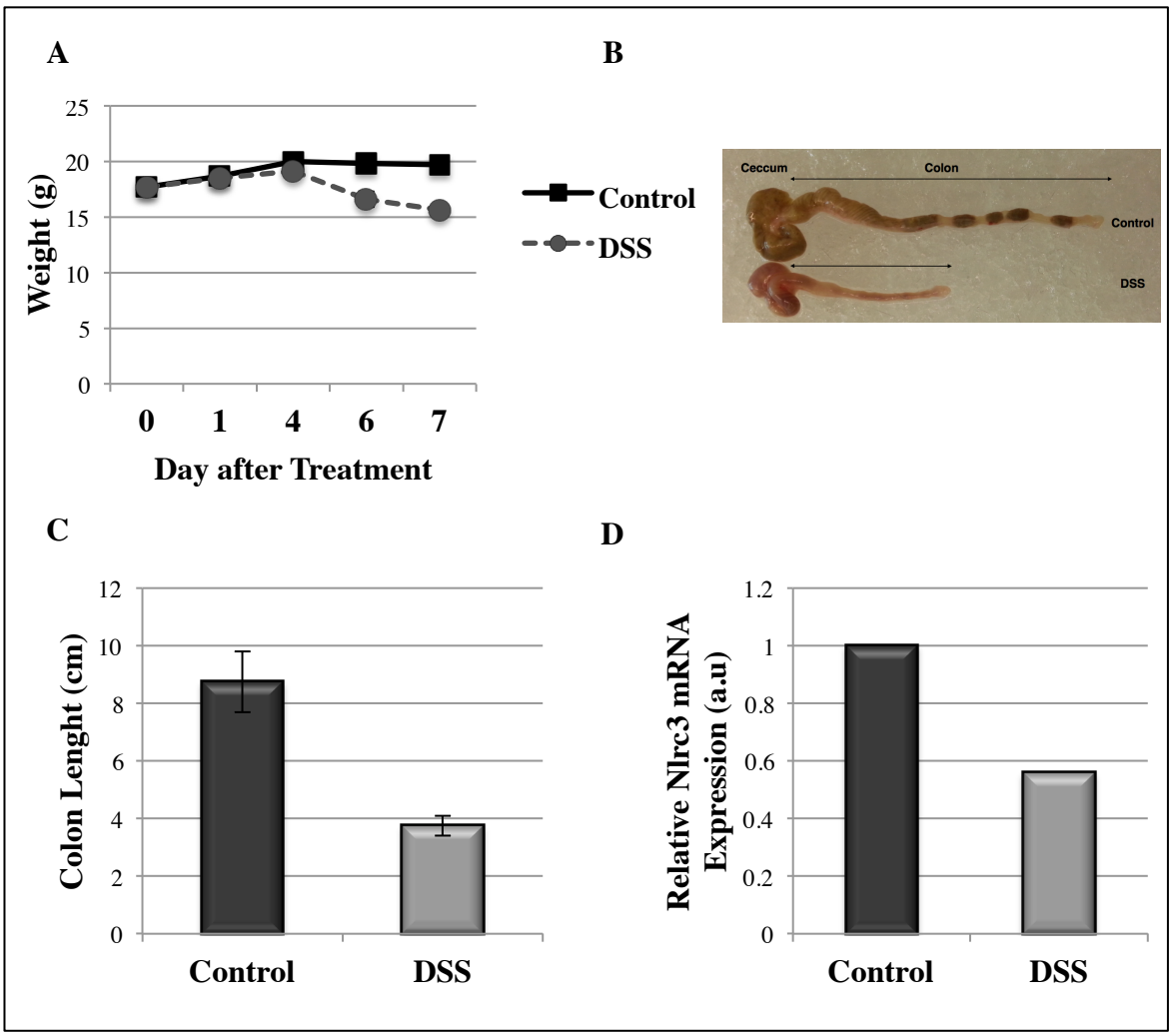

Figure 5.14. Nlrc3 expression is down-regulated during acute colitis. (A) Weight of control mice and mice treated with 3% DSS *ad libidium* for 7 days. Two mice were used for each group. (B) Pictures of colon of control and DSS-treated mice. (C) Graphical representation of colon lengths. (D) Relative Nlrc3 mRNA expression in control and DSS-treated mice (n=1 for each group). mRNA levels were normalized to Actin mRNA. Nlrc3 levels in control sample was assigned as 1 arbitrary unit.

5.1.15. NLRC3 Levels are Negatively Regulated During NFκB Pathway Activation

It is now well established that NLRC3 inhibits NFκB pathway by inducing the degradation of TRAF6 an activator of the pathway (Schneider *et al*., 2012). NFκB pathway

activation through TLR receptors and inflammasome induction are parallel pathways. To elucidate if the NFκB pathway has an effect on NLRC3 levels, THP-1 cells were stimulated with LPS. Activation of NFκB is very fast and IκB is degraded as early as 15' after LPS stimulation. NLRC3 protein levels are downregulated at 30' until 2 hours and come to the basal level at 3 hours after stimulation (Figure 5.15). Thus, NLRC3 levels are negatively regulated by the NFκB pathway.

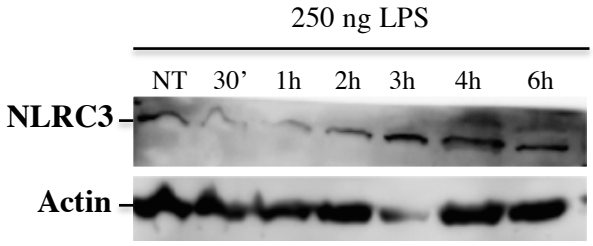

Figure 5.15. NLRC3 levels are negatively regulated during NFκB pathway activation. THP-1 cells were treated with 250 ng LPS for the indicated times.

5.2. Nlrc3, Stemness and Tumorigenesis

5.2.1. Nlrc3 is Expressed in the Small Intestine and Colon

Previous microarray analysis suggested that Nlrc3 is highly expressed in immune cells such as lymphocytes, T-cells and B-cells. Crypts from mouse small intestine and colon were isolated to determine whether Nlrc3 is expressed in these tissues. Validated primers located at the exon/intron junction and specific to Nlrc3 were chosen. Nlrc3 was expressed in both the small intestine and the colon of C56BL/6 and Webster mice (Figure 5.16a). Nlrc3 expression in the colon was higher than its expression in the small intestine (Figure 5.16b).

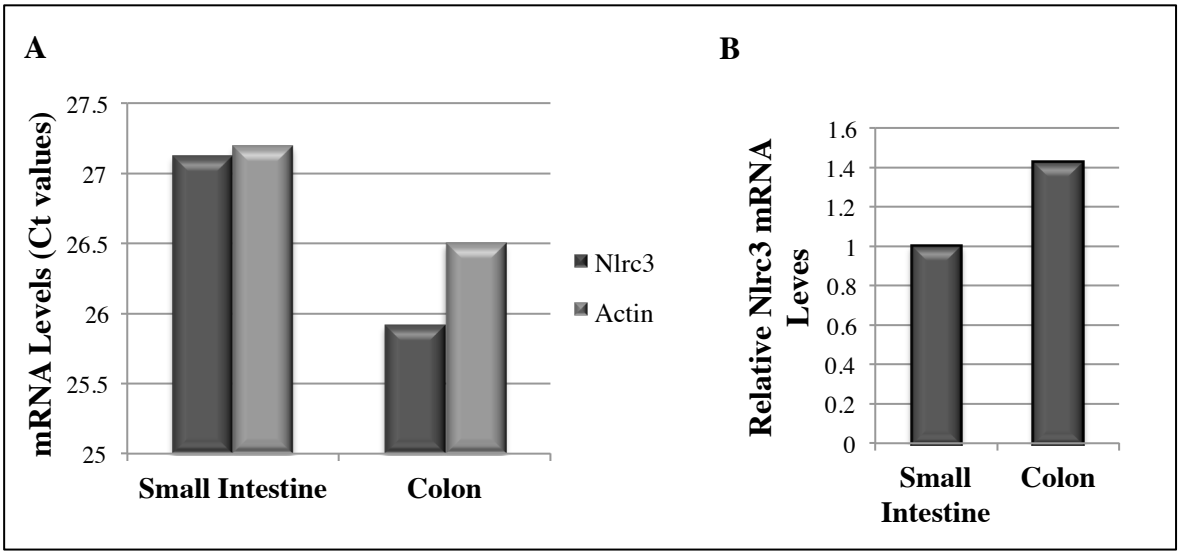

Figure 5.16. Nlrc3 is expressed in the small intestine and the colon of mice. (A) qPCR results. Ct values of Nlrc3 and Actin are shown. (B) Relative Nlrc3 expression. 2^delta Ct value of Nlrc3 in the small intestine was assigned as 1 a.u and its expression in the colon was normalized to the small intestine.

5.2.2. Nlrc3 is Less Expressed in Cells Prone to Form Tumors

APC mutations are the major cause of colorectal cancers. Apc KO organoids from both the small intestine and the colon were generated by using pUSCC-mApc and pLenti-CRISPR-RFP-mApc, two different CRISPR vectors containing a guide targeting exon 16 of Apc. Apc KO was verified by quantifying Axin2, a component of beta-Catenin degradation complex known to be a target of the Wnt pathway. As expected, Apc KO activated Wnt pathway and Axin2 levels were more than 10 fold upregulated in Apc KO organoids proving Apc loss and an active Wnt pathway (Figure 5.17a and b). Moreover, known Wnt pathway target genes c-Myc, CyclinD1, Vegf and EphB2 were also upregulated in Apc KO organoids.

Once making sure Apc was knocked out, Nlrc3 levels were measured in control and Apc KO organoids. Nlrc3 levels were about 10 fold lower in Apc KO organoids from both the colon and the small intestine compared to the control organoids expressing Apc (Figure 5.17a and b).

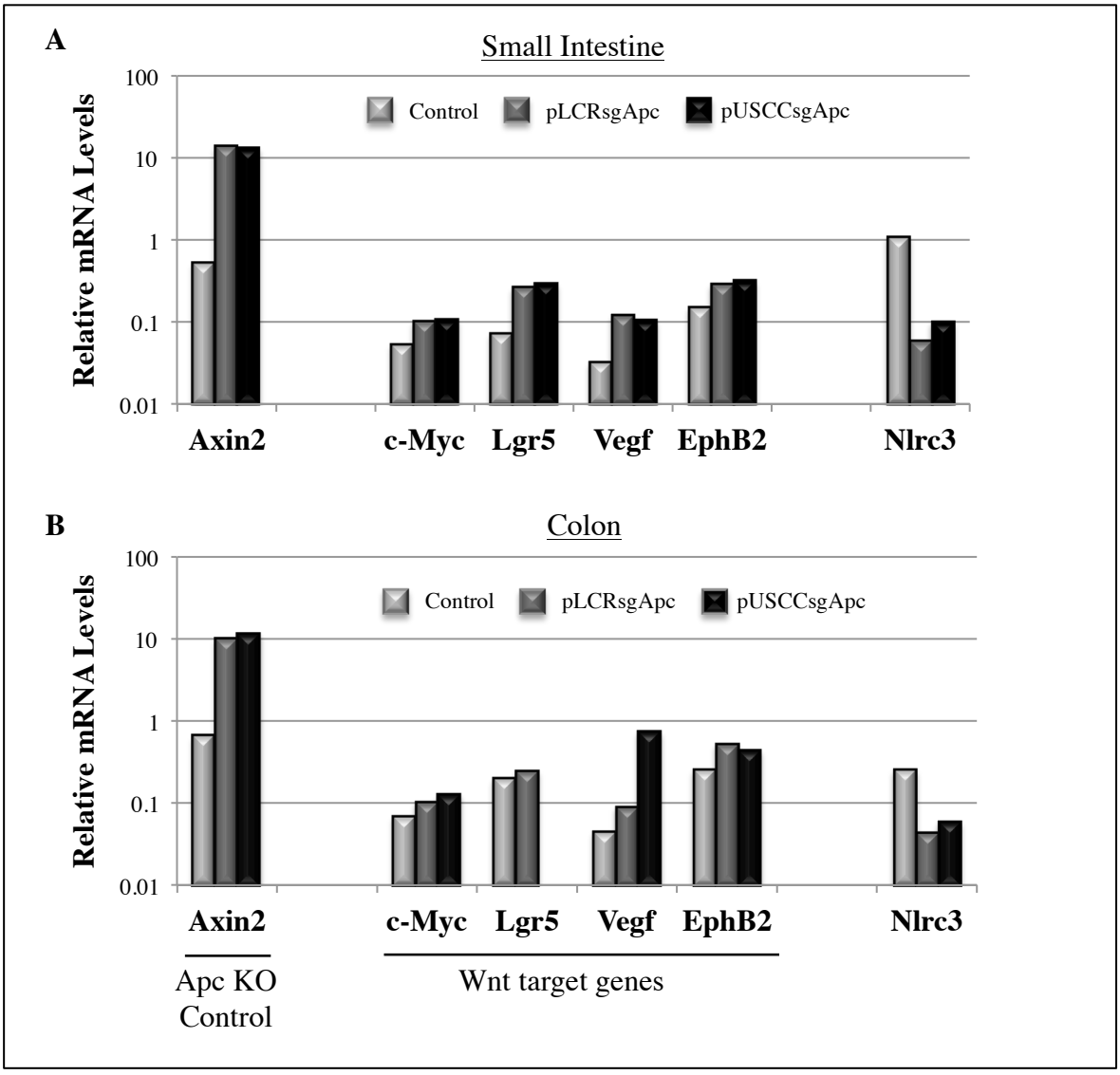

Figure 5.17. Nlrc3 expression is decreased in Apc KO organoids. Apc KO organoids were generated by using CRISPR. pLenti-CRISPR-sgApc-tRFP or pUSCC-sgApc plasmids were used to generate Apc KO organoids. Non-infected organoids were used as control. (A) Nlrc3 and Wnt target gene qPCR results in organoids from the small intestine. (B) Nlrc3 and Wnt target gene qPCR results in organoids from the colon.

Because colorectal cancer is aggrieved by accumulation of mutations and Apc and Kras mutations are known to lead to a more severe tumorigenic phenotype, Nlrc3 levels were tested in organoids from Apc, Kras double knock-out mouse (Figure 5.18a and b). A gradual decrease in Nlrc3 levels was observed from control towards Apc KO and Apc Kras

KO organoids whereas Axin2 levels were increasing (Figure 5.18c). As a conclusion, there was a negative correlation between Nlrc3 expression and tumorigenesis.

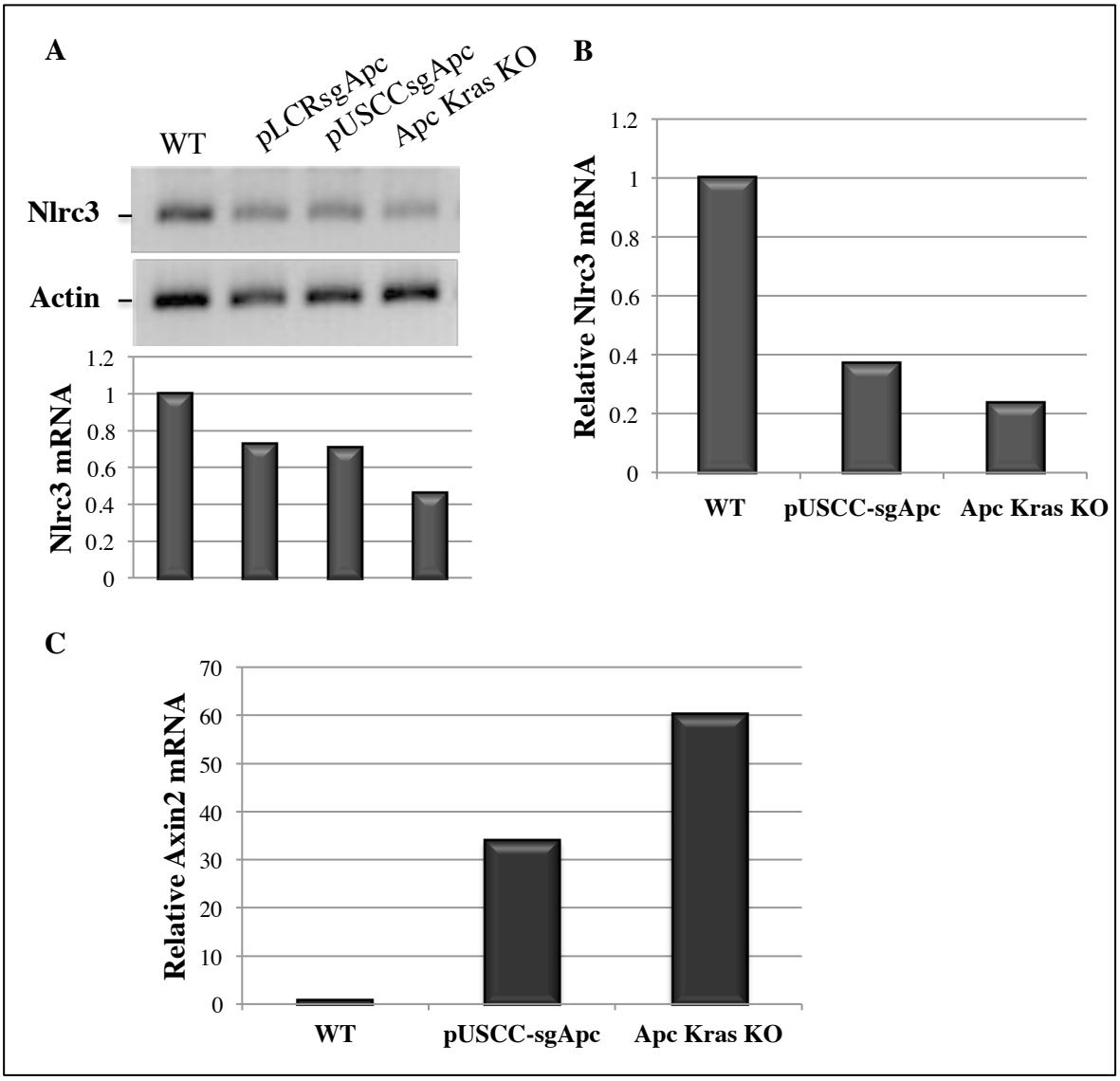

Figure 5.18. Nlrc3 expression decreases in organoids from Apc/Kras KO mice. (A) RT-PCR results of Nlrc3 and Actin levels from Apc KO organoids from the small intestine and organoids from Apc and Kras KO mice. Bottom: quantification of semi-quantitative PCR results. (B) qPCR Results of relative Nlrc3 mRNA levels normalized to WT. (C) Axin2 levels in different organoids.

5.2.3. Nlrc3 is More Expressed in Paneth Cells Compared to the Stem Cells

Expression levels of Nlrc3 were determined in sorted stem cells (GFP high), transit amplifying cells (GFP low) and Paneth cells (Figure 5.19). Whereas Nlrc3 levels were similar in both stem cells and transient amplifying cells, Nlrc3 levels tend to be higher in Paneth cells (p=0,09) that are quiescent cells. Thus Nlrc3 is more expressed in less proliferative cells.

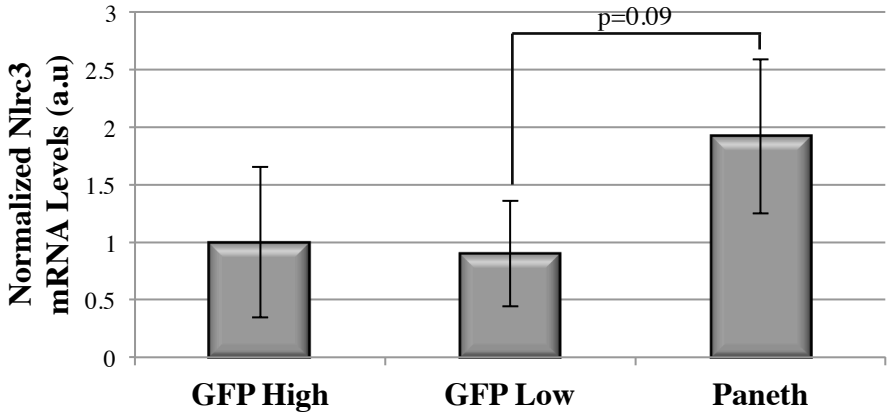

Figure 5.19. Nlrc3 is more expressed in Paneth cells compared to stem cells. qPCR results of Nlrc3. Intestinal crypts were isolated and GFP High, GFP Low and c-kit^{+} Paneth cells were sorted by flow cytometry. Nlrc3 mRNA levels were normalized to Actin and ratio obtained for the GFP high samples was assigned as 1 a.u. and other samples were normalized to GFP high.

5.2.4. Nlrc3 KO Organoids Were Generated with CRISPR

In order to determine if the decrease in Nlrc3 levels seen in Apc KO organoids is the cause or the consequence of proliferation, Nlrc3 KO and KD organoids were generated and the organoid formation capacity of these cells were measured.

Nlrc3 knock-out organoids were generated by using inducible CRISPR technology. Two different guide RNA molecules against Nlrc3 and control guide to tdTomato were designed by using Benchling online software. sgNlrc3-G1 was chosen in the exon 1 corresponding to the 5'UTR of *Nlrc3* and gave the highest on-target score. sgNlrc3-G2 on the other hand, was designed against the exon 2, which is a coding sequence. Neither sgNlrc3-G1 nor sgNlrc3-G2 blasted significantly with any other non-specific genes.

These guide RNAs were cloned downstream of human U6 promoter into a vector containing turboRFP gene under the control of EFS. Because the vector did not contain Cas9, Cas9-EGFP-Lox-STOP-Lox; Villin-Cre mice were used (Platt *et al*., 2014; Figure 5.20a). Tamoxifen injection to mice induced the expression of Cre in the epithelial cells of the colon and small intestine and Cre allowed Cas9-EGFP expression. Intestinal crypts were isolated from these mice and cultured into conditioned medium to let them form organoids. After they were formed, organoids were infected with a virus-expressing our guides of interest and GFP^+ RFP^+ cells were sorted (Figure 5.20b).

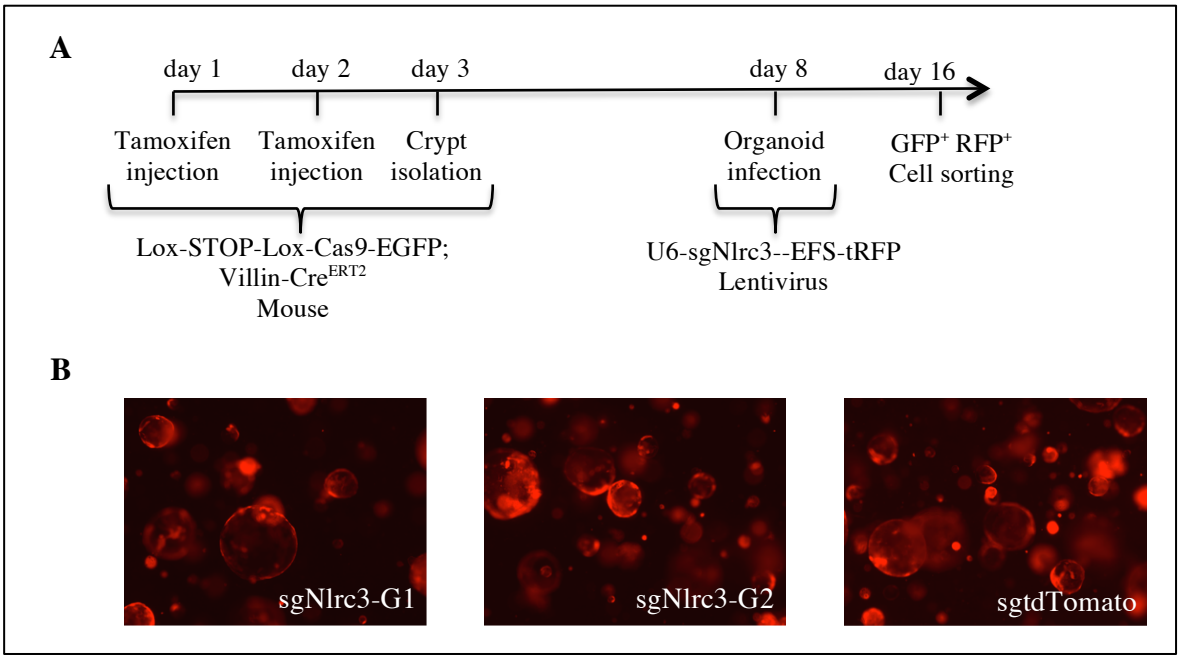

Figure 5.20. Nlrc3 knockout and knockdown organoids were generated. (A) Experimental strategy. (B) Pictures of infected organoids.

Genomic DNA was isolated from sorted cells, the targeted regions were PCR amplified and cloned into TOPO vector. Ten TOPO positive bacterial colonies were sent for sequencing for each guide RNA. All ten colonies for sgNlrc3-G1 were WT (data not shown) whereas only one colony was WT for sgNlrc3-G2 and the remaining nine colonies had insertion/deletions at homozygous or heterozygous states (Figure 5.21a).

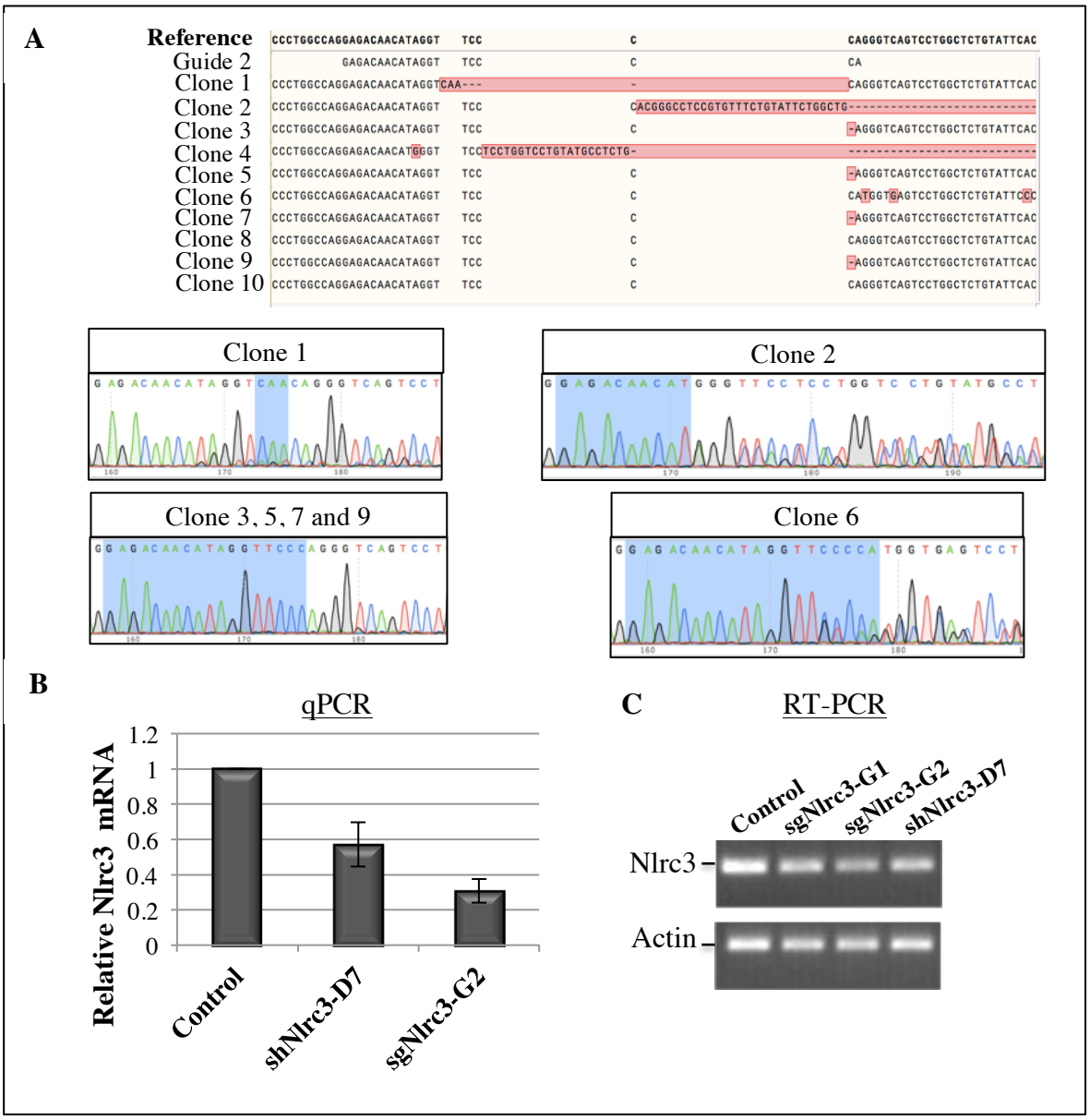

Figure 5.21. Nlrc3 KO and KD organoids results. (A) Results of surveyor assay. Reference *Nlrc3* sequence and sequences of Nlrc3 KO organoids are presented. Sequences highlighted in red: insertions/deletions. (B) Relative Nlrc3 mRNA Levels in control, shNlrc3-D7 and sgNlrc3-2 organoids by qPCR. (C) RT-PCR results of Nlrc3 levels in control, sgNlrc3-G1, sgNlrc3-G2 and shNlrc3-D7 organoids.

To confirm that these modifications affect Nlrc3 levels, RT-PCR and qPCR were performed from sorted organoids. In fact, Nlrc3 mRNA levels were reduced by 74% in sgNlrc3-G2 organoids compared to sgtdTomato infected ones (Figure 5.21b). Decrease of Nlrc3 levels was further confirmed by RT-PCR (Figure 5.21c).

To also make knock-down Nlrc3 primary cells, a puromycin cassette of pLKO.1-shNLRC3-D7 (that was the only shRNA targeting both human and mouse Nlrc3) was replaced with turboRFP. Similarly, organoids infected with shNLRC3-D7, RFP^+ cells were sorted and qPCR analysis showed that Nlrc3 is reduced by 34% in these cells (Figure 5.21b and c).

5.2.5. Nlrc3 KD and KO Cells Formed More Organoids

Stem cells forming the intestinal crypts give rise to a mini-gut structure called organoids in culture. Since a negative correlation between Nlrc3 expression and cell proliferation was found, the effect of Nlrc3 KD or KO on organoid formation was tested (Figure 5.22). Infected cells were sorted and an equal number of cells was plated for each condition and the number of spontaneously formed organoids was counted (Figure 5.22a).

sgNlrc3-G2 infected cells formed 1.8 fold more organoids compared to sgtdTomato infected cells (Figure 5.22b and c). Similarly, shNlrc3 infected cells formed 2.3 fold more organoids compared to shcontrol infected cells (p=0,02, Figure 5.23a and b).

In conclusion, KD or KO of Nlrc3 resulted in higher organoid formation, meaning higher stemness capacity and higher proliferation.

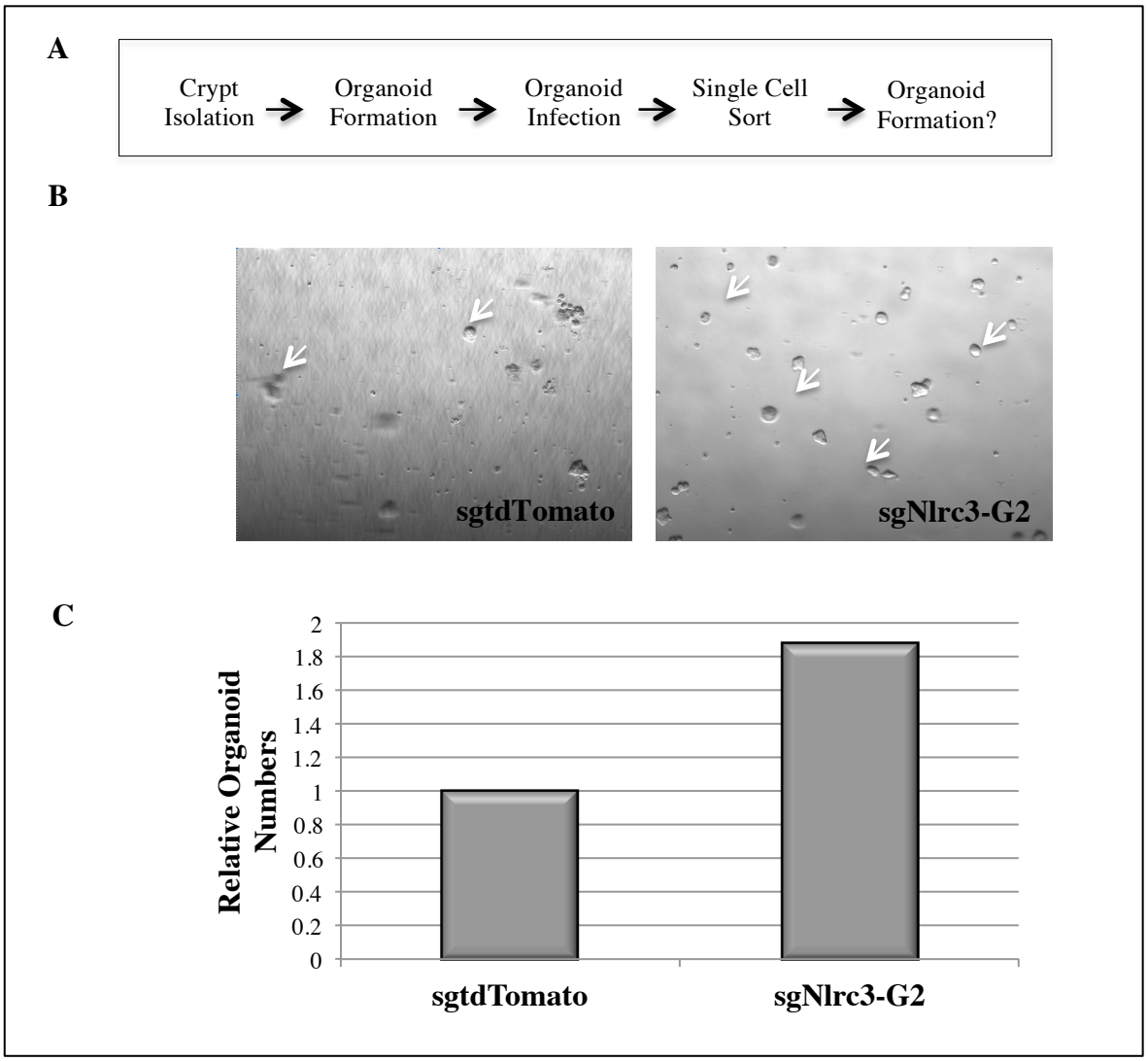

Figure 5.22. Nlrc3 KO cells form more organoids. (A) Experimental strategy. (B) Pictures of organoids formed by Nlrc3 KO and control cells 4 days after sorting. (C) Quantification of organoid formation by Nlrc3 KO and control cells.

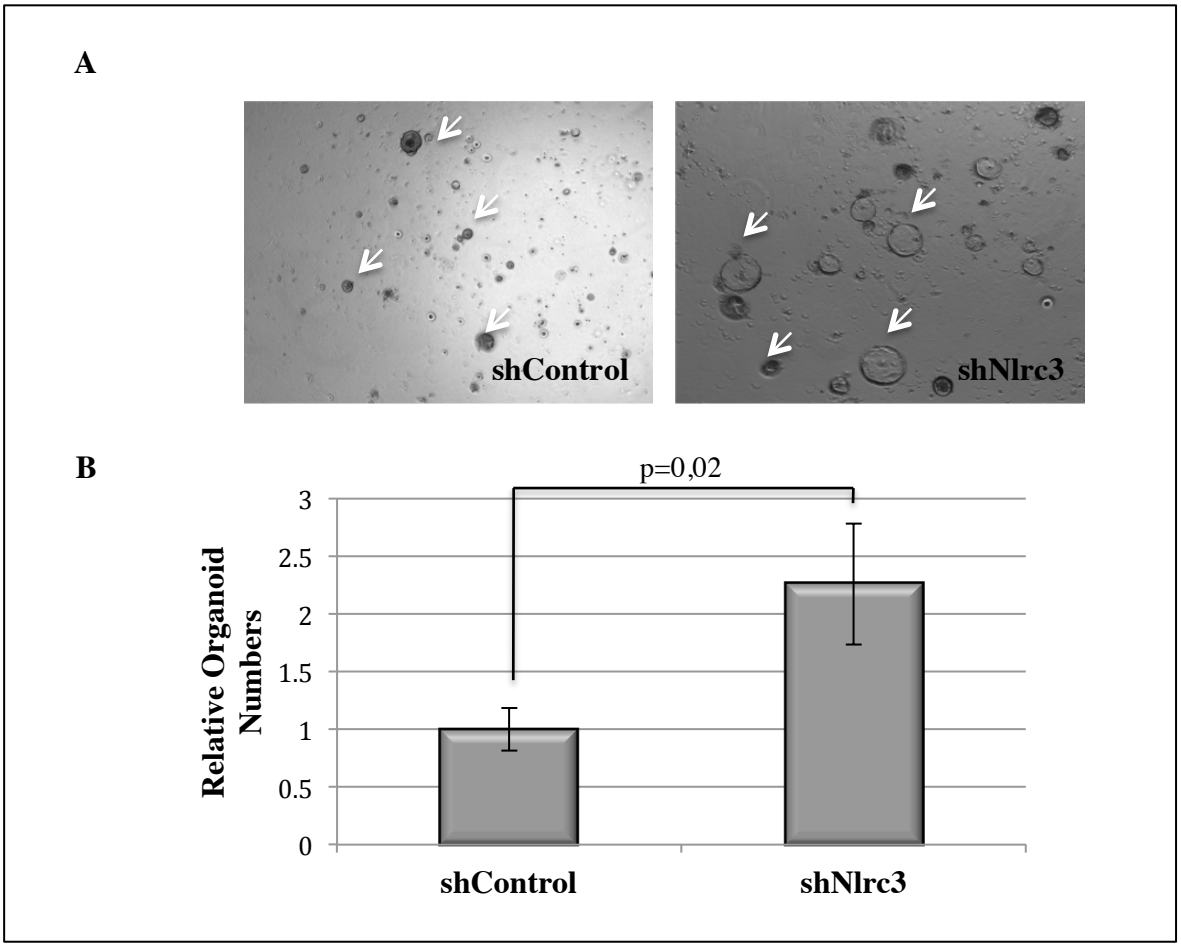

Figure 5.23. Nlrc3 KD cells form more organoids. (A) Pictures of organoids formed by Nlrc3 KD and control cells 7 days after sorting. (B) Quantification of organoid formation by Nlrc3 KD and control cells. Arrows show organoids.

5.2.6. NLRC3 Overexpression Inhibited Organoid Formation

NLRC3 was cloned into pLenti-CMV vector in order to be able to overexpress it in cells (Figure 5.24a). Organoids from the small intestine were infected with pLenti-CMV-NLRC3 or control pLenti-CMV vectors and selected with blasticidin. Live cells were sorted and equal amount of cells were plated to assess organoid formation.

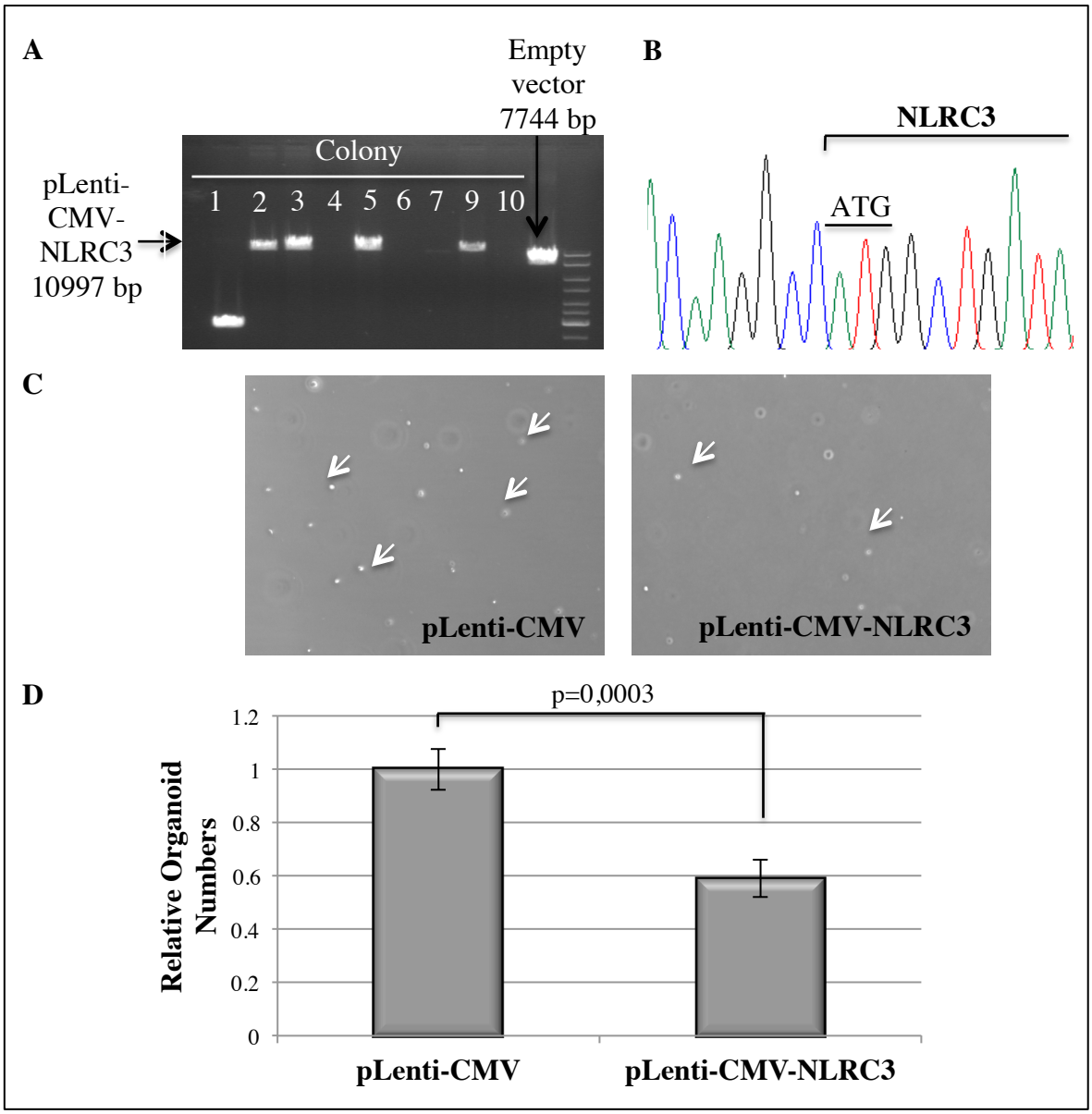

Figure 5.24. NLRC3 overexpression inhibits organoid formation. (A) Analytic digestion with XbaI enzyme result. (B) Sequencing result of NLRC3 cloning with CMV-F primer. (C) Pictures of organoids formed by NLRC3 overexpressing and control cells three days after sorting. Arrows show organoids. (D) Quantification of organoids. The number of organoids was counted in four different wells for each condition and normalized to the total number of cells. The ratio for pLenti-CMV was assigned as 1 a.u.

Whereas pLenti-CMV control cells formed 128 ± 9,8 organoids 3 days after sorting, pLenti-CMV-NLRC3 expressing cells only formed 75,6 ± 9 organoids (p=0,0003, Figure 5.24).

Thus, overexpression of NLRC3 in cells inhibited proliferation. Both control and NLRC3 expressing cells stopped growing and died 2 weeks after sorting probably due to the stress induced by blasticidin selection and sorting. Total RNA could not be isolated to verify NLRC3 overexpression in infected cells.

5.2.7. Molecular Mechanism of the Inhibition of Organoid Formation by Nlrc3

To determine the molecular mechanism that leads to less organoid formation in NLRC3 overexpressing cells and higher organoid formation in Nlrc3 KD and KO cells, stem cell marker (Lgr5) and proliferation marker (CyclinD1) levels were determined in control and Nlrc3 KO organoids (Figure 5.25). Both Lgr5 (8 fold) and CyclinD1 (2 fold) mRNA levels were upregulated in Nlrc3 KO organoids compared to control Nlrc3 expressing counterparts. Taken together, one can speculate that silencing of Nlrc3 gives a stemness character to cells and makes them proliferate.

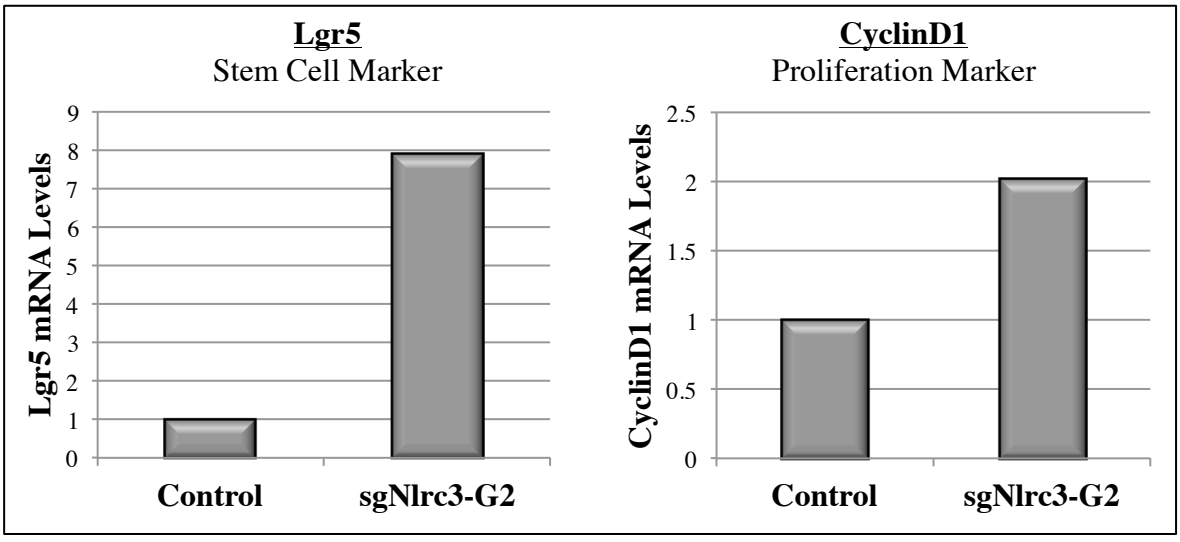

Figure 5.25. Nlrc3 KO organoids express higher Lgr5 and CyclinD1. RNA was isolated from sgNlrc3-G2 and sg-tdTomato (control) organoids and Lgr5 and CyclinD1 mRNA levels were determined by qPCR. Lgr5/Actin and CyclinD1/Actin mRNA levels normalized to control ratios are shown.

5.3. NLRC3's Role in Immune Tolerance Mechanisms

5.3.1. NLRC3 Is Expressed in Cell Lines From Immune Tolerance Sites

NLRC3 was previously shown to be highly expressed in T-cell lines by RT-PCR (Conti *et al*., 2005). To test its expression in immune privileged sites, human cell lines from endometrium cancer (Hec1A and Hec1B), from trophoblast (Swan71), from placental choriocarcinoma (JAR) and from testicular seminoma (Tera-2) were purchased. MIO-M1 glial cell lines from human retina were also used. THP-1 and Jurkat cells were used as positive controls for NLRC3 expression (Figure 5.26).

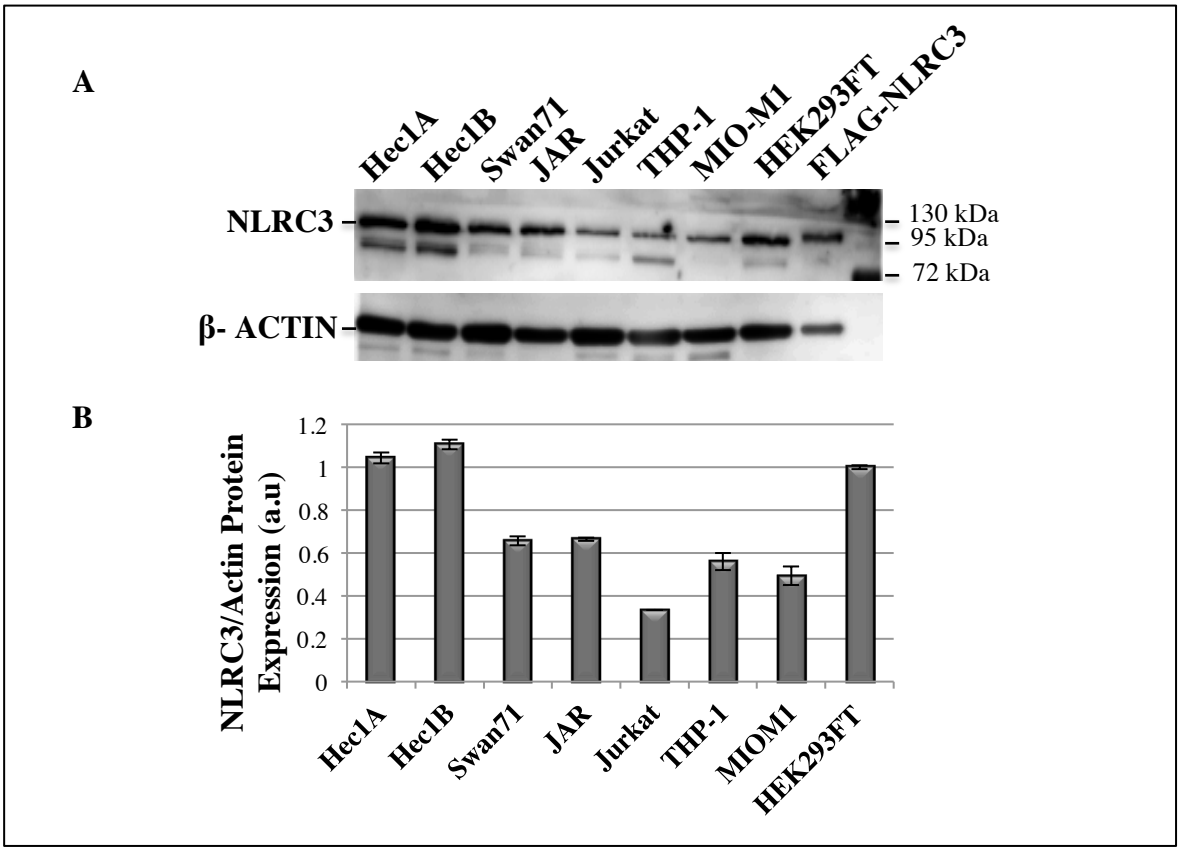

Figure 5.26. NLRC3 is expressed in cell lines from immune tolerant sites. (A) Western blot results of NLRC3 and β-Actin expression. (B) Quantification of Western blot results by ImageJ software. NLRC3/Actin bands intensity for HEK293FT were set as 1 and others were normalized to it.

NLRC3 was expressed in all cell lines tested (Figure 5.26a). NLRC3 protein was highly expressed in endometrium cell lines (Hec1A and Hec1B) compared to other lines and its level was similar between trophoblastic and placental cell lines (Swan71 and JAR respectively) and monocytic cell line THP-1 (Figure 5.26b). Tera-2 cells also expressed NLRC3 (Figure 5.27b).

According to these results, NLRC3 is expressed in all human cell lines derived from immune privileged sites and may be still a potential immune tolerance regulator.

5.3.2. Nlrc3 is Expressed in Tissues From Immune Tolerance Sites

A previous study showed that NLRC3 was expressed at very low levels in the testis, uterus, placenta and brain of mice by microarray. These levels were higher in human brain and uterus compared to other tissues in human and to mice tissues (Conti *et al*., 2005). After determining that NLRC3 is expressed in human cell lines, Nlrc3 expression in primary tissues was detected by Western blotting (Figure 5.27) and immunohistochemistry analyses (Figure 5.27).

Four tissues from mouse immune privileged sites (brain, eye, ovary and testis) were examined for Nlrc3 protein expression by Western blotting (Figure 5.27a). Nlrc3 was abundantly present in mouse brain and moderately expressed in the eye and testis. On the other hand, Nlrc3 protein was absent in the ovary. Nlrc3 expression in the eye and testis were further confirmed by extracting a second set of eye and testis tissues (Figure 5.27b and 5.27c).

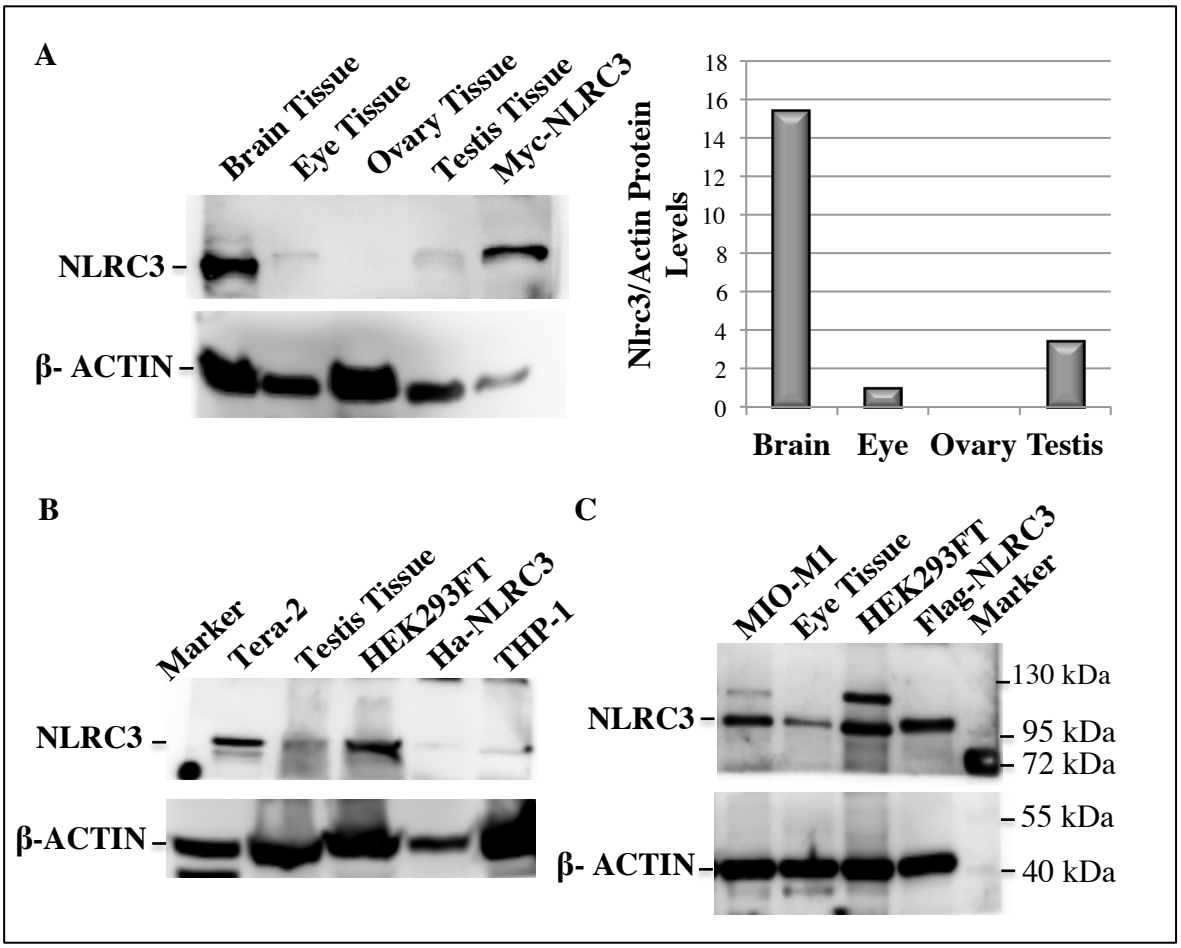

Figure 5.27. Nlrc3 is expressed in tissues from immune tolerance sites. (A) Nlrc3 expression in BALB/c mouse immune privileged tissues. Left: Western blot results. Right: Quantification of Western results with ImageJ software. Nlrc3 expression in eye which was the lowest between brain and testis was considered as 1 arbitrary unit and Nlrc3 protein expression in other tissues were normalized to 1. (B) Nlrc3 expression in BALB/c mouse eye. (C) Nlrc3 expression in BALB/c mouse testis.

Nlrc3 expression was also verified by immunostaining in the brain (Figure 5.28). Tissue sections were taken and stained with anti-NLRC3 antibody or only the secondary antibody as negative control. DAPI staining was also performed to visualize cell nuclei. Nlrc3 protein was expressed in different sections of the brain (Figure 5.28a and 5.28b) thus confirming Western blot results.

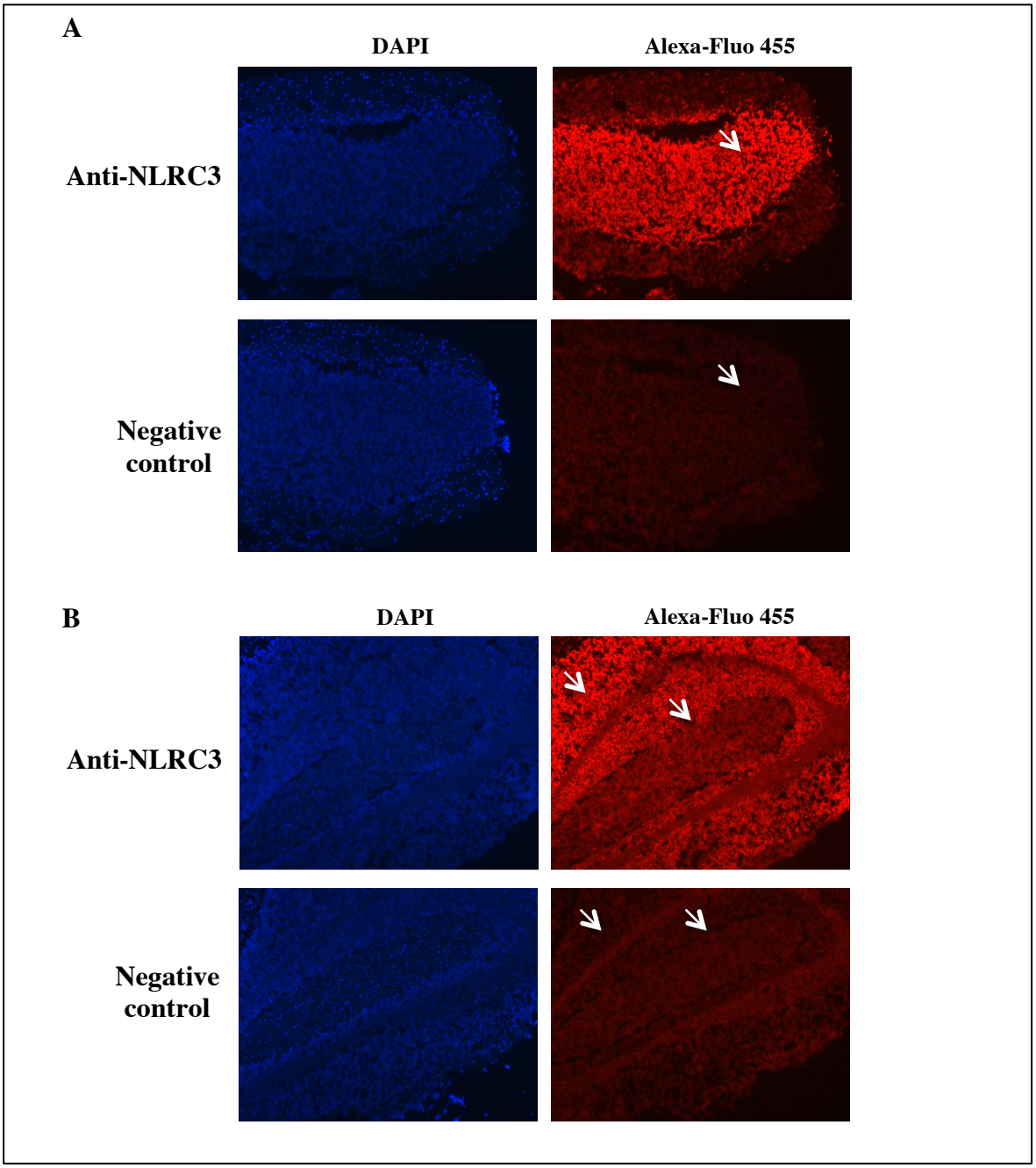

Figure 5.28. Immunohistochemistry of Nlrc3's expression in mouse brain. 10 µm medial (mid-sagital) sections of the brain at 10X magnification from (A) Olfactory bulb; (B) Cerebellum. Arrows show differences in Nlrc3 expression between negative control and anti-NLRC3 antibody treated samples. Representative images are shown.

In conclusion, NLRC3 was expressed in all human cell lines derived from endometrium, trophoblast, placenta, eye and testis. Furthermore, Nlrc3 protein was present in mouse brain, eye and testis but not in ovary.

5.3.3. Cryopyrin Inflammasome Components Expression in IPS

One of the possible mechanism through which NLRC3 may regulate immune tolerance is through Cryopyrin inflammasome inhibition. To validate this hypothesis, we determined whether inflammasome components Cryopyrin, ASC and Caspase-1 were expressed in human cells from immune privileged sites (IPS).

According to our Western blot results, Cryopyrin were endogenously expressed in Hec1A, Hec1B endometrium cells; Swan71, JAR placental cells and Tera-2 testicular seminoma lines. Jurkat, THP-1 and HEK293FT cells were used as positive controls for Cryopyrin expression. MIO-M1 derived from eye expressed very low levels of Cryopyrin (Figure 5.29a).

The adaptor protein ASC was not expressed in any cell line from immune privileged sites. Its expression was only seen in THP-1 monocytic cells used as positive control. HEK293FT cells were used as negative control for ASC expression (Figure 5.29b). Caspase-1, the downstream element of Cryopyrin inflammasome, was expressed in all tested cell lines (Figure 5.29c). THP-1 cells were used as positive control for Caspase-1 expression.

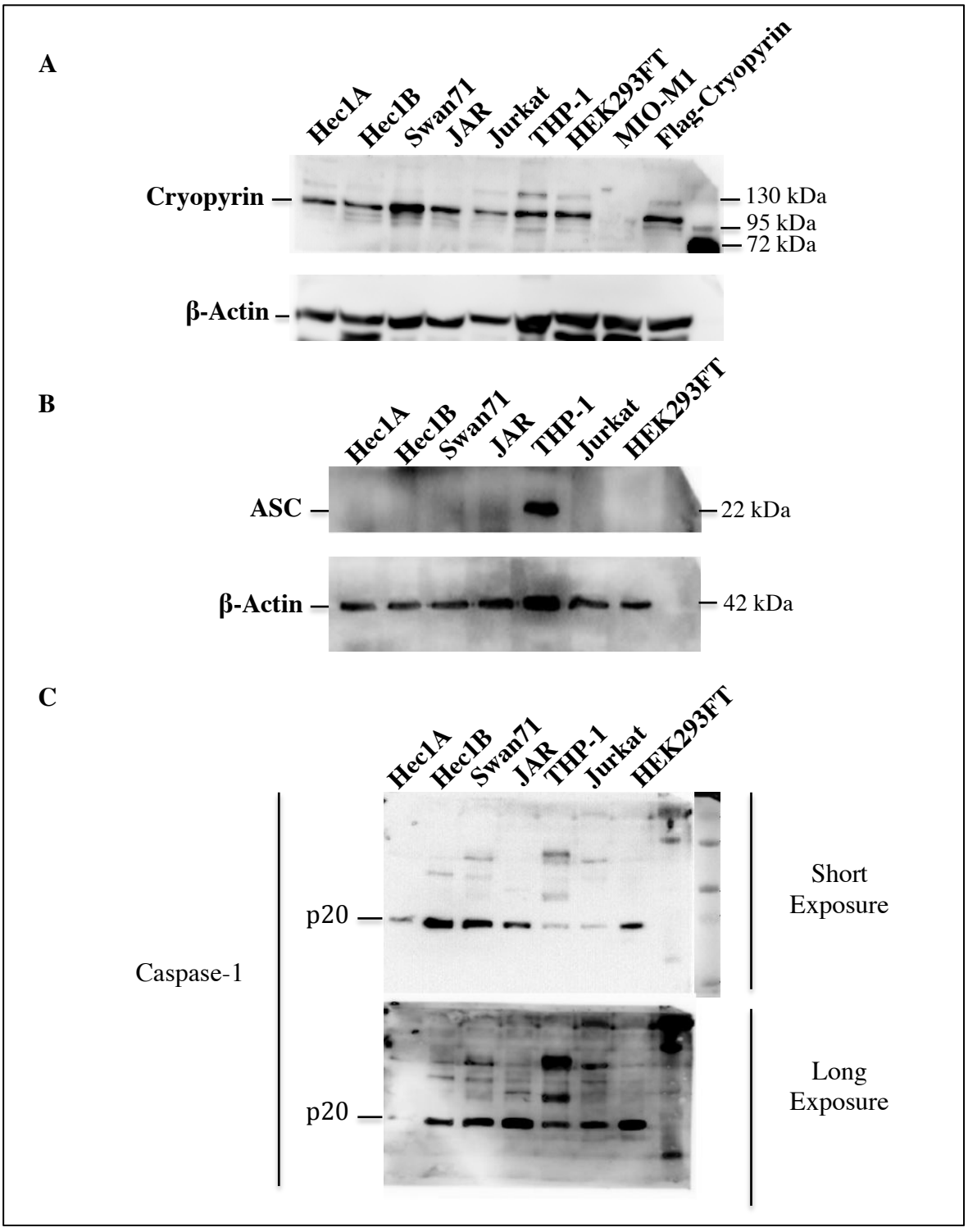

Figure 5.29. Inflammasome components are expressed in cell lines from IPS. (A) Cryopyrin expression; (B) ASC expression; (C) Caspase-1 expression in immune privileged sites.

We also tested inflammasome components expression in mouse tissues (Figure 5.30). Cryopyrin protein was present in the eye of BALB/c mice. THP-1 and Ha-NLRC3 transfected HEK293FT cells were used as positive controls for Cryopyrin expression. However, MIO-M1 cells derived from human eye did not express Cryopyrin at the basal state (Figure 5.30a).

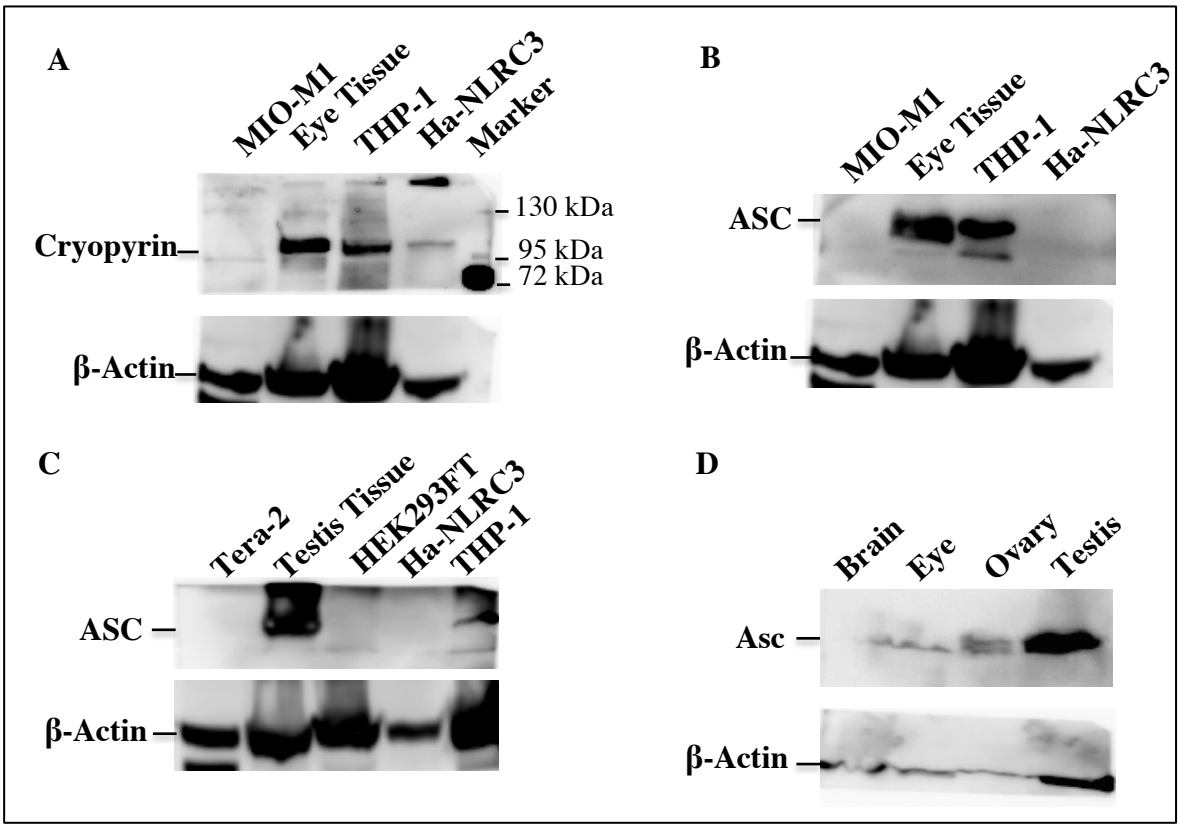

Figure 5.30. Cryopyrin and Asc are expressed in primary tissues. Eye and testis were extracted from BALB/c mice and 60 μg of proteins were loaded on gel. (A) Cryopyrin expression in the eye and MIO-M1 cell lines. (B) Asc expression in the eye and MIO-M1 cells lines derived from eye. (C) Asc expression in testis and Tera-2 cell lines derived from testis. (D) Asc expression in different tissues.

Asc adaptor protein was expressed in the eye and the testis tissues but not in MIO-M1 and Tera-2 cell lines derived from human eye and teratoma respectively. HEK293FT and Ha-NLRC3 transfected HEK293FT cells were used as negative control for ASC expression whereas THP-1 monocytic cell lines were positive controls (Figure 5.30b and 5.30c).

Overall, NLRC3 was found to be expressed in all cell lines (**Table 5.1**) and tissues tested except for the ovary (**Table 5.2**). While Cryopyrin and Caspase-1 were expressed in all cells, ASC protein was absent in cell lines but expressed in primary tissues.

Table 5.1. Summary of protein expression in human cell lines. +: indicated proteins are expressed, -: indicated proteins are not expressed, nd: non-determined.

	Hec1A	Hec1B	Swan71	JAR	Tera-2	MIO-M1	Jurkat	THP-1	HEK293FT
NLRC3	+	+	+	+	+	+	+	+	+
Cryopyrin	+	+	+	+	+	-	+	+	+
ASC	-	-	-	-	-	-	-	+	-
Caspase-1	+	+	+	+	nd	nd	+	+	+

Table 5.2. Summary of protein expression in mouse tissues. +: indicated proteins are expressed, -: indicated proteins are not expressed, nd: non-determined.

	Brain	Eye	Ovary	Testis
Nlrc3	+	+	-	+
Cryopyrin	nd	+	nd	nd
Asc	-	+	+	+

5.3.4. NLRC3 is Localized in the Nucleus

Because of potential modulation of HLA proteins' transcription by NLRC3, subcellular localization of NLRC3 was determined (Figure 5.31).

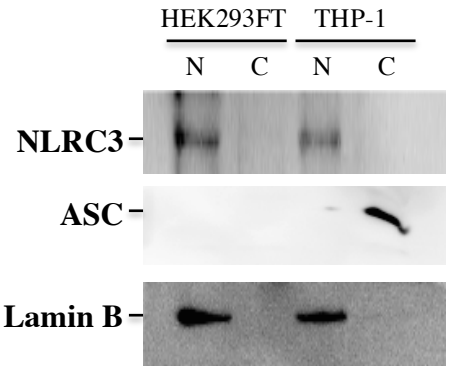

Figure 5.31. Subcellular localization of NLRC3. Lysates from HEK293FT and THP-1 cells were separated into nuclear (N) and cytoplasmic (C) fractions.

Endogenous NLRC3 was localized into the nucleus of HEK293FT and THP-1 cells. NLRC3 had the same expression pattern as Lamin B which was also in the nucleus as expected. ASC was used as negative control, since it is well known that ASC is not expressed in HEK293FT cells and that ASC is into the cytoplasm of THP-1 cells.

6. CONCLUSION and DISCUSSION

6.1. NLRC3 is a Novel Inhibitor of the Cryopyrin Inflammasome

In the first part of this PhD thesis, we characterized the function of NLRC3, a novel protein belonging to the NLR family, with very limited number of groups that was working on it and that had one publication at the time we started the project. Because the Cryopyrin inflammasome was associated with many diseases and a large number of stimulants were identified, we investigated whether NLRC3 could have an effect on specifically this inflammasome. Based on the inhibitory effect of NLRC3 on the NFκB pathway that was previously described, we hypothesized that NLRC3 may also be a suppressor of the Cryopyrin inflammasome.

In order to elucidate the physiological roles of NLRC3, we decided to study endogenous NLRC3 protein's function. For this purpose, we cloned full-length His-tagged NLRC3 and NLRC3's domains separately into a bacterial expression vector to generate polyclonal and monoclonal antibodies (not shown). In parallel, commercially available anti-NLRC3 antibody was purchased and optimized in order to detect endogenous NLRC3. Endogenous NLRC3 was detected using the commercial antibody at about 104 kDa, in comparison to by tagged NLRC3 proteins that were 1 kDa higher in the gel (Figure 5.1). The specificity of the antibody was further confirmed by NLRC3 knockdown experiments, where we showed that the band suspected to be NLRC3 disappeared in KD cells (Figure 5.4a). Since the commercial antibody was working perfectly, the generation of a novel NLRC3 antibody process was ended after successful immunization of mouse because of time concerns.

The expression of NLRC3 was detected at protein level in HEK293FT and THP-1 cells (and some other epithelial cells from immune privileged sites that will be discussed later). To be able to control each component of the complex, HEK293FT cells that do not express ASC protein and negligible levels of pro-Caspase-1 and pro-IL-1β at the basal level were used. These proteins were transfected into HEK293FT cells together with

Cryopyrin or Cryopyrin and NLRC3. Overexpression of Cryopyrin bypassed the priming step by NFκB pathway that is necessary for inflammasome activation and induced IL-1β in a concentration dependent manner (Figure 5.2). Interestingly, when Cryopyrin was co-transfected with NLRC3, IL-1β levels in the supernatant significantly decreased suggesting that NLRC3 has an inhibitory role on Cryopyrin-induced IL-1β secretion independently of the NFκB pathway.

NLRC3's function was then tested in THP-1 human monocytes. Inflammasome activation protocol was established in WT THP-1 cells for known Cryopyrin inflammasome stimulants ATP, Nigericin and MSU (Figure 5.3). Treatments were performed on 10^6 to 2 x 10^6 cells in 6 well-plate instead of 12 or 24 well-plates and longer incubation times were used compared to the literature. For these reasons, higher IL-1β concentrations than usual were obtained. Optimal stimulant concentrations and treatment times were determined.

Then, different shRNAs directed against NLRC3 were obtained from the Broad Institute and their efficacy was determined by transient infection of HEK293FT cells. All tested shRNAs reduced NLRC3 protein levels (Figure 5.4b). NLRC3 KD THP-1 stable cell lines were generated (Figure 5.4) by lentiviral infection of these cells and selection with Puromycin which concentration was determined with a kill curve (not shown). shD7-infected THP-1 cells were lost during culture. Whereas shD8 did not have an effect on NLRC3 levels compared to the control (shLuc), shD9 reduced NLRC3 levels by 76% and shD6 by 34%. Since they had the highest decrease in NLRC3 levels, shD9 cell lines were used in our experiments. The difference seen in the efficacy of shRNA between HEK293FT and THP-1 cells can be explained by two fundamental phenomenon: first of all, HEK293FT are cells that grow very well in culture and into which transfection is very easy whereas culture of THP-1 cells is very delicate and can only be transfected by spinoculation. Thus, shRNAs may be less effective in THP-1 compared to HEK293FT cells due to a decrease of transduction efficiency coming from the nature of the cells. Secondly, HEK293FT cells were transiently transduced whereas THP-1 cells underwent longer antibiotic selection process that could give time to shRNAs integrated into the genome to be completely lost or silenced by methylation.

Treatment of Cryopyrin inflammasome by ATP, Nigericin and MSU resulted in significantly higher IL-1β secretion in shNLRC3 cells compared to shLuc (Figure 5.5). Experiments were conducted in 3-4 independent sets of experiment and gave the same secretion pattern. IL-1β secretion was not significantly different in THP-1 only differentiated into macrophage between WT and NLRC3 KD cells. Moreover, not only secretion but also cleavage of pro-IL-1β into the cell was higher in NLRC3 KD cells compared to the control in response to Nigericin treatment. Pro-IL-1β levels were similar in the WT and KD cells (Figure 5.6).

In summary, NLRC3 inhibited Cryopyrin inflammasome in endogenous system independently of the stimulant, confirming the previous results. ATP and Nigericin activate Cryopyrin inflammasome by inducing potassium efflux whereas MSU trigger lysosomal rupture. Results show that NLRC3 KD has an effect on both pathways. Thus, the inhibition is exerted upstream of potassium efflux and lysosomal rupture.

We also tried to show how pro-Caspase-1 cleavage is affected in treated cells however we could not optimize Western blotting to detect cleaved 10 kDa p10 band on membrane with the commercially available antibody. Detection of the cleaved band is known to be problematic and most of the time irreproducible.

To determine whether NLRC3 is an inhibitor specific of Cryopyrin inflammasome or if it can also inhibit other inflammasomes, THP-1 cells were stimulated with *Pseudomonas aeroginosa* which is a specific activator of IPAF inflammasome. shNLRC3 cells secreted significantly more IL-1β compared to the WT (Figure 5.7), suggesting that NLRC3 also inhibits IPAF inflammasome. Because Cryopyrin and IPAF have ASC, pro-Caspase-1 and IL-1β in common, we concluded that NLRC3 inhibits downstream of the receptor proteins.

Once we identified that besides suppression of NFκB pathway, NLRC3 also inhibits Cryopyrin and IPAF inflammasomes, we decided to elucidate molecular mechanism of this inhibition. NLRC3 was shown to inhibit NFκB pathway by ubiquitination of TRAF6 on K63 and targeting to proteaosome for degradation (Schneider *et al*., 2012). NLRC3 did not change Cryopyrin, ASC and IL-1β levels (Figure 5.8). Thus, NLRC3 may inhibit Cryopyrin inflammasome by a mechanism other than the degradation of proteins.

When Cryopyrin inflammasome gets activated, ASC and Caspase-1 interacts with each other and form a protein complex called “speck” which constitutes a platform for pro-IL-1β activation. First of all, we showed that ASC speck formation correlates with Cryopyrin inflammasome activation in both THP-1 ASC-EGFP stable lines treated with Nigericin and Nigericin treated WT THP-1 cells stained for endogenous ASC specks. Whereas Cryopyrin overexpression induced ASC speck formation in HEK293FT ASC-EGFP cells, NLRC3 transfection had no effect alone (Figure 5.9). However, co-transfection of Cryopyrin and NLRC3 significantly inhibited Cryopyrin-induced ASC speck formation in NLRC3-concentration dependent manner. We concluded from this experiment that NLRC3 disrupts Cryopyrin inflammasome assembly by interfering with ASC speck formation.

We next investigated whether NLRC3 interacts with Cryopyrin inflammasome components. NLRC3 did not interact with Cryopyrin (Figure 5.10). Since Cryopyrin does not have a CARD domain, NLRC3 may need ASC adaptor protein to interact with Cryopyrin. Co-transfection of Cryopyrin, ASC and NLRC3 did not induced NLRC3 and Cryopyrin interaction, suggesting that NLRC3 is not in contact with Cryopyrin. This finding is in favor with our previous results that showed that NLRC3 was acting downstream of effector proteins on probably ASC/Caspase-1 interface. On the opposite, NLRC3 interacted endogenously with both ASC and pro-Caspase-1 (Figure 5.10). Because of the bands that were detected, we determined that NLRC3 interacts with the CARD domain of pro-Caspase-1.

Endogenous immunostaining of THP-1 cells reveled that NLRC3 protein does not co-localize in ASC specks (Figure 5.11). The absence of NLRC3 in ASC speck was further confirmed by western blotting (Figure 5.11). Thus, NLRC3 inhibitory effect might be exerted before ASC speck formation. It may bind to CARD domain of ASC and pro-Caspase-1 and block ASC/pro-Caspase-1 interaction by occupying their CARD domain and disrupt ASC speck formation.

To further elucidate the molecular mechanism of NLRC3’s inhibition, we identified the domain of NLRC3 responsible for the inhibition. Similar to the full-length NLRC3, separate domains had no effect on ASC speck formation on their own (not shown).

However, the expression of CARD, LRR, CARD/NACHT and NACHT/LRR significantly decreased Cryopyrin-induced ASC speck formation (Figure 5.13). Only NACHT domain alone did not disrupt ASC speck assembly. It is understandable that CARD and CARD/NACHT affect ASC speck formation because NLRC3's CARD may compete for ASC binding with pro-Caspase-1. However, it is unclear to us why LRR domain which exact function is not yet known may inhibit speck formation. LRR domain is in general associated with pathogen sensing.

CARD domain mediates assembly of ASC and pro-Caspase-1 and speck formation (Proel *et al*., 2013). ASC and pro-Caspase-1 residues indispensable for speck formation were previously identified (Narayanan *et al*., 2014 and Narayanan *et al*., 2015). When one of these residues was mutated, ASC speck formation was inhibited. Alignment of NLRC3's CARD domain with ASC and pro-Caspase-1 showed that overall CARD domains are 30% identical between NLRC3 and pro-Caspase-1 and 41% identical between NLRC3 and ASC. Some of the residues important for ASC/pro-Caspase-1 binding and ASC speck formation were conserved between ASC, Caspase-1 and NLRC3 (Figure 6.1).

A protein encoding only a CARD domain named CARD8 was shown to inhibit Cryopyrin inflammasome by binding to pro-Caspase-1 (Razmara *et al*., 2002) and ASC speck formation (Ito *et al*., 2014). NLRC3 contains a CARD domain and may interfere with ASC and Caspase-1 CARD/CARD interaction, then disrupting ASC specks. This hypothesis could be confirmed by competition assay and co-immunoprecipitation of ASC and Caspase-1 in the presence of increasing concentrations of NLRC3.

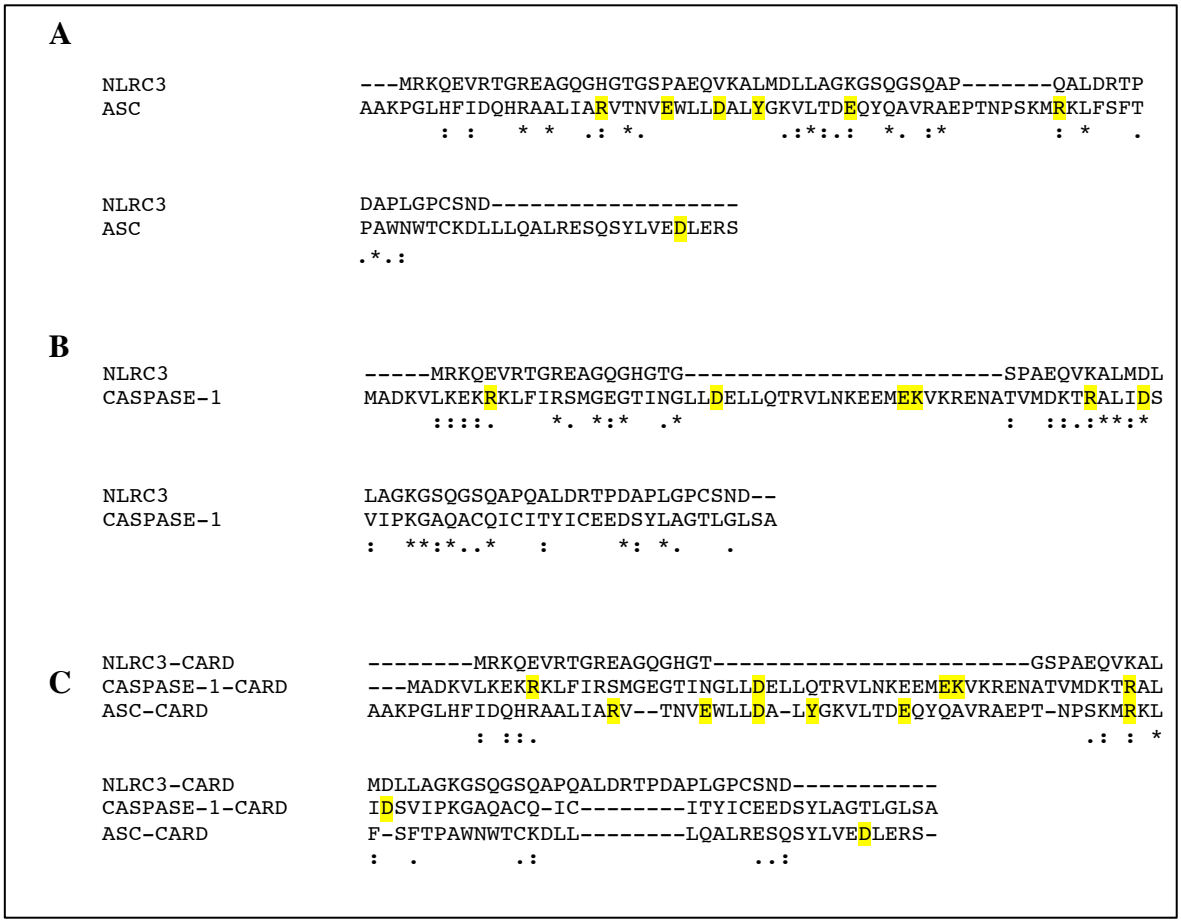

Figure 6.1. Alignment of CARD domains. CARD of human NLRC3 and ASC (A) or NLRC3 and pro-Caspase-1 (B) or all three (C) were aligned. Residues necessary for ASC speck formation are highlighted. "*" means identical residue, ":" means conservative, "." means semi-conservative alignments.

Finally, we also investigated NLRC3's *in vivo* effect on Cryopyrin inflammasome. Since we did not have NLRC3 KO mouse to isolate peritoneal macrophages, stimulate them with Cryopyrin activators and compare their IL-1β secretion with control macrophages, we followed a different experimental strategy. Acute conjunctivitis was induced in rat eye by injection of LPS into the vitreous. Myc alone and Myc-tagged NLRC3 proteins were expressed in HEK293FT cells and purified by anti-Myc immunoprecipitation and injected into the eye. In preliminary experiments that are not shown in this thesis, Myc-NLRC3 injected eye secreted less IL-1β compared to Myc injected control.

As an alternative, we used an *in vivo* Cryopyrin inflammasome activation model, by inducing acute colitis by DSS treatment. We showed that colitis occurred since colons were shortened and mice lost weight. Interestingly, NLRC3 mRNA levels were down-regulated in crypts isolated from colitis induced intestines compared to control (Figure 5.14). So, NLRC3's expression was also negatively correlated with Cryopyrin inflammasome activation *in vivo*. Another interesting aim was to induce colitis and put NLRC3 protein back by injection of pLenti-CMV-NLRC3 containing virus. Because virus transduction efficiency was very low in the colon (tested with Apc KD encoding virus by a colleague) and because even if we could express NLRC3, the expression would be local and we could not see a change in the structure of the colon or in cytokine secretion, this experiment was not performed. For publication, MSU-induced peritonesis and acute conjunctivitis will be induced in mice and purified NLRC3 or pLenti-CMV-NLRC3 virus will be introduced to the infection site and a potential *in vivo* inhibition of Cryopyrin-induced inflammation by NLRC3 will be determined.

The regulation of NLRC3's protein level in response to NFκB activation was also investigated and we found that NLRC3 protein levels are decreased when NFκB pathway is activated (Figure 5.15). Then, NFκB pathway negatively regulates NLRC3 levels.

In summary, we propose that when the cells are treated by pro-inflammatory stimulants, TLR receptors are activated and induce NFκB pathway. NFκB signaling in turn induces the expression of pro-inflammatory cytokines and inflammasome components and represses NLRC3 expression. Once Cryopyrin inflammasome proteins reach a certain expression level, the inflammasome gets activated resulting in IL-1β secretion from cells. During inflammasome activation, NLRC3 protein levels increase gradually and exerts its inhibitory effect on two levels: first of all, NLRC3 inhibits NFκB pathway by targeting TRAF6 protein (inflammasome protein and pro-inflammatory cytokine levels are decreased) and secondly, it may disrupt ASC/Caspase-1 interaction thus inactivating inflammasome complex (Figure 6.2).

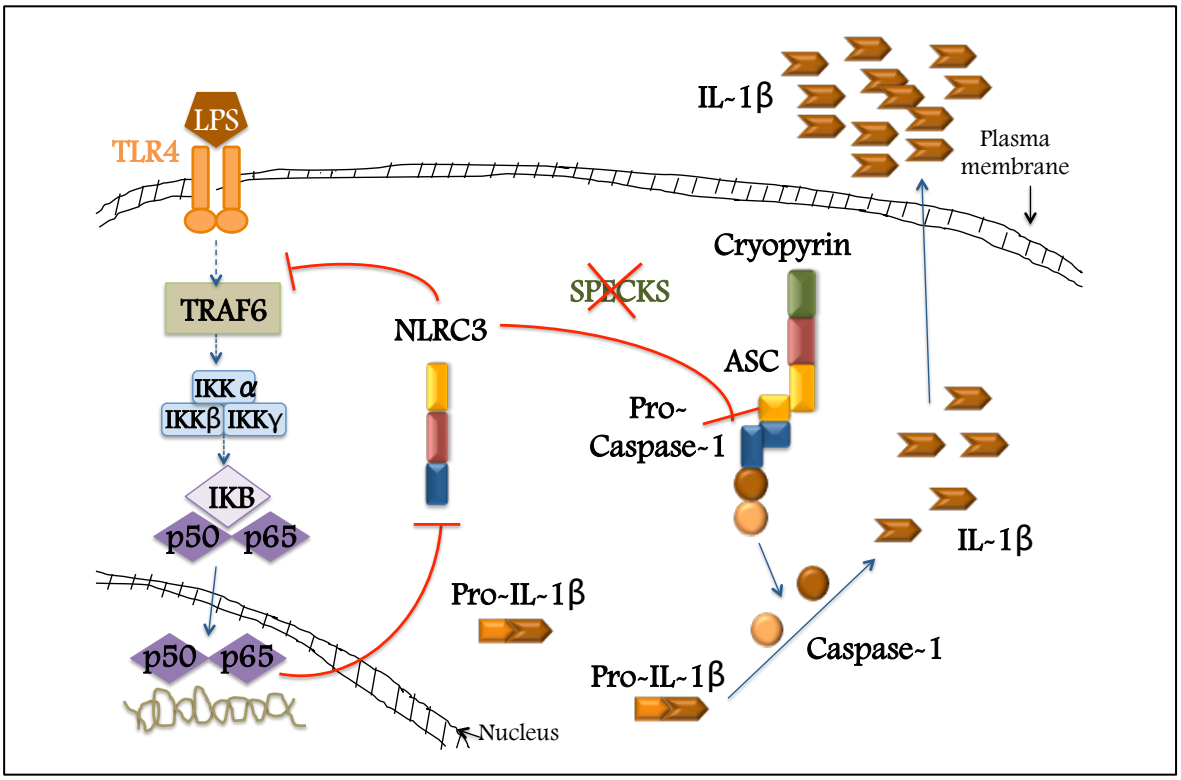

Figure 6.2. Proposed model of inflammasome regulation by NLRC3.

6.2. Nlrc3 Inhibits Cell Proliferation and Tumor Formation

In the second part of this thesis we determined whether Nlrc3 has an effect on cell proliferation and tumorigenesis. Nlrc3 was expressed in both the small intestine and colon and its expression was higher in the colon compared to the small intestine (Figure 5.16).

Since some inflammasome forming proteins, such as AIM2, are implicated in cancer, we assessed whether Nlrc3 expression is changing during cancer formation. For this purpose, Apc KO organoids from the colon and the small intestine were generated and Apc KO was confirmed by visualization of an increase of Wnt pathway's target genes Axin2 and others genes (Figure 5.17). Interestingly, Nlrc3 levels were down-regulated by 8 to 10 fold in the small intestine and colon in Apc KO organoids compared to controls. Cancer is aggravated by accumulation of Apc and Kras mutations. Nlrc3's mRNA levels were

decreasing gradually from control to Apc and Apc Kras KO organoids. Thus, there was a negative correlation between Nlrc3 expression and cancer stage. In favor of our findings, a very recently published paper has shown that Nlrc3 levels are down-regulated in patients with colorectal cancer (Liu *et al*., 2015).

To assess whether Nlrc3 is differentially expressed in different cells of the intestine, stem cells, Paneth cells and transit amplifying cells were isolated and qPCR was performed. Because only 500 cells were used, RNA quality was not that good and we got huge error bars for our samples obtained. Nonetheless, in cells isolated from four different mice, Nlrc3's expression was higher in Paneth cells compared to stem cells and transient amplifying cells. In terms of cellular function, this result was expected because Paneth cells are immune cells of the intestine and Nlrc3 expression as an immune modulator in Paneth cells make senses. However, when considered with the decrease in Nlrc3 expression when cancer progresses, we can also withdraw the conclusion that Nlrc3's expression may negatively correlate with stemness and proliferation of cells. These hypotheses were further confirmed when Nlrc3 expression was analyzed in organoids from antibiotic treated and germ-free mice. In another project conducted in order to elucidate the effect of the microbiome on stemness, we found that in absence of any pathogen, organoids grew faster (not shown). Interestingly, Nlrc3's expression was higher in control organoids compared to more proliferative organoids from germ-free or antibiotic treated mice.

To clarify whether Nlrc3 has a directly role on the proliferation or whether the down-regulation of its expression is just a consequence of Wnt pathway activation, Nlrc3 KO, KD and Nlrc3-overexpressing organoids were generated. Nlrc3 KO organoids were generated by using CRISPR-Cas9 system. Between the two guides designed only one induced DNA cleavage and introduced mutations (Figure 5.20 and 5.21). qPCR analysis of these organoids reveled 70% reduction in Nlrc3 levels in sgNlrc3-G2 compared to the control (Figure 5.22). Because CRISPR-Cas9 is time consuming to generate, Nlrc3 was also knocked-down in organoids by using pLKO.1-shD7-tRFP vector. 40% of reduction in Nlrc3 expression was obtained in these KD cells (Figure 5.23).

Infected organoids were dissociated into single cells and cultured to measure their organoid formation capacity. Both Nlrc3 KO and KD cells produced significantly higher number of organoids than the control (Figure 5.22 and 5.23).

NLRC3-overexpressing organoids were also generated by using pLenti-CMV-NLRC3. Organoids were blasticidin selected but we did not obtain enough cells to perform qPCR. NLRC3-overexpressing cells formed less organoids compared to the control. If we assume that NLRC3 was overexpressed in these organoids, NLRC3 inhibited proliferation. These organoid formation assays should be repeated by doing a second independent infection of organoids.

We tried to rescue phenotype by re-expressing NLRC3 in Nlrc3 KD cells. However, transfection of Nlrc3 did not work. Rescue of phenotype in Apc KO organoids was also tried by re-introducing Nlrc3 without success.

In future experiments, Nlrc3 will be KO and KD in different cancer cell lines and will be tested for *in vivo* tumor formation, *in vitro* migration and its effect on cell cycle. NLRC3 could be also re-activated in Apc KO organoids to inhibit cell proliferation. For this purpose, pLenti-CMV-NLRC3 can be used or activator Cas9 system can be designed to bind NLRC3's promoter and activate endogenous NLRC3 in an inducible manner.

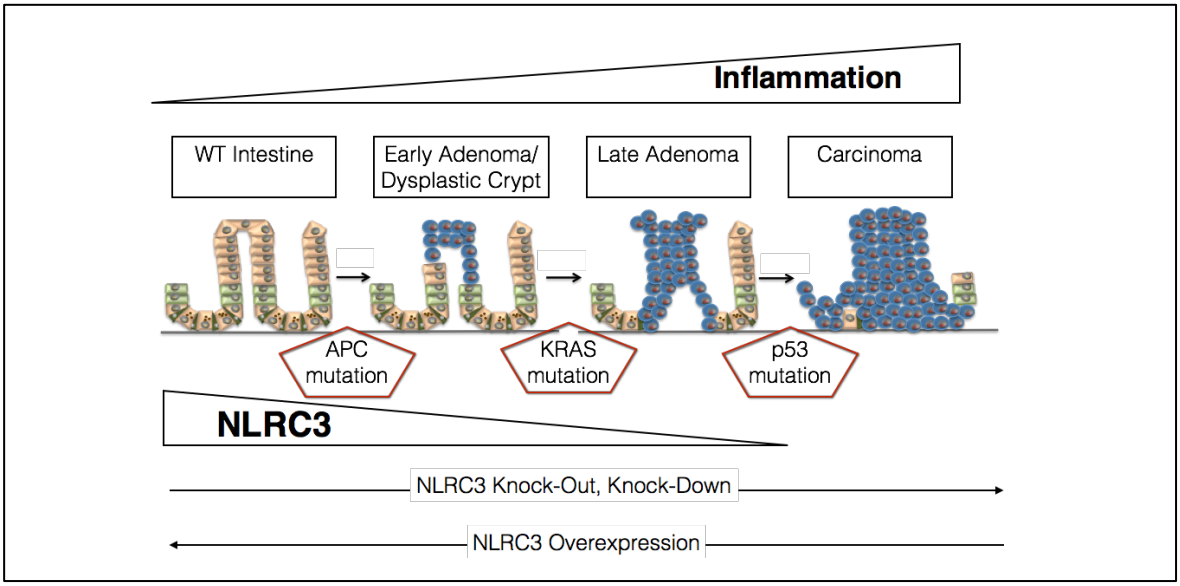

Figure 6.3. Proposed model for Nlrc3 and cancer.

6.3. NLRC3 and Immune Tolerance

In the third part of this thesis, potential implication of NLRC3 in immune tolerance mechanisms was investigated. Since some NLR family members were shown to be highly expressed only in tissues from immune tolerant organs, NLRC3 expression in these sites was checked out. Human cell lines from placenta, trophoblast, endometrium, brain, eye and testis were used. All the cells tested as well as THP-1 cells used as positive control expressed NLRC3 protein at the basal level without any treatment (Figure 5.26). So, NLRC3's expression was not restricted to immune cells but was also expressed in epithelial cells.

To confirm results obtained in human cell lines, primary tissues from mouse brain, eye, ovary and testis were analyzed for Nlrc3 expression. Nlrc3 was expressed in the brain, testis and eye at basal level, without any treatment but was absent in ovary (Figure 5.27). Western blot results were confirmed by immunohistochemistry in the brain, where Nlrc3 was present in the olfactory bulbs and cerebellum (Figure 5.28).

Nlrc3 protein was only absent in mouse ovary. As we did not have access to human tissues and did not have any cell line from human ovary, we do not know whether NLRC3 is expressed in human ovary or not. It can be also absent in human ovary or a different expression profile may exist between mouse and human.

In our experiments, anti-human NLRC3 antibody also recognized mouse Nlrc3. This commercially available antibody was derived from human C-terminal "ISEAIKTNAPTCTVE" sequence which is 100% identical to mouse C-terminal motif (e-value= 3e-16 in protein blast). Thus, it is expected that our antibody recognizes mouse Nlrc3.

The presence of NLRC3 in cell lines and primary tissues from immune privileged sites suggest that NLRC3 may have a role in immune tolerance mechanisms. Since we have shown that NLRC3 is a novel inhibitor of Cryopyrin inflammasome, its role can be through the regulation of this complex. Cryopyrin was expressed in all tested cell lines and

at a very negligible level in MIO-M1 cells. Caspase-1 was expressed in all tested cells. On the other hand, ASC was not expressed in any cell line used. It is known that Cryopyrin inflammasome components expressions are tightly regulated. These proteins' expression are activated by NFκB pathway induction. In our experiments, cells were not treated with any NFκB activator stimuli. This may be the reason of absence of Cryopyrin in MIO-M1 and ASC expression in the cell lines.

When primary mouse tissues were analyzed, Cryopyrin and Asc were expressed in the mouse eye. Asc was also expressed in testis and ovary but not in the brain (Figure 5.30). These differences between human cell lines and primary mouse tissues may result from differences from the two species or these proteins may be silenced in cell lines during immortalization. ASC is known to be silenced in cancer by DNA methylation (Salminen *et al*., 2014). It may undergo such a regulation in cell lines and in the mouse brain.

The second hypothesis is the regulation of tolerance by modulation of HLA proteins' expression by NLRC3. NLR family member CIITA was found to a transcriptional activator of MHC molecule expression (Steimle *et al*., 1994). Similarly, NLRC5 regulated the transcription of MHC class I molecules (Meissner *et al*., 2010) through its nucleotide binding domain (NBD, Meissner *et al*., 2012). To test if NLRC3 could have such a transcriptional factor activity, subcellular localization of NLRC3 was determined. In confocal microscopy of THP-1 cells stained with anti-NLRC3 antibody, NLRC3 formed a ring around the nucleus (not shown). Because the antibody we use is polyclonal, we could not decide whether it is an artifact or if NLRC3 is really located in the nucleus. To clarify this issue, subcellular fractionation was performed in HEK293FT and THP-1 cells. NLRC3 was present in the nucleus at the basal level (Figure 5.31).

Online Nuclear Localization Signal (NLS) detector software did not find any NLS in NLRC3's sequence. NLS sequence of NLRC5 was found to be in its CARD domain by mutational analysis and was identified as "HHGL**KR**PHQSCGSSP**RRK**QCKKQQ" (Meissner *et al*., 2012). Mutation of residues represented in bold inhibited nuclear transport of NLRC5. NLRC3 did not contain these NLS motifs in its sequence. Localization of each domain of NLRC3 in the nucleus should be tested and after the domain that translocates to the nucleus is identified, the NLS motif should be identified by site directed mutagenesis.

The localization of NLRC3 can also be determined by transfecting cells with GFP-tagged NLRC3 and co-staining with DAPI. Moreover, Leptomycin B that inhibits nuclear export can be used to see whether NLRC3 shuttles in the nucleus. If NLRC3 is localized in the nucleus, transcription of HLA molecules in GFP and GFP-NLRC3 expressing cells will be compared.

6.4. NLRC3: on the Crossroad of Inflammation, Stemness and Immune Tolerance

In summary, we showed for the first time in this PhD thesis that NLRC3 is an inhibitor of Cryopyrin inflammasome. NLRC3 inhibits pro-IL-1β cleavage, IL-1β secretion and ASC speck formation by interacting with ASC and/or pro-Caspase-1. Secondly, we showed that Nlrc3's expression negatively correlates with cell proliferation and stemness. We generated primary cells KO for NLRC3 with CRISPR-Cas9 technology. And finally, we showed that NLRC3's expression is not restricted to immune cells and that NLRC3 is also expressed in epithelial cells from immune tolerance sites. We determined that NLRC3 localizes in the nucleus.

REFERENCES

Aganna, E., F. Martinon, P. N. Hawkins, J. B. Ross, D. C. Swan, D. R. Booth, H. J. Lachmann, A. Bybee, R. Gaudet, P. Woo, C. Feighery, F. E. Cotter, M. Thome, G. A. Hitman, J. Tschopp and M. F. McDermott, "Association of mutations in the NALP3/CIAS1/PYPAF1 gene with a broad phenotype including recurrent fever, cold sensitivity, sensorineural deafness, and AA amyloidosis", *Arthritis and Rheumatology*, Vol. 46, No. 9, pp. 2445-52, 2002.

Allen, I. C., C. B. Moore, M. Schneider, Y. Lei, B. K. Davis, M. A. Scull, D. Gris, K. E. Roney, A. G. Zimmermann, J. B. Bowzard, P. Ranjan, K. M. Monroe, R. J. Pickles, S. Sambhara and J. P. Ting, "NLRX1 protein attenuates inflammatory responses to infection by interfering with the RIG-I-MAVS and TRAF6-NF-kappaB signaling pathways", *Immunity*, Vol. 34, No. 6, pp. 854-65, 2011.

Barker, N., J. H. van Es, J. Kuipers, P. Kujala, M. van den Born, M. Cozijnsen, A. Haegebarth, J. Korving, H. Begthel, P. J. Peters and H. Clevers, "Identification of stem cells in small intestine and colon by marker gene Lgr5", *Nature*, Vol. 449, No. 7165, pp. 1003-7, 2007.

Bauer, C., P. Duewell, C. Mayer, H. A. Lehr, K. A. Fitzgerald, M. Dauer, J. Tschopp, S. Endres, E. Latz and M. Schnurr, "Colitis induced in mice with dextran sulfate sodium (DSS) is mediated by the NLRP3 inflammasome", *Gut*, Vol. 59, No. 9, pp. 1192-9, 2010.

Bauernfeind, F. G., G. Horvath, A. Stutz, E. S. Alnemri, K. MacDonald, D. Speert, T. Fernandes-Alnemri, J. Wu, B. G. Monks, K. A. Fitzgerald, V. Hornung and E. Latz, "Cutting edge: NF-kappaB activating pattern recognition and cytokine receptors license NLRP3 inflammasome activation by regulating NLRP3 expression", *Journal of Immunology*, Vol. 183, No. 2, pp. 787-91, 2009.

Bauernfeind, F., A. Ablasser, E. Bartok, S. Kim, J. Schmid-Burgk, T. Cavlar, and V. Hornung, "Inflammasomes: current understanding and open questions", *Cellular and Molecular Life Sciences*, Vol. 68, No. 5, pp. 765-83, 2011.

Bianchi, D. W., L. D. Platt, J. D. Goldberg, A. Z. Abuhamad, A. J. Sehnert, R. P. Rava and MatErnal BLood IS Source to Accurately diagnose fetal aneuploidy (MELISSA) Study Group. "Genome-wide fetal aneuploidy detection by maternal plasma DNA sequencing", *Obstetrics and Gynecology*, Vol. 119, No. 5, pp. 890-901, 2012.

Billingham, R. E. and W. K. Silvers, "Studies on homografts of foetal and infant skin and further observations on the anomalous properties of pouch skin grafts in hamsters", *Proceedings of the Royal Society of London Series B Biological Sciences*, vol. 161, pp. 168-90, 1964.

Carter, J., A. Newport, K. D. Keeler and D. W. Dresser, "FACS analysis of changes in T and B lymphocyte populations in the blood, spleen and lymph nodes of pregnant mice", *Immunology*, Vol. 48, No. 4, pp. 791-97, 1983.

Chen G. Y., M. H. Shaw, G. Redondo and G. Núñez, "The innate immune receptor Nod1 protects the intestine from inflammation-induced tumorigenesis", *Cancer Research*, Vol. 68, No. 24, pp. 10060-7, 2008.

Chen, M., H. Wang, W. Chen and G. Meng, "Regulation of adaptive immunity by the NLRP3 inflammasome", *International Immunopharmacol*ogy, Vol. 11, No 5, pp. 549-54, 2011.

Chen, G. Y., M. Liu, F. Wang, J. Bertin and Núñez G, "A functional role for Nlrp6 in intestinal inflammation and tumorigenesis", *Journal of Immunology*, Vol. 186, No. 12, pp. 7187-94, 2011.

Clevers, H., "Wnt/beta-catenin signaling in development and disease", *Cell*, Vol. 127, No.3, pp. 469-80, 2006.

Conti, B. J., B. K. Davis, J. Zhang, W. Jr. O'connor, K. L. Williams and J. P. Ting, "CATERPILLER 16.2 (CLR16.2), a novel NBD/LRR family member that negatively regulates T cell function", *Journal of Biological Chemistry*, Vol. 280, No. 18, pp. 18375-85, 2005.

Cruz, C. M., A. Rinna, H. J. Forman, A. L. Ventura, P. M. Persechini and D. M. Ojcius, "ATP activates a reactive oxygen species-dependent oxidative stress response and secretion of proinflammatory cytokines in macrophages", *Journal of Biological Chemistry*, Vol. 282, No. 5, pp. 2871-79, 2007.

Cui, J., L. Zhu, X. Xia, H. Y. Wang, X. Legras, J. Hong, J. Ji, P. Shen, S. Zheng, Z. J. Chen and R. F. Wang, "NLRC5 negatively regulates the NF-kappaB and type I interferon signaling pathways", *Cell*, Vol. 141, No. 3, pp. 483-96, 2010.

Dode, C., N. Le Du, L. Cuisset, F. Letourneur, J. M. Berthelot, G. Vaudour, A. Meyrier, R. A. Watts, D. G. Scott, A. Nicholls, B. Granel, C. Frances, F. Garcier, P. Edery, S. Boulinguez, J. P. Domergues, M. Delpech and G. Grateau, "New mutations of CIAS1 that are responsible for Muckle-Wells syndrome and familial cold urticaria: a novel mutation underlies both syndromes", *The American Journal of Human Genetics*, Vol. 70, No. 6, pp. 1498-1506, 2002.

Dowds, T. A., J. Masumoto, L. Zhu, N. Inohara and G. Nunez, "Cryopyrin-induced interleukin 1beta secretion in monocytic cells: enhanced activity of disease-associated mutants and requirement for ASC", *Journal of Biological Chemistry*, Vol. 279, No. 21, pp. 21924-8, 2004.

Eisenbarth, S. C. and R. A. Flavell, "Innate instruction of adaptive immunity revisited: the inflammasome", *EMBO Molecular Medicine*, Vol. 1, No. 2, pp. 92-8, 2009.

Fearon, E. R. and B. Vogelstein, "A genetic model for colorectal tumorigenesis", *Cell,* Vol. 61, No. 5, pp. 759-67, 1990.

Fernandes-Alnemri, T., J. Wu, J. W. Yu, P. Datta, B. Miller, W. Jankowski, S. Rosenberg, J. Zhang and E. S. Alnemri, "The pyroptosome: a supramolecular assembly of ASC dimers mediating inflammatory cell death via caspase-1 activation", *Cell Death and Differentiation*, Vol. 14, No. 9, pp. 1590-604, 2007.

Franchi, L., J. H. Park, M. H. Shaw, N. Marina-Garcia, G. Chen, Y. G. Kim and G. Nunez, "Intracellular NOD-like receptors in innate immunity, infection and disease", *Cell Microbiology*, Vol. 10, No. 1, pp. 1-8, 2008.

Gillen, C. D., H. A. Andrews, P. Prior, R. N. Allan, "Crohn's disease and colorectal cancer", Gut, Vol. 35, No. 5, pp. 651-5, 1994.

Gültekin, Y., 2011, "Cloning and Characterization of Novel Nod Like Receptors as Cytoplasmic Immune Sensors", M.Sc. thesis, Boğaziçi University.

Gültekin, Y., E. Eren, N. "Overexpressed NLRC3 acts as an anti-inflammatory cytosolic protein", *Journal of Innate Immunity,* Vol. 7, No. 1, pp. 25-36, 2015.

Gregorieff, A. and H. Clevers, "Wnt signaling in the intestinal epithelium: from endoderm to cancer", *Genes and Development*, Vol. 19, No. 8, pp. 877-90, 2005.

Hogquist, K. A., T. A. Baldwin and S. C. Jameson, "Central tolerance: learning self-control in the thymus", *Nature Reviews Immunology*, Vol. 5, No. 10, pp. 772-82, 2005.

Hornung, V., F. Bauernfeind, A. Halle, E. O. Samstad, H. Kono, K. L. Rock, K. A. Fitzgerald and E. Latz, "Silica crystals and aluminum salts activate the NALP3 inflammasome through phagosomal destabilization", *Nature Immunolology*, Vol. 9, No. 8, pp. 847-56, 2008.

Huang, J. Y., M. Su, S. H. Lin and P. L. Kuo, "A genetic association study of NLRP2 and NLRP7 genes in idiopathic recurrent miscarriage", *Human Reproduction*, Vol. 28, No. 4, pp. 1127-34, 2013.

Ito, S., Y. Hara and T. Kubota, "CARD8 is a negative regulator for NLRP3 inflammasome, but mutant NLRP3 in cryopyrin-associated periodic syndromes escapes the restriction", *Arthritis Research and Therapy*, Vol. 16, No. 1, pp. R52, 2014.

Jin, C. and R. A. Flavell, "Molecular mechanism of NLRP3 inflammasome activation", *Journal of Clinical Immunology*, Vol. 30, No. 5, pp. 628-31, 2010.

Kaufmann, S. H., "The contribution of immunology to the rational design of novel antibacterial vaccines", *Nature Reviews Microbiology,* Vol. 5, No. 7, pp. 491-504, 2007.

Kanneganti, T. D., N. Ozoren, M. Body-Malapel, A. Amer, J. H. Park, L. Franchi, J. Whitfield, W. Barchet, M. Colonna, P. Vandenabeele, J. Bertin, A. Coyle, E. P. Grant, S. Akira and G. Nunez, "Bacterial RNA and small antiviral compounds activate caspase-1 through cryopyrin/Nalp3", *Nature*, Vol. 440, No. 7081, pp. 233-6, 2006.

Koch, C. A. and J. L. Platt, "T cell recognition and immunity in the fetus and mother", *Cellular Immunology*, Vol. 248, No. 1, pp. 12-7, 2007.

Liu, R., A. D. Truax, L. Chen, P. Hu, Z. Li, J. Chen, C. Song, L. Chen and J. P. Ting, "Expression profile of innate immune receptors, NLRs and AIM2, in human colorectal cancer: correlation with cancer stages and inflammasome components", *Oncotarget,* Vol. 6, No. 32, pp. 33456-69, 2015.

Man, S. M., Q. Zhu, L. Zhu, Z. Liu, R. Karki, A. Malik, D. Sharma, L. Li, R. K. Malireddi, P. Gurung, G. Neale, S. R. Olsen, R. A. Carter, D. J. McGoldrick, G. Wu, D. Finkelstein, P. Vogel, R. J. Gilbertson and T. D. Kanneganti, "Critical Role for the DNA Sensor AIM2 in Stem Cell Proliferation and Cancer", *Cell*, Vol. 162 No. 1, pp. 45-58, 2015.

Mariathasan, S., D. S. Weiss, K. Newton, J. McBride, K. O'Rourke, M. Roose-Girma, W. P. Lee, Y. Weinrauch, D. M. Monack and V. M. Dixit, "Cryopyrin activates the inflammasome in response to toxins and ATP", *Nature*, Vol. 440, No. 7081, pp. 228-32, 2006.

Mariathasan, S., "ASC, Ipaf and Cryopyrin/Nalp3: bona fide intracellular adapters of the caspase-1 inflammasome", *Microbes and Infection*, Vol. 9, No. 5, pp. 664-71, 2007.

Martinon, F., L. Agostini, E. Meylan and J. Tschopp, "Identification of bacterial muramyl dipeptide as activator of the NALP3/cryopyrin inflammasome", *Current Biology*, Vol. 14, No. 21, pp. 1929-34, 2004.

Martinon, F., V. Petrilli, A. Mayor, A. Tardivel and J. Tschopp, "Gout-associated uric acid crystals activate the NALP3 inflammasome", *Nature*, Vol. 440, No. 7081, pp. 237-41, 2006.

Martinon, F., O. Gaide, V. Petrilli, A. Mayor and J. Tschopp, "NALP inflammasomes: a central role in innate immunity", *Seminars in Immunopathology*, Vol. 29, No. 3, pp. 213-29, 2007.

Martinon, F., "Signaling by ROS drives inflammasome activation", *European Journal of Immunology*, Vol. 40, No. 3, pp. 616-9, 2010.

Medzhitov, R., P. Preston-Hurlburt and C. A. Janeway Jr., "A human homologue of the Drosophila Toll protein signals activation of adaptive immunity", *Nature*, Vol. 388, No. 6640, pp. 394-7, 1997.

Meissner, T. B., A. Li, A. Biswas, K. H. Lee, Y. J. Liu, E. Bayir, D. Iliopoulos, P. J. van den Elsen and K. S. Kobayashi, "NLR family member NLRC5 is a transcriptional regulator of MHC class I genes", *Proceedings of the National Academy of Sciences U S A*, Vol. 107, No. 31, pp. 13794-9, 2010.

Meissner, T. B., A. Li, Y. J. Liu, E. Gagnon and K. S. Kobayashi, "The nucleotide-binding domain of NLRC5 is critical for nuclear import and transactivation activity", *Biochemical Biophysical Research Communications*, Vol. 418 No. 4, pp. 786-91, 2012.

Murdoch, S., U. Djuric, B. Mazhar, M. Seoud, R. Khan, R. Kuick, R. Bagga, R. Kircheisen, A. Ao, B. Ratti, S. Hanash, G. A. Rouleau and R. Slim, "Mutations in NALP7 cause recurrent hydatidiform moles and reproductive wastage in humans", *Nature Genetics*, Vol. 38, No. 3, pp. 300-2, 2006.

Murphy, K., P. Travers and M. Walport, Janeway's Immunobiology, 887 pp. 7th ed. Garland Science, New York, 2008.

Narayanan, K. B., T. H. Jang and H. H. Park, "Self-oligomerization of ASC PYD domain prevents the assembly of inflammasome in vitro", *Applied Biochemistry and Biotechnology,* Vol. 172 No. 8, pp. 3902-12, 2014.

Narayanan, K. B. and H. H. Park, "Purification and analysis of the interactions of caspase-1 and ASC for assembly of the inflammasome", *Applied Biochemistry and Biotechnology*, Vol. 175, No. 6, pp. 2883-94, 2015.

Ogura, Y., S. Lala, W. Xin, E. Smith, T. A. Dowds, F. F. Chen, E. Zimmermann, M. Tretiakova, J. H. Cho, J. Hart, J. K. Greenson, S. Keshav and Nuñez G, "Expression of NOD2 in Paneth cells: a possible link to Crohn's ileitis", Gut, Vol. 52, No. 11, pp. 1591-7, 2003.

Özören, N., J. Masumoto, L. Franchi, T. D. Kanneganti, M. Body-Malapel, I. Erturk, R. Jagirdar, L. Zhu, N. Inohara, J. Bertin, A. Coyle, E. P. Grant and G. Nunez, "Distinct roles of TLR2 and the adaptor ASC in IL-1beta/IL-18 secretion in response to Listeria monocytogenes", *Journal of Immunology*, Vol. 176, No. 7, pp. 4337-42, 2006.

Perregaux, D. and C. A. Gabel, "Interleukin-1 beta maturation and release in response to ATP and nigericin. Evidence that potassium depletion mediated by these agents is a necessary and common feature of their activity", *Journal of Biological Chemistry*, Vol. 269, No. 21, pp. 15195-203, 1994.

Platt, R. J., S. Chen, Y. Zhou, M. J. Yim, L. Swiech, H. R. Kempton, J. E. Dahlman, O. Parnas, T. M. Eisenhaure, M. Jovanovic, D. B. Graham, S. Jhunjhunwala, M. Heidenreich, R. J. Xavier, R. Langer, D. G. Anderson, N. Hacohen, A. Regev, G. Feng, P. A. Sharp and F. Zhang, "CRISPR-Cas9 knockin mice for genome editing and cancer modeling", *Cell*, Vol. 159, No. 2, pp. 440-55, 2014.

Proell, M., M. Gerlic, P. D. Mace, J. C. Reed and S. J. Riedl, "The CARD plays a critical role in ASC foci formation and inflammasome signaling", *Biochemical Journal*, Vol. 449, No. 3, pp. 613-21, 2013.

Polk, D. B. and R. M. Jr. Peek, "Helicobacter pylori: gastric cancer and beyond", *Nature Reviews Cancer*, Vol. 10, No. 6, pp. 403-14, 2010.

Py, B. F., M. S. Kim, H. Vakifahmetoglu-Norberg and J. Yuan, "Deubiquitination of NLRP3 by BRCC3 critically regulates inflammasome activity", *Molecular Cell*, Vol. 49, No. 2, pp. 331-8, 2013.

Razmara, M., S. M. Srinivasula, L. Wang, J. L. Poyet, B. J. Geddes, P. S. DiStefano, J. Bertin and E. S. Alnemri, "CARD-8 protein, a new CARD family member that regulates caspase-1 activation and apoptosis", *Journal of Biological Chemistry*, Vol. 277, No. 16, pp. 13952-8, 2002.

Redman, C. W., A. J. McMichael, G. M. Stirrat, C. A. Sunderland and A. Ting, "Class 1 major histocompatibility complex antigens on human extra-villous trophoblast", *Immunology*, Vol. 52, No. 3, pp. 457-68, 1984.

Roberts, R. L., R. B. Gearry, M. D. Allington, H. R. Morrin, B. A. Robinson, F. A. Frizelle, "Caspase recruitment domain-containing protein 15 mutations in patients with colorectal cancer", *Cancer Research*, Vol. 66, No. 5, pp. 2532-5, 2006.

Saito, S., T. Shima, A. Nakashima, A. Shiozaki, M. Ito and Y. Sasaki, "What is the role of regulatory T cells in the success of implantation and early pregnancy?", *Journal of Assisted Reproduction and Genetics*, Vol. 24, No. 9, pp. 379-86, 2007.

Salminen, A., A. Kauppinen, M. Hiltunen and K. Kaarniranta, "Epigenetic regulation of ASC/TMS1 expression: potential role in apoptosis and inflammasome function", *Cellular and Molecular Life Sciences*, Vol. 71, No. 10, pp. 1855-64, 2014.

Sato, T., R. G. Vries, H. J. Snippert, M. van de Wetering, N. Barker, D. E. Stange, J. H. van Es, A. Abo, P. Kujala, P. J. Peters and H. Clevers, "Single Lgr5 stem cells build crypt-villus structures in vitro without a mesenchymal niche", *Nature*, Vol. 459, No. 7244, pp. 262-5, 2009.

Sato, T., J. H. van Es, H. J. Snippert, D. E. Stange, R. G. Vries, M. van den Born, N. Barker, N. F. Shroyer, M. van de Wetering and H. Clevers, "Paneth cells constitute the niche for Lgr5 stem cells in intestinal crypts", *Nature*, Vol. 469, No. 7330, pp. 415-8, 2011.

Sato, T. and H. Clevers, "Growing self-organizing mini-guts from a single intestinal stem cell: mechanism and applications", *Science*, Vol. 340, No. 6137, pp. 1190-4, 2013.

Schepers, A. G., H. J. Snippert, D. E. Stange, M. van den Born, J. H. van Es, M. van de Wetering and H. Clevers, "Lineage tracing reveals Lgr5+ stem cell activity in mouse intestinal adenomas", Science, Vol. 337, No. 6095, pp. 730-5, 2012.

Schjenken, J. E., J. M. Tolosa, W. Jonathan W. Paul, Vicki L. Clifton and Roger Smith Mechanisms of Maternal Immune Tolerance During Pregnancy, Recent Advances in Research on the Human Placenta, Dr. Jing Zheng (Ed.), ISBN: 978-953-51-0194-9, InTech, DOI: 10.5772/33541, 2012.

Schneider, M., A. G. Zimmermann, R. A. Roberts, L. Zhang, K. V. Swanson, H. Wen, B. K. Davis, I. C. Allen, E. K. Holl, Z. Ye, A. H. Rahman, B. J. Conti, T. K. Eitas, B. H. Koller and J. P. Ting, "The innate immune sensor NLRC3 attenuates Toll-like receptor signaling via modification of the signaling adaptor TRAF6 and transcription factor NF-kappaB", *Nature Immunology*, Vol. 13, No. 9, pp. 823-31, 2012.

Schroder, K. and J. Tschopp, "The inflammasomes", *Cell*, Vol. 140, No. 6, pp. 821-32, 2010.

Sha, Z., J. W. Abernathy, S. Wang, P. Li, H. Kucuktas, H. Liu, E. Peatman and Z. Liu, "NOD-like subfamily of the nucleotide-binding domain and leucine-rich repeat containing family receptors and their expression in channel catfish", *Developmental and Comparative Immunology*, Vol. 33, No. 9, pp. 991-9, 2009.

Shi, C. S., K. Shenderov, N. N. Huang, J. Kabat, M. Abu-Asab, K. A. Fitzgerald, A. Sher and J. H. Kehrl, "Activation of autophagy by inflammatory signals limits IL-1beta production by targeting ubiquitinated inflammasomes for destruction", *Nature Immunology*, Vol. 29, No. 13, pp. 255-63, 2012.

Shaw, M. H., T. Reimer, Y. G. Kim and G. Nunez, "NOD-like receptors (NLRs): bona fide intracellular microbial sensors", *Current Opinion in Immunology*, Vol. 20, No. 4, pp. 377-82, 2008.

Shiau, C. E., K. R. Monk, W. Joo, W. S. Talbot, "An anti-inflammatory NOD-like receptor is required for microglia development", *Cell Reports,* Vol. 5, No. 5, pp. 1342-52, 2013.

Siegmund, B., H. A. Lehr, G. Fantuzzi and C. A. Dinarello, "IL-1 beta -converting enzyme (caspase-1) in intestinal inflammation", *Proceedings of the National Academy of Sciences U S A,* Vol. 98 No. 23, pp. 13249-54, 2001.

Starr, T. K., S. C. Jameson and K. A. Hogquist, "Positive and negative selection of T cells", *Annual Review of Immunology*, Vol. 21, pp. 139-76, 2003.

Steimle, V., C. A. Siegrist, A. Mottet, B. Lisowska-Grospierre and B. Mach, "Regulation of MHC class II expression by interferon-gamma mediated by the transactivator gene CIITA", *Science*, Vol. 265, No.5168, pp. 106-9, 1994.

Sutterwala, F. S., L. A. Mijares, L. Li, Y. Ogura, B. I. Kazmierczak and R. A. Flavell "Immune recognition of *Pseudomonas aeruginosa* mediated by the IPAF/NLRC4 inflammasome", *Journal of Experimental Medicine*, Vol. 204, No. 13, pp. 3235-45, 2007.

Takeda, K. and S. Akira, "TLR signaling pathways", *Seminars in Immunology*, Vol. 16, No. 1, pp. 3-9, 2004.

Takeda, K. and S. Akira, "Toll-like receptors in innate immunity", *International Immunology*, Vol. 17, No. 1, pp. 1-14, 2005.

Tallon, D. F., D. J. Corcoran, E. M. O'Dwyer and J. F. Greally, "Circulating lymphocyte subpopulations in pregnancy: a longitudinal study", *Journal of Immunology*, Vol. 132, No. 4, pp. 1784-7, 1984.

Vallejo, A. N., E. Davila, C. M. Weyand and J. J. Goronzy, "Biology of T lymphocytes", *Rheumatic Disease of Clinics of North America*, Vol. 30, No. 1, pp. 135-57, 2004.

Verma, D., M. Lerm, R. Blomgran Julinder, P. Eriksson, P. Soderkvist and E. Sarndahl, "Gene polymorphisms in the NALP3 inflammasome are associated with interleukin-1 production and severe inflammation: relation to common inflammatory diseases?", *Arthritis and Rheumatology*, Vol. 58, No. 3, pp. 888-94, 2008.

Watanabe, M., Y. Iwatani, T. Kaneda, Y. Hidaka, N. Mitsuda, Y. Morimoto and N. Amino, "Changes in T, B, and NK lymphocyte subsets during and after normal pregnancy", *American Journal of Reproductive Immunology*, Vol. 37, No. 5, pp. 368-77, 1997.

Xia, X., J. Cui, H. Y. Wang, L. Zhu, S. Matsueda, Q. Wang, X. Yang, J. Hong, Z. Songyang, Z. J. Chen and R. F. Wang, "NLRX1 negatively regulates TLR-induced NF-kappaB signaling by targeting TRAF6 and IKK", *Immunity*, Vol. 34, No. 6, pp. 843-53, 2011.

Yan, Y., V. Kolachala, G. Dalmasso, H. Nguyen, H. Laroui, S. V. Sitaraman, D. Merlin, "Temporal and spatial analysis of clinical and molecular parameters in dextran sodium sulfate induced colitis", *PLoS One*, Vol. 4 No. 6, pp. e6073, 2009.

Yu, H. B. and B. B. Finlay, "The caspase-1 inflammasome: a pilot of innate immune responses", *Cell Host and Microbe*, Vol. 4, No. 3, pp. 198-208, 2008.

Yu, J. R. and K. S. Leslie, "Cryopyrin-associated periodic syndrome: an update on diagnosis and treatment response", *Current Allergy and Asthma Reports*, Vol. 11, No. 1, pp. 12-20, 2011.

Yüksel, Ş., E. Eren, G. Hatemi, A. C. Sahillioğlu, Y. Gültekin, D. Demiröz, C. Akdiş, İ. Fresko and N. Özören, "Novel NLRP3/cryopyrin mutations and pro-inflammatory cytokine profiles in Behçet's syndrome patients", *International Immunology*, Vol. 26, No. 2, pp. 71-81, 2014.

Zaki, M. H., P. Vogel, R. K. Malireddi, M. Body-Malapel, P. K. Anand, J. Bertin, D. R. Green, M. Lamkanfi, T. D. Kanneganti, "The NOD-like receptor NLRP12 attenuates colon inflammation and tumorigenesis", *Cancer Cell*, Vol. 20, No. 5, pp. 649-60, 2011.

Zhang, L., J. Mo, K. V. Swanson, H. Wen, A. Petrucelli, S. M. Gregory, Z. Zhang, M. Schneider, Y. Jiang, K. A. Fitzgerald, S. Ouyang, Z. J. Liu, B. Damania, H. B. Shu, J. A. Duncan and J. P. Ting, "NLRC3, a member of the NLR family of proteins, is a negative regulator of innate immune signaling induced by the DNA sensor STING", *Immunity,* Vol. 40, No. 3, pp. 329-41, 2014.